CERN/PS/DL 80-7

16 May 1980

DESIGN STUDY OF A FACILITY FOR EXPERIMENTS WITH LOW ENERGY ANTIPROTONS (LEAR)

PREFACE

After the decision, in June 1979, to pursue at CERN the field of physics with slow antiprotons, an informal Working Group was set up in the PS Division with the task to work out a design study of a facility for experiments with low energy antiprotons. Because of the many projects currently under way in the Division only three staff members could devote full time to this study. Many others contributed, despite the heavy responsiblities and tight schedules, the necessary technical input so that parameters and budgets contained in this project report can now be submitted with a good degree of confidence. Several aspects of the project were discussed in the LEAR Liaison Group which includes representatives of the future users of the facility. We want to acknowledge the efforts of all who contributed to the study; in particular, some of the users for their intense collaboration : P. Dalpiaz, U. Gastaldi and K. Kilian ; J.L. Laclare and G. Leleux (CERN-Saclay) and M. Conte (Genova) for advice; and R. Klapisch, E. Lohrmann, G.L. Munday and V. Soergel for their encouragement. Finally, we thank the Design Office and the secretaries for the devotion and hard work that has allowed this report to be issued on time.

G. Plass
Editor

PARTICIPANTS IN THE STUDY :

Full-time

W. Hardt

P. Lefèvre

D. Möhl

Part-Time

R. Bertolotto

B. Bianchi

M. Bouthéon

D. Fiander

J.Y. Freeman

C. Germain

M. Giesch

H. Haseroth

G. Heritier

M. Hoefert

L. Hoffmann

W. Kubischta

R. Mosig

H. Poth

P. Riboni

C. Rufer

D. Simon

A. Sullivan

A. Susini

U. Tallgren

M. Thivent

L. Thorndahl

LEAR LIAISON GROUP

F. Bonaudi

P. Dalpiaz

U. Gastaldi

L. Hoffmann

K. Kilian

P. Lefèvre (Secretary)

D. Möhl

G.L. Munday

G. Plass (Chairman)

V. Soergel

DESIGN STUDY OF A FACILITY FOR EXPERIMENTS WITH LOW ENERGY ANTIPROTONS (LEAR)

C O N T E N T S

1. INTRODUCTION

This report is concerned with the proposal to build a small synchrotron (called LEAR for Low Energy Antiprotons Ring) which will provide intense antiproton beams for a variety of $\bar{p}$ experiments at low energy. It will receive at regular intervals batches of $\bar{p}$ extracted from the Antiproton Accumulator (AA) [4] and decelerated in the PS. This machine will primarily be used as an accelerator/decelerator and as a beam stretcher, i.e., the beam will be accelerated or slowed down from the fixed transfer momentum to that required by the experiments, where it will be extracted in a very long spill for fixed target experiments. Other options are being considered, such as fast extraction, the installation of internal jet targets, co-rotating H^- and $\bar{p}$ beams, and $p\bar{p}$ collision experiments.

At CERN, early versions [1] of such a machine were proposed in 1977, in papers submitted by U. Gastaldi, K. Kilian and D. Möhl to the International Accelerator Conference and by P. Dalpiaz to the CERN $p\bar{p}$ study week [*]. A summary of these proposals was presented by the "Lohrmann Group" [2a] to the Workshop on the Future of Intermediate Energy Physics [2b] held at CERN in the autumn of 1977 where it was given an enthusiastic response, and to the PS and SC Committees [2c] who gave further support. The CERN Scientific Policy Committee in its meeting in November 1978, gave a positive recommendation for such a facility to be built at CERN. Thereafter, a Workshop [3a] on Physics with Cooled Low-Energy Antiprotons was attended by more than 70 interested physicists in Karlsruhe on March 19-21, 1979 and on the basis of the physics proposed there, a report [3b] was discussed by the PS + SC Experiments Committee. This Committee and the CERN Research Board recommended the construction of a facility for experiments with intense beams of low energy $\bar{p}$ in their meetings in June 1979. Upon the invitation issued by the PSSC to submit letters of intent for experiments at this facility, 17 letters have so far been received involving 24 Institutes from Member States and two from non-member States.

On the basis of the conceptual studies [5] made previously a detailed study of the facility was launched in September 1979 and the design of LEAR is now presented in this report. The cost of the first stage, i.e., the beam stretcher, is estimated at 10.65 MFr. ; it will take 65 man-years of staff effort, and if authorized in May 1980, it is expected to begin the running-in in the second half of 1982.

---

*) References to earlier work are contained in these papers.

2. DESCRIPTION OF THE PROJECT

2.1 General layout

LEAR is located in the South Hall of the PS as indicated in Figs. 1 and 2. The position chosen was conditioned by several constraints such as size (now 1/8 of the PS circumference), ejected beam and experimental areas, access, and the condition to provide for the later implementation of the options. The area for experiments using the $\bar{p}$ beam from LEAR is in the East part used at present for test beams.

It turned out, on balance, that the injection line is best taken through a new separate tunnel as indicated in Fig. 1 (rather than through the linac tunnel). The $\bar{p}$ beam is ejected from the PS straight sector 26 and the ejection septum magnet is compatible with the injection into the PS of protons and ions coming from the old (or the new) linac. 50 MeV protons from the old linac will be essential for testing and running-in of LEAR. Particles from the old linac are brought to the injection line through the loop indicated in Fig. 1.

The new linac control room will also serve as the Control Center for LEAR. Experimenters will obtain information and limited control on mobile terminals. Special supplies and electronic equipment for sub-systems (injection, ejection, etc.) will be located in the area between LEAR and the linacs. The power supplies for the LEAR magnets and quadrupoles and the beam elements will be installed inside or near the South generator and South Rectifier buildings.

The necessary power and water installations exist in the area as well as the network of cable trenches.

LEAR will be enclosed in concrete shielding walls designed to keep the radiation level in the PS Main Control Room, which is permanently occupied, at tolerable levels.

2.2 Brief description of LEAR

The machine is discussed in detail in Chapters 3 and 4 ; a summary is given here for convenience.

The circumference is equal to one eighth of the PS or one half of the AA. It has an almost square shape in order to provide long straight sectors where large equipment can be installed (e.g., a low β section and/or large experiments around an internal target or a collision point). The four sector magnets and a quadrupole doublet at either side of it provide for short straights of 1 m length between dipole and quadrupoles and long straights of 8 m between the doublets (Fig. 3). The beam height is 1.66 m above the floor of the hall. The machine parameters are given in Table 2.2-1.

The all metal vacuum system will be designed for baking at 300° and with the ultimate goal of achieving the vacuum limits obtained in the ISR. The acceleration system consists of one or two ferrite cavities. Controls will be based on the PDP 11/45 computers of the Linac control system, to which a third CAMAC branch is being added.

Injection and ejection make use of a common septum magnet in SL 1. The injected beam receives its final deflection by a fast ferrite kicker and space is reserved in SL 4 for a second septum/kicker system for the case that a beam circulating in opposite direction is required. The ejected beam is deflected across the common magnetic septum by a thin electrostatic septum device in SS 11, and it receives a final deflection by a thick septum magnet.

A special ejection system providing a very long spill is necessary in order to obtain a continuous ejected beam between two refills. To achieve this, one uses the phenomenon that a RF signal containing noise of a certain bandwidth induces in the beam a diffusion process inside a momentum band. This techniques is used first to flatten the particle distribution and then to make particles diffuse towards the momentum where they find themselves in the transverse resonance which leads to ejection (then called stochastic extraction) (see Fig. 12).

The installation of stochastic cooling systems for transverse and momentum phase-space has been studied and space reserved for the necessary elements. It is expected that some material for a first modest set-up can be recuperated from the ICE ring. The necessary provisions, in particular for the pick-ups, will be implemented in the design of the vacuum chambers from the outset.

Table 2.2-1

LEAR BASIC PARAMETERS.

Momentum (kinetic energy) range	0.1 - 2 GeV/c (5.3 MeV - 1.3 GeV)
Injection momentum (kinetic energy)	0.6 GeV/c (175.4 MeV)
Circumference	78.54 m (= 2π x 12.5 m)
Typical cycle	$10^9 \bar{p}$ injected every 10^3 s
Typical extracted beam	10^6 $\bar{p}$/s
Typical spill length	≈ 900 s
Long straight sections	4 of 8 m length each
Short straight sections (between quadrupoles and Bending Magnet)	8 of 1 m length each
Bending magnets ,No, arc length ,field at 2 GeV/c	4, 6.55 m, B = 1.6 T
Quadrupoles, No, magnetic length, max gradient at 2 GeV/c	16, 0.5 m, k = 1.8 m^{-2} (g = 12 T/m)
Focusing structure	4 superperiods, seperated function BoDFOFDoB
Betatron wavenumbers and momentum compaction (stretcher mode)	$Q_H \approx 2.3$ $Q_V \approx 2.7$ $\alpha = \gamma_t^{-2} = -4.8 \times 10^{-3}$
Aperture limitation	$a_H = \pm 70$ mm $a_V = \pm 29$ mm
Acceptances (stretcher mode)	$E_H = 240\ \pi \times 10^{-6}$ rad m $E_V = 48\ \pi \times 10^{-6}$ rad m $\Delta p/p = \pm 1.1$ %
Vacuum system, design pressure (N_2 - equivalent)	10^{-11} - 10^{-12} Torr
Bake out temperature, bake out and pump down time	300^oC, ≈ 40 h
Rf - system frequency range (h = 1)	0.4 - 3.5 MHz
Peak voltage per turn (stretcher mode)	12 KV
PS beam bunch properties at transfer (h = 10 in PS), area, total bunch length	A = 15 mrad, l_b = 250-300 ns
Acceptance of transfer system	$E_H = 40\ \pi \times 10^{-6}$ rad m $E_V = 20\ \pi \times 10^{-6}$ rad m $\Delta p/p = \pm 5 \times 10^{-3}$
Assumed AA beam properties at 3.5 GeV/c (unstacking of 10^9 $\bar{p}$)	$E_H \leq 3\pi \times 10^{-6}$ rad m $E_V \leq 1.5\pi \times 10^{-6}$ rad m A = 6 mrad (at h = 1 in AA)

As to the options, the location of a jet target for experiments on the circulating beam is planned in straight sector SL 2, where also the quadrupoles for the low beta scheme will be installed. One or two jet targets for the production of secondary $\bar{n}$ beams can be located in the center of the magnet sectors 1 and 2. Space for the electron cooling system is reserved in straight sector SL 3. For the experiments with co-rotating $\bar{p}$ and H^- beams, the neutral $(p\bar{p})$ states formed in SS11, SL 1 and SS12 fly along the neutral beam line indicated in Fig. 2. The collisions region in the $p\bar{p}$ collision option would be in SL 2, replacing the jet target.

2.3 Development of the Facility

During all discussions to date it has been assumed that the LEAR facility would come in phases, beginning with the operation as a beam stretcher. A possible programme of the development making the optimistic assumption that the basic facility is ready by mid-1982 is briefly discussed below.

2.3.1 The stretcher

Some running-in of experiments using the external beam can be expected to begin (on a parasite basis) concurrently with the development of the slow ejection system. Beam would first be available at the PS-LEAR transfer momentum i.e., 0.6 GeV/c approximately, and an increasing range of momenta would become accessible as the acceleration system comes into operation. It is now estimated that the momentum range 0.3 to 1.6 GeV/c will be accessible with the initial acceleration system early in 1983.

Extension of the range down to 100 MeV/c can be expected once transverse stochastic cooling has come into operation. Extension upwards to about 2 GeV/c may be limited by the efficiency of the extraction system and practical experience will be essential. These two latter developments are expected in the course of 1983.

Fast ejection at medium momentum, using the inflection kicker could be available rather early. For high and low momenta (large beams) an additional fast kicker would be necessary.

2.3.2 The options

The options for the further development, which are described in Chapter 6, are briefly commented below.

Amongst the options, the installation of an electron cooling system is of most general interest, as it would improve the performance of the basic machine as well as of two of the other options (jet target, H^- beams). A system designed to specification for LEAR (momenta up to about 0.6 GeV/c, short cooling times) will constitute a major development and take some time to build ; it could become usable in 1984 if seriously undertaken in the second half of 1980. The possibility to adapt the ICE test set-up is therefore being investigated.

Gas jet targets are at present being developed for possible use in the SPS and the ISR, the main problem being compatibility with the vacuum requirements in these machines. If these developments were successful, a jet for LEAR presumably of the cryogenic cluster type could probably be obtained on a rather short time-scale. A target of low luminosity, with a total thickness no larger than the integrated rest-gas density, could be installed rather early on. A target of high luminosity, typically one used for antineutron production, will have to await the availability of the electron cooling system for the compensation of multiple Coulomb scattering.

The two further options, co-rotating H^- and $\bar{p}$ beams, and $p\bar{p}$ collision experiments, impose more stringent requirements on the machine in order to reach full potential. Though weak ($p\bar{p}$) beams will be obtained as soon as H^- ions are injected, electron cooling of the H^- beam is essential for more sophisticated experiments, and then a very precise velocity match between the electrons and the H^- ions must be maintained to avoid stripping. Similarly, the luminosity obtained in $p\bar{p}$ collisions in the "bare" machine would be very low. The electron cooling system required to improve the luminosity in this option would have to work at momenta around 2 GeV/c which is a high momentum for the conventional electron cooling and low for relativistic electron cooling. The short bunch length required in the collider option necessitates a special high voltage RF system.

At the present stage, parameters and choices have been avoided which would exclude the implementation of any of the options and studies to data have established the probable feasibility of the jet

As to the options, the location of a jet target for experiments on the circulating beam is planned in straight sector SL 2, where also the quadrupoles for the low beta scheme will be installed. One or two jet targets for the production of secondary $\bar{n}$ beams can be located in the center of the magnet sectors 1 and 2. Space for the electron cooling system is reserved in straight sector SL 3. For the experiments with co-rotating $\bar{p}$ and H^- beams, the neutral $(p\bar{p})$ states formed in SS11, SL 1 and SS12 fly along the neutral beam line indicated in Fig. 2. The collisions region in the $p\bar{p}$ collision option would be in SL 2, replacing the jet target.

2.3 Development of the Facility

During all discussions to date it has been assumed that the LEAR facility would come in phases, beginning with the operation as a beam stretcher. A possible programme of the development making the optimistic assumption that the basic facility is ready by mid-1982 is briefly discussed below.

2.3.1 The stretcher

Some running-in of experiments using the external beam can be expected to begin (on a parasite basis) concurrently with the development of the slow ejection system. Beam would first be available at the PS-LEAR transfer momentum i.e., 0.6 GeV/c approximately, and an increasing range of momenta would become accessible as the acceleration system comes into operation. It is now estimated that the momentum range 0.3 to 1.6 GeV/c will be accessible with the initial acceleration system early in 1983.

Extension of the range down to 100 MeV/c can be expected once transverse stochastic cooling has come into operation. Extension upwards to about 2 GeV/c may be limited by the efficiency of the extraction system and practical experience will be essential. These two latter developments are expected in the course of 1983.

Fast ejection at medium momentum, using the inflection kicker could be available rather early. For high and low momenta (large beams) an additional fast kicker would be necessary.

2.3.2 The options

The options for the further development, which are described in Chapter 6, are briefly commented below.

Amongst the options, the installation of an electron cooling system is of most general interest, as it would improve the performance of the basic machine as well as of two of the other options (jet target, H^- beams). A system designed to specification for LEAR (momenta up to about 0.6 GeV/c, short cooling times) will constitute a major development and take some time to build ; it could become usable in 1984 if seriously undertaken in the second half of 1980. The possibility to adapt the ICE test set-up is therefore being investigated.

Gas jet targets are at present being developed for possible use in the SPS and the ISR, the main problem being compatibility with the vacuum requirements in these machines. If these developments were successful, a jet for LEAR presumably of the cryogenic cluster type could probably be obtained on a rather short time-scale. A target of low luminosity, with a total thickness no larger than the integrated rest-gas density, could be installed rather early on. A target of high luminosity, typically one used for antineutron production, will have to await the availability of the electron cooling system for the compensation of multiple Coulomb scattering.

The two further options, co-rotating H^- and $\bar{p}$ beams, and $p\bar{p}$ collision experiments, impose more stringent requirements on the machine in order to reach full potential. Though weak $(p\bar{p})$ beams will be obtained as soon as H^- ions are injected, electron cooling of the H^- beam is essential for more sophisticated experiments, and then a very precise velocity match between the electrons and the H^- ions must be maintained to avoid stripping. Similarly, the luminosity obtained in $p\bar{p}$ collisions in the "bare" machine would be very low. The electron cooling system required to improve the luminosity in this option would have to work at momenta around 2 GeV/c which is a high momentum for the conventional electron cooling and low for relativistic electron cooling. The short bunch length required in the collider option necessitates a special high voltage RF system.

At the present stage, parameters and choices have been avoided which would exclude the implementation of any of the options and studies to data have established the probable feasibility of the jet target in conjunction with electron cooling. The implementation of the other two options will still need much study and development and will not be possible before 1985.

2.4 Operation and performance

The Antiproton Accumulator is expected to accumulate 6.10^{11} $\bar{p}$ per day when the PS runs for $\bar{p}$ production exclusively. Taking into account transfer losses, 4 to 5.10^{6} $\bar{p}$/s is the max. flux obtainable in the external beam from LEAR. It is unlikely that LEAR will be the only facility in operation and the possibilities of running in parallel with PS and SPS physics will be considered below.

Two basic schemes of beam sharing are possible

i) sharing protons, i.e., using one or two 25 GeV cycles within a PS/SPS supercycle for $\bar{p}$ production, the AA being used for LEAR exclusively.

ii) sharing antiprotons, i.e., taking a small fraction of a $\bar{p}$ stack being prepared in the AA for the SPS (or ISR).

The first of these possibilities looks quite straightforward. One would take one or two hours to create in the AA a stack of about 5.10^{10} $\bar{p}$ and unstack batches of the order of 10^{9} $\bar{p}$ at intervals of 1000 s which after transfer to LEAR would be available as an extracted beam with a flux of 10^{6} $\bar{p}$/s. The batch size of 10^{9} $\bar{p}$ is the minimum which the present PS beam control system needs to function safely.

The second possibility, parasitic running during SPS $\bar{p}$ experiments, would be very interesting if, say, 5% of the stack could be allowed for low energy $\bar{p}$ physics. LEAR could then typically receive 30 batches of 10^{9} $\bar{p}$, and run about 8 hours per day in the normal way. If the PS beam control, on the other hand, could be made more sensitive so that smaller batches can be transferred, or if the slow extraction of LEAR could be stretched out by another factor of three, a parasitic beam of 2 to 3.10^{5} $\bar{p}$/s would be available around the clock.

For setting-up experiments (as well as the machine) it is interesting to note that a proton beam will be available, and possibly also an H^{-} beam for which no polarity reversal would be necessary.

A small team of machine physicists/engineers will be available for running-in, machine development and setting-up the machine as well as for trouble-shooting. The continuous surveillance during runs will be the charge of some members of teams running experiments at LEAR, helped by the possibilities of a computer-based control system.

3. LATTICE AND BEAM PARAMETERS

3.1 LATTICE

3.1.1 General considerations

Several types of lattices have been studied, including FODO, doublet and triplet arrangements with and without special long straight sections. Our final choice is for a symmetric four period machine with compact 90^{o} bending magnets and very strong focusing (phase advance of almost 250^{o} per period) by eight quadrupole doublets. This arrangement meets best the requirements of a 2 GeV/c ring in the South Hall, into which acceleration/deceleration, ultra slow ejection, cooling, internal gas targets and eventually operation with co-rotating $\bar{p}$ and H^{-} and with colliding beams of p and $\bar{p}$ can be included. The main properties of the lattice are summarized in Table 3.1-1 and in Fig. 4-9.

Special weight was put on the requirements to have small aperture, to obtain at least 3 long and unobstructed straight sections and to push transition energy above the working range. The circumference has been chosen to be 1/8 of the PS. This is the maximum size of a regular machine that fits into the South Hall. The integer radius ratio with PS and AA will permit multiturn injection schemes that might become desirable for the colliding beam option.

The resulting four long straight sections of LEAR (with a free length of 8 m each) are adequate to accommodate injection and ejection of antiprotons (LS1), the apparatus for physics with internal beams (LS2), RF and electron cooling (LS3), and injection of protons and further RF (LS4). The eight short straight sections (about 1 m length each) between magnet and doublet house the remaining equipment for beam observation, stochastic cooling, electrostatic septum, etc. Some pick-up electrodes for beam observation and cooling can be installed in the central blocks of the magnet quadrant as the vertical beam size is small in these places (see Figs 4, 6, 8).

The small beam size in the centre of the long straight section makes this location suited for electron cooling. By the same token, this focal point, as well as the other beam waists occurring in the magnet centre are strategic locations for the jet targets as at these points the scattering acceptance (maximum deflection of a particle not leading to loss) is large. This behaviour can be emphasized by tuning to a suitable working point. In addition, a low β optic can be inserted in LS2 to further increase the scattering acceptance and to improve the luminosity of $\bar{p}$-p collisions.

A peculiarity of the doublet structure concerns transition energy. In fact, with the BDFOFDB arrangement, transition can be shifted to energies much above the working range despite the low periodicity of the machine. For the preferred working point γ_{tr} is imaginary , that is to say that the "momentum compaction" $\gamma_{tr}^{-2} = \Delta C/C / \Delta p/p$ relating the change of orbit circumference to the momentum error of a particle is negative.

This is very favourable for stochastic cooling because the dispersion of particle revolution periods ($\Delta T/T/\Delta p/p = \eta = \frac{1}{\gamma_t^2} - \frac{1}{\gamma^2}$) and hence the mixing of particles of different momenta remains large even when the momentum spread has become small. Operation below transition (η negative) is advantageous in order to alleviate certain beam density limitations (longitudinal self-bunching instability and intra beam scattering), which may become important with efficient cooling.

3.1.2 Tuning and correction

With the separated function structure and the quadrupole strength of $|k| \leq 2\ m^{-2}$, it is possible to explore a full range of working points Q_H, Q_V between 1 and 3.5 ("Forbidden" bands around $Q \approx 2$ corresponding to instability of the betatron equation have, of course, to be avoided, in addition to the usual stop-bands $n_1 Q_H + n_2 Q_V = m$). For the principal mode of operation, the working point will be close to $Q_H = 2.3$; $Q_V = 2.7$ which is near to the third integer resonance ($Q_H = 2\ 1/3$) used for extraction and in a working range sufficiently free of systematic resonances (Fig. 5). For dedicated operation with internal targets and for $\bar{H}\bar{p}$ beams, a higher working point ($Q_H \approx 3.3$) is advantageous (Figs 8, 9 and Table 3.1-2). It is possible to go from the BDFOFDB to a BFDODFB or even to an asymmetric BFDOFDB excitation of the superperiods and this might be favourable in the colliding beam option.

Short air cored correction magnets (ℓ = 30 cm) including sextupole and dipole windings will be used for chromaticity and orbit correction as detailed in Table 3.1-3. The D correctors are located between

Table 3.1-1

General lattice parameters and performances for stretcher working point

Momentum range	0.1 - 2 GeV/c	
Circumference	78.54 m (= 2 π x 12.5 m)	
Total length of straight section	52.3 m	
Free length of long straight section	8.0	
Number of long straight sections	4	
Length of short straight section	1.16 m	
Free length (including bellows)	∿1.0 m	
Number of short straight sections	8	
Approximate working point for stretcher	Q_H = 2.3	
	Q_V ≃ 2.7	
	γ_t^2 = $-(14.5)^2$	
Maxima of lattice functions	β_H = 9.4 m	
	β_V = 21.0 m	
	α_p = 3.9 m	
Maxima in bending magnets	β_H = 9.4 m	
	β_V = 11.8 m	
	α_p = -0.9 m	
Aperture limitations	a_H = ± 70 mm in F quadrupole	
	a_V = ± 29 mm at entrance of magnets	
Corresponding lattice functions	β_H = 8.4 m	
	β_V = 11.8 m	
	α_p = 3.9 m	
Assumed beam apertures ($\pm$ 5 mm allowance for orbit distortion)	$a_{H\beta}$ = ± 45 mm	
	a_{Hp} = ± 45 mm	
	a_V = ± 24 mm	
Maximum acceptances	E_H = 240 π 10^{-6} rad.m	
	E_V = 48 π 10^{-6} rad.m	
	Δp/p = ± 1.1 %	
Momentum	2 GeV/c	0.1 GeV/c
Bending field	1.6 T	0.08 T
Integrated quadrupole gradient (Q_H = 2.33 ; Q_V = 2.75)	QD 4.7 T	0.24 T
	QF 4.1 T	0.21 T

TABLE 3.1-2

Working point for internal target and H^--$\bar{p}$ operation

Approximate tune values	Q_H = 3.2 Q_V = 2.7 $\gamma_t^2 = -(2.5)^2$
Maxima of lattice functions	β_H = 14 m β_V = 25 m α_p = 2.7 m
Maxima in bending magnets	β_H = 4.3 m β_V = 14.0 m α_p = −2.6 m
Aperture limitations	a_H = ±70 mm in F quadrupole a_V = ±29 mm at entrance of magnets
Corresponding lattice functions	β_H = 14.0 m β_V = 13.8 m α_p = 2.6 m
Assumed beam apertures (± 5 mm allowance for orbit distortion)	$a_{H\beta}$ = ±45 mm a_{Hp} = ±45 mm a_V = ±24 mm
Maximum acceptance	E_H = 145 π mm.mrad E_V = 40 π mm.mrad $\frac{\Delta p}{p}$ = ± 1.7%
Lattice functions and acceptance angle in centre of straight sections	β_H = 1.3 m β_V = 5.0 m θ_H = 10 mrad θ_V = 2.9 mrad $\theta = \sqrt{\theta_H \cdot \theta_V}$ = 5.5 mrad
Lattice functions and acceptance angle in magnet centre	β_H = 3.9 m β_V = 0.8 m θ_H = 6.1 mrad θ_V = 7.2 mrad $\theta = \sqrt{\theta_H \cdot \theta_V}$ = 6.6 mrad

TABLE 3.1-3

CHROMATICITY AND ORBIT CORRECTION

(Working point $Q_H = 2.3$; $Q_V = 2.7$)

Chromaticity $\xi = \frac{\partial Q/Q}{\partial p/p}$ without correction*	
– horizontal	$\xi_H = -1.9$
– vertical	$\xi_V = -2.7$
Number of sextupoles	
– at F location (either end of long straight section)	8
– at D location (between lenses of each doublet)	8
Magnetic length of each element	0.3 m
Strength $k' = \frac{\partial^2 B/\partial x^2}{B\rho}$ (in m^{-3}) to have:	
$\xi_H = 0$; $\xi_V = 0$	$k'_F = 2.1$; $k'_D = -2.3$
$\xi_H = 1$; $\xi_V = 0$	$k'_F = 2.75$; $k'_D = -2.8$
Number of dipoles (integrated with sextupole correctors	
– horizontal (at F location)	8
– vertical (at D location)	8
Deflection $\theta = B\ell/B\rho$ at maximum energy	1 mrad
Corresponding "half wave bump" at $\beta_c = 5$ m	
– horizontal	± 6.3 mm
– vertical	± 8.6 mm
Single quadrupole misalignement to produce similar deflection	1.2 mm
Field error ($\Delta B/B$) of one magnet quadrant for similar deflection	6.4×10^{-4}

* Values obtained using the computer code SYNCH. The code AGS gives more favourable values.

the lenses of each doublet where the vertical focusing function (β_V) is large and the action thus mainly in the vertical plane. At the "F" correctors (located on either side of the long straight sections), the horizontal and vertical β functions are about equal. A more favourable F position where $\beta_H >> \beta_V$ is not easily accessible. The lens strength required for orbit correction and for chromaticity tuning to $\xi_H \simeq 0.6$ and $\xi_V = 0$, necessary for slow ejection, can just be provided by the lens design described in section 4.1 although little margin is left at the highest LEAR energies.

3.2 Beam transfer into LEAR

The low energy antiproton facility will require a beam in two different conditions :

- small batches of $\bar{p}$ in the stretcher mode and for operation with an internal jet target or with H^- beams ;
- the full stack of the AA (6×10^{11} $\bar{p}$) for the p-$\bar{p}$ collider mode.

The "small batch" transferred every 10 to 15 minutes, will typically contain 10^9 $\bar{p}$. This number is given by the sensitivity of the beam observation and control systems of the PS. Modifications of these systems in order to increase their sensitivity will be examined. Transfer of the whole stack will follow the line adopted for the AA-PS-SPS transfer of batches of up to 10^{11} $\bar{p}$.

3.2.1 $\bar{p}$ transfer from AA to LEAR

The batches are obtained in the AA by unstacking part of the stack, as it is done for SPS or ISR transfer, typically in RF buckets of 6 mrad size. For the small batches, the same bucket will be used but the density of the $\bar{p}$ bunch is smaller, by taking either the tail of the main stack in parasitic mode, or by creating a stack of 10^3 $\bar{p}$/eV and unstacking a momentum bite about 1 MeV wide.

The beam is decelerated in the PS, where harmonic number 10 is chosen in order to provide sufficient bucket size. The RF matching at 3.5 GeV/c and deceleration at harmonic 10 in the PS need some extension of the developments underway for the high energy $p\bar{p}$ scheme. This deceleration will be operated on the decreasing part of the PS magnetic cycles for high energy (B cycle) which must be slightly modified, see Fig. 10 . The duration of the total cycle (incl. dead time) will remain unchanged. Typical values of the beam parameters are indicated in Table 3.2-1. Enough margin is left for small transverse and longitudinal blow-up.

For the ejection from the PS at .6 GeV/c a new thin septum magnet is foreseen to replace the electrostatic septum in SS 26. A fast kicker will be installed in SS28. This ejection system is compatible with the 50 MeV multiturn injection for p, deuterons and alpha particles in the PS.

TABLE 3.2-1 - AA-PS-LEAR TRANSFER PARAMETERS

- 3.5 GeV/c	AA-PS transfer	AA	PS
	Harmonic number h	1	10
	Bunch emittance (unstacking bucket)	6 mrad	15 mrad
	RF voltage	14 kV	7 kV
	Emittance [6] (2 rms) at 3.5 GeV/c	$E_H = 3\pi \times 10^{-6}$ rad m; $E_V = 1.5\pi \times 10^{-6}$ rad m (partially cooled*)	$E_H = 1.5\pi \times 10^{-6}$ rad m; $E_V = 1\pi \times 10^{-6}$ rad m (totally cooled)
-	Bucket acceptance for PS deceleration	25 mrad	
- .6 GeV/c	PS ejection, transfer, LEAR injection	PS	LEAR
	Slope of magnetic field $\dot{B}$	$-0.3\ TS^{-1}$	0
	Magnetic guide field	0.0286 T	0.48 T
	Harmonic number h	10	1
	Bucket acceptance	25 mrad	20 mrad
	RF voltage	70–120 kV	12 kV
	max. momentum acceptance	$\Delta p/p = \pm 5.10^{-3}$	
	Bunch length	250 - 300 ns	
	Transverse acceptances	$E_H = 40\pi \times 10^{-6}$ rad m; $E_V = 20\pi \times 10^{-6}$ rad m	

*) In most schemes of taking small batches of $\bar{p}$ from the AA, the particles may not stay long enough in the AA to undergo complete transverse cooling.

3.2.2 Protons and H^- for LEAR at 50 MeV

Protons and H^- ions come from the old linac. A loop (Chapter 4.9) will be constructed in order to transfer p and H^- from the Linac to the antiproton transfer line towards LEAR. Testing of LEAR with protons, and in the future with H^-, will thus be completely independent of PS operation (H^- will have the advantage to circulate with the LEAR elements in the same polarity as for antiprotons).

For the collider option, protons can also be taken from the Linac and a second anticlockwise injection path into LEAR is provided.

3.3 ULTRA SLOW EJECTION

The extraction of LEAR has two aspects:

- the transverse, which is similar in concept to other synchrotrons, i.e. a transverse resonance condition is set up for particles of a certain momentum which makes them jump across a septum and they are led out of the machine from there on;
- the longitudinal, which introduces a new method in order to guarantee a good duty factor during the unusually long spill i.e. the application of RF noise embracing the resonance over a limited bandwidth makes the spill rate insensitive to ripple.

3.3.1 The transverse aspect

It is proposed to use a third integer resonance and to install an electrostatic septum in SS11 (located inside the vacuum envelope), and a magnetic septum in SL1 (located outside the vacuum envelope). A further magnet with a thick septum will deflect the beam onto its final trajectory. The parameters of the ejection system are specified in Table 3.3-1.

The third integer resonance will be excited by the sextupoles foreseen for chromaticity correction. It is then important not to alter the adjusted chromaticity and to limit the additional sextupole strength required. This can be achieved by powering pairs of sextupoles (to each positive sextupole belongs a diametrically opposite sextupole of negative polarity). They are selected such that they contribute to the desired Fourier component. An example for such a repartition is given in Table 3.3-1. During extraction, particles of different momenta and betatron amplitudes are driven into the resonance simultaneously. Although they experience the same kick at the electrostatic septum and thus have the same separation at the magnetic septum, they do not (generally) arrive with the same displacement there. An analytic condition has been found to align the particles at the magnetic septum. It requires a particular ratio of chromaticity to sextupole excitation and contains the phase of the excitation as the only parameter to play with. For reasonable values of this phase, the chromaticity must be positive, thus chromaticity correction is essential since the natural chromaticity is negative.

Ejection appears straightforward at medium momenta. At momenta near 2 GeV/c, the deflection provided by the electrostatic septum is marginal as can be seen from Table 3.3-1. Only the ideal geometry (concerning septa position, bumps and chromaticity correction) avoids losses at the magnetic septum up to 1.98 GeV/c.

Another problem arises due to the large emittance of the beam at very low energy. Again, a positive chromaticity is favourable since the separatrix configuration as shown in Fig. 11a allows a tighter beam-septum spacing than that in Fig. 11b , which belongs to negative chromaticity and positive $\Delta Q = Q - Q_{res}$ (coming from above). At momenta below 0.3 MeV/c, cooling is indispensable.

3.3.2 The longitudinal aspect

The duty factor F of a spill with the low frequency structure $\phi(t)$ is given by

$$F = \langle\phi\rangle^2 / \langle\phi^2\rangle$$

For conventional extraction, when the beam is swept across the resonance with a speed v, we find $F = 2/3$ for $v = \omega r$ where r is the ripple and ω the ripple angular frequency, assuming one essential ripple frequency for simplicity and measuring v/ω and r in the same units, preferably in $\Delta p/p$. As r has a lower limit for technical reasons and $v \simeq a/T_s$ (beam width over spill time), it is clear that it is impossible to achieve a good duty factor with conventional extraction. The way-out is to embed the resonance by a noisy region [7] which makes the spill rather insensitive to ripple. v is replaced then by $v_\omega = \sqrt{2\omega D}$ (velocity of diffusion waves) so that $F = 2/3$ for $D = \frac{1}{2}\omega r^2$ which value may be taken as a lower limit for the required diffusion constant.

In addition, a method must be applied to drive the beam into the noisy region. The following proposal seems the simplest and has been tried successfully at the PS [8]. It consists of three steps (Fig. 12):

i) the beam is debunched and its distribution made rectangular by applying noise with carrier frequency at point X_1 and bandwidth ΔX_1 (Fig. 12a),

ii) the carrier frequency is tuned quickly to point X_2 and simultaneously the bandwidth is changed to ΔX_2 such that the low momentum edge of the noise coincides with the high momentum edge of the beam (Fig. 12b),

iii) the carrier frequency is tuned slowly, with speed $v = a/T_s$ (Fig. 12c).

The requirement for a constant spill rate imposes a few constraints on the choice of parameters. The density at the edge of the noise should remain small compared to the unperturbed density. As the corresponding ratio is given by $1 - \exp\left(-\frac{vb}{D}\right)$ we must have $vb \ll D$. Furthermore, there is also a lower limit for vb (or an upper limit for D). That comes from the inevitable intermodulation beyond the intended bandwidth. It depends in turn on the power level and the bandwidth and thus there is no easy expression to describe the degradation of the distribution function beyond the noise edge. But crudely one can derive an expression for the accessible spill duration T_s

$$\frac{1}{\omega} N \left(\frac{a}{r}\right)^2 \gg T_s \gg \frac{1}{\omega} \left(\frac{a}{r}\right)^2 ;$$

where N is the factor full power/intermodulation power. If D is increased significantly above ωr^2 this inequality becomes

$$\frac{Na^2}{D} \gg T_s \gg \frac{a^2}{D}$$

now with a smaller N and shorter time T_s.

For very large T_s, it will no longer be possible to meet the left hand part of this inequality. Then the low momentum "edge" of the distribution will be degraded. Here it should help to apply stochastic cooling (acceleration) and in this way extend T_s further. For T_s in the 10 s range, machine experiments at the PS have given encouraging results [8].

TABLE 3.3-1

Specification of extraction elements

- Electrostatic septum SE1 as specified in Table 4.6-1 (page 29)
Centre of SE1: 5.93 m upstream of middle of SL1; preferred radial position from axis : 55 mm (together with a 20 mm orbit displacement). Some typical data for various momenta:

Momentum (pc/GeV)	Field strength (MV/m)	Gap (mm)	Voltage (kV)	Kick (mrad)	Separation at SM1 (mm)
2	8.1	10	81	3.13	9
0.3	0.8	20	16	6.13	17.6
0.1	0.1	20	2	6.13	17.6

- Magnetic septa : SM1 and SM2 as specified in Table 4.7-1 (page 30).

- Sextupolar excitation
The phases of the 2 sextupoles XF in SL1 are $\pm \psi_1$ ($\psi_1 = 51.7^o$). If they and the 2 sextupoles XF in SL2 are powered with the strength K_s together with the 4 other XF in SL3 and LS4 of strength $-K_s$, the total excitation sums up to a strength $-4 \cdot \sqrt{2} \cdot \cos(3\psi_1) \cdot K_s = 5.14\ K_s$. The phase of the relevant outgoing separatrix in normalized phase plane at the electrostatic septum becomes 30^o (Fig. 11a). The jump size increases with the distance orbit - SE1, with K_s and the emittance. As an example: for a distance of 35 mm, $K_s = .202/m^2$ and 0 and 10 π emittance values, the jump is 6.5 mm and 8.2 mm respectively.

4. SUBSYSTEMS

4.1 Magnet

The dipole field is provided by four 90° sector magnets. Each sector magnet is made of six blocks. Each block consists of an upper and a lower core which are built of laminated steel. Two excitation coils cover the whole 90° sector (Fig. 13). A wedge-shaped gap in the center of each sector permits access to the vacuum chamber. It can be used to locate a jet target or other components. Half cores and coils will be delivered separately and will be assembled in their final position in the South Hall. A cross-section of the dipole is shown in Fig. 14. It is a C-magnet with the opening directed to the outside of the ring, which facilitates the layout for injection and ejection and the neutral beam lines. The main parameters of the magnet are given in Table 4.1.1.

A cross-section of the quadrupoles is shown in Fig. 15. The cores are made from stacks of glued laminations without end-plates. The main parameters of these quadrupoles are given in Table 4.1-2.

Superposed dipoles and sextupoles of the air core type will be used for closed orbit correction and chromaticity correction. Their magnetic length is 0.3 m, the maximum deflection and the sextupole strength at 2 GeV/c are $\theta = \pm 1$ mrad, $k' = \pm 2.6\ m^{-3}$. A cross-section of these magnets is shown in Fig. 15.

The power supply used to date for the ICE magnet (R5 type) will be used for the dipoles and two standard units of type R21 will be made for the quadrupoles.

TABLE 4.1-1 - LEAR DIPOLE - MAIN PARAMETERS

A. BASIC	
Aperture (useful field region) height x width	160 x 80 mm^2
Nom. field at 2.0 GeV/c	1.6 T
Bending radius	4.170 m
B. COIL	
Maximum Excitation current	4450 A
	2 x 12 turns
Conductor	33.5x33.5 mm^2
Cooling hole	11.5 mm
Current density	4.4 A/mm^2
C. MAGNET (4 quadrants)	
Resistance at nom. excitation	0.027 Ω
Inductance	0.1 H
Max.Diss. Power	530 kW
Weight copper	14
steel	226

TABLE 4.1-2 - LEAR QUADRUPOLE - MAIN PARAMETERS

A.	BASIC	
	Aperture (inscr. circle)	r_o = 73 mm
	Useful field width	± 100 mm
	Maximum strength at 2 GeV/c	$k = 1.8\ m^{-2}$
	Corresponding gradient	g = 12.0 T/m
	Magnetic length	ℓ = 0.5 m
B.	COIL	
	Maximum excitation (for $k = 1.8\ m^{-2}$ at 2 GeV/c)	I = 640 A
	Number of turns	N = 42
	Conductor	wxh = 13 x 13 mm^2
	Cooling hole diameter	d = 5.0 mm
C.	MAGNET	
	Resistance at 30°C	R = 0.032 Ω
	Inductance	L = 0.05 H
	Diss. power per quad. (for $k = 1.8\ m^{-2}$ at 2 GeV/c)	P = 13 kW
	Core length	0.438 m
	Total length	0.652 m
	Weight : copper	380 Kg
	steel	2800 Kg

4.2 Vacuum

4.2.1 Vacuum requirements

The residual gas has several effects on beams circulating in LEAR :

i) single Coulomb scattering leading to beam loss ;

ii) multiple Coulomb scattering leading to emittance growth ;

iii) stripping of H^- ions limiting the H^- life-time ;

iv) contribution to background when operating with internal beams.

These effects lead to the specification of an ultimate mean vacuum below 10^{-11} Torr and the concepts and procedures chosen, based on ISR practice[8a)], ought to be compatible with this goal. Nevertheless, a pressure one to two orders of magnitude higher can be accepted in the initial period of exploitation. It is also worth noting that emittance blow-up due to multiple scattering can be compensated by beam cooling techniques.

4.2.2 Chambers, flanges and gaskets

The vacuum envelope will essentially be made from AISI 316 LN stainless steep properly treated according to ISR standards. Con-Flat flanges with copper disc gasket will be used for the diameters up to 200 mm. Cu wire flanges are foreseen for larger diameters.

In the gap of the four bending magnets, an oval cross-section chamber (see Fig. 16) will fit between the poles of the magnet and will house in its central part pick-ups for horizontal stochasting cooling and orbit observation.

The chambers for the quadrupoles and free straight sections are less critical : some difficulties could be encountered for the large flanges of the tanks housing kickers and electrostatic septa. We intend to use the same Wheeler type flanges that have been used by AA group. This taking advantage of their experience.

4.2.3. Valves

Bakable all metal valves are still very delicate pieces of equipment, especially if they must be activated during bake out. For this reason the number of sectors will be kept to a minimum. Similarly, turbo-pump valves are also a problem but the experience being now obtained with the AA project will serve as a guide.

4.2.4 Pumping system

Evacuation of the vacuum chambers from atmospheric pressure down to 10^{-5} Torr will be done by rotary and turbomolecular pumps. The same pump groups will be operated during bake-outs for removing the gases liberated from the surfaces. The nominal pumping capacity of the primary pump will be in the range of 12÷15 m^3/hr and the pumping speed of the turbopumps in the region of 100÷200 l/sec. Sputter ion pumps of a nominal speed of 30 and 400 l/sec will be used. Their capability to pump also noble gases will supplement the 50 Ti sublimation pumps distributed around the ring.

4.2.5 Residual pressure measurement

Special ionisation gauges with no X-ray limitations in the region of 10^{-12} Torr will be used from the beginning. They are available on the market from different companies and a choice will be made after evaluation of the advantages of the 2 or 3 existing types. Two or three residual gas analysers will be installed in critical points of the machine. In addition, a number of Pirani and Penning type gauges will also be installed on the system. They are needed for controlling the pumping system during pump down and bake outs or in case of very large leaks.

4.2.6 Bake out

A baking at $300^{\circ}C$ for 24h is required to reduce the typical out-gassing of SS from 1×10^{-12} to $1 \div 2 \times 10^{-13}$ Torr l $sec^{-1} cm^{-2}$ as required for LEAR. The same technique as largely developed by ISR specialists and used for the AA vacuum system, will be employed.

Tubular elements of the chamber will be wraped with heating tapes and conveniently insulated. Thermocouples distributed around the circumference of the machine will control and monitor the temperature. Heating tapes will be doubled by spare ones. Tanks and other special shaped vacuum envelopes will be surrounded by special heating jacket.

Power installed for tubular element is of the order of ~ 0.6kW per meter of chamber and of the order of $1.2 \div 1.3$ kW per m^2 of tank surface. With this power a gradient of $50^{\circ}C/h$ is easily obtainable.

4.2.7 Control

The controls philosophy of the vacuum system will be to have as much as possible self-protected and autoregulated equipment. Control circuitry will be such that in case of mains failure or any other fault in a part of the installation the system will react automatically in order to prevent major damage, making intervention by an operator or a computer unnecessary. Parameters like residual pressure, status and controls of valves and pumps will be available at the Linac PDP computer. As a first estimate about 200 bits for status acquisition, 180 bits for control and 115 analog signals will be used. This controls equipment will be installed in about 20 racks.

4.3 RF

The acceleration cavities must fulfil the following specifications :

I) The frequency range needed is .4 MHz to 4 MHz. If the available ferrite cannot cover this range, it is possible, though less convenient, to accept a reduced range from .8 MHz to 4 MHz (i.e. between .2 GeV/c to 2 GeV/c), and a mechanical switch to cover the total deceleration domain down to .4 MHz (.1 GeV/c).

II) The accelerating voltage should be at least 12 kV.

III) There are two possible options which define the cavity length :

a) two cavities each one 1.5m long between flanges ;

b) 1 cavity 2.5m to 3m long between flanges.

No restrictions on the cavity diameter.

IV) The beam should see a low cavity impedance, say 50 Ω. Strong feedback has to be applied at the power amplifier.

V) High vacuum bakable beam pipes, no appreciable radiation damages.

Ferrite loaded cavities [9] will be used. A capacitor could be connected across the gap for deceleration in order to reduce the tuning range. The present market situation concerning ferrites is being investigated. Special ferrites for low frequency duty appear still to be lacking despite the demand from several accelerator projects.

Table 4.3.1 gives a set of tentative parameters pending the final choice of ferrite. Fig. 17 gives a tentative circuit layout.

The low-level beam control system can largely be based on our existing machines.

Table 4.3-1 : Tentative parameter list

Harmonic number	1
Frequency range	0.4 to 3.5 MHz
Ferrite type	8C12 Philips
Total number of rings	76
Maximum voltage	12 kV
Maximum RF power	40 kW
Installed power	100 kW

4.4 Controls

A preliminary survey of the LEAR project shows that we have to handle up to 400 parameters.

4.4.1 Computer

It has been decided to connect the LEAR controls to the DEC PDP 11/45 back-up computer of the New Linac control system [10]. This computer has 128 kword of memory and runs under the RSX-11M operating system. Apart from emergency situations, it will be possible to run the LEAR and Linac processes on separate computers. We can profit from the ten man-years of effort which has been put into the development of control software for the New Linac (R2), and the experience of more than one year of continuous operation.

For the development of application programs, the user has at his disposal several high level languages, such as Fortran, Pascal and Basic. In any of these languages, the user program is linked to the control system by the specification of three buffers : a parameter name list, a data buffer and an error buffer. These facilities were appreciated by the physicists and engineers involved in writing beam measurement programs and setting-up procedures for the New Linac.

4.4.2 Consoles

We intend to run LEAR from the same console as the one presently being used for the New Linac operation. This console is heavily occupied only at the startup of the Linac, - when normally LEAR will not work -, and is thereafter practically deserted, until problems develop in the Linac operation.

The Linac main console permits up to four operators to work in an independent manner. It will be so arranged that the operator can, by selection with touch buttons, work either on the LEAR or the Linac process. Following the initial selection, his future work will automatically be directed to the computer handling the process he has selected.

Remote consoles, equipped with a colour TV display, a touch panel, and a video terminal, will be available in the equipment room of LEAR, and, at a later stage, for the experimental teams.

4.4.3 Interface equipment

The LEAR process and the Old Linac will be connected to the computer over a separate Serial CAMAC Highway (Fig. 18). We expect to use about eight CAMAC crates for LEAR and two for the Old Linac. Local intelligence might be needed in some CAMAC crates, e.g., for function generators.

4.4.4 Operation

The operator will be able, with the help of touch buttons, to select any four parameters from the LEAR process for simultaneous display and command. A log-in procedure makes the system "busy-set" the parameters selected for command, so that two users cannot attempt to control the same parameters. Synoptic displays will be prepared, giving the operator an overall view on the colour TV display of a sub-system, such as a beam line or the vacuum system. For the latter, a scheduled task will come in at regular intervals to read gauge pressures into a computer file, which afterwards may be used to produce a display of the evolution of the vacuum in LEAR and its beam lines.

For quick setting of a whole group of parameters, such as the focussing elements of a beam line, a facility known as LIP, the LIst Processor (R3) is available. A computer file with a Name List and a corresponding Value File are both linked to a touch button. Pressing this button, after a log-in, switftly sets up to one hundred parameters. Using the same Name List but different Value Lists, the user can prepare several different settings in advance with separately named touch buttons to help his choice.

Programs for different logs exist already. Only a computer file with the Name List of the desired parameters has to be prepared.

Two analog stations are available on the Linac main console. Up to four parameters can be selected with touch buttons and displayed on two double beam scopes. The bandwidth for the analog transmission is 5 MHz.

4.5 INSTRUMENTATION

A set of beam diagnostic devices is foreseen for the machine itself, the transfer lines from PS and Linac into LEAR, and for the ejection channel. The general layout (Fig. 3) shows the distribution of the main measuring equipment in LEAR.

Wherever possible places in the vacuum chamber in the bending magnets and quadrupoles are used in order to keep long straight sections free. On the other hand, one adopted the standard equipment used in the PS, developed for AA or experimented in ICE. The equipment has to be adopted for the very low intensity in LEAR, and some special new measuring devices have to be developed.

4.5.1 Eight electrostatic position pick-up electrodes will be installed in the second and fifth block of each magnet for radial and vertical orbit measurements.

Standard P.U. will also be placed in the transfer lines. A set of independent Schottky noise pick-up electrodes will be installed in the vacuum chambers inside the quadrupoles.

4.5.2 Scintillator screens and TV's, with special vidicon and image intensifiers, will be placed at adequate places in the transfer line and in LEAR for desctructive beam observation. A beam scraper inside one of the LEAR magnets will be used to measure beam size and also to serve as an internal dump.

4.5.3 A low intensity beam transformer has to be developed for the machine to measure the circulating intensity ; in the transfer lines one can use more standard transformers.

4.5.4 A non-destructive beam profile monitor using electrons from ionization of residual gas by the beam is envisaged. The low intensity and the low local pressure seems to put this equipment near the technological limit and perhaps one will be pushed to use a kind of gas curtain based on the jet target development.

4.5.5 Secondary emission grid chambers will be developed to be installed near the PS septum 26 in the transfer line, and for measurement during the first turn in the machine.

4.5.6 A special beam measurement line will be installed in the dump line, in which standard measurements are foreseen with the fast extracted beam.

4.6 The Electrostatic Septum

The design of the electrostatic septum (SE1) for LEAR is to some extent inspired by the SE's installed in the PS for the slow ejection and the continuous transfer. However, certain conditions specific to LEAR, have made it necessary or possible, to introduce some important changes in the design of this new SE , namely :

- operation in ultra high vacuum ($\sim 10^{-9}$Pa, i.e., 10^{-11} Torr),
- reversible polarity on the high voltage electrode, for both p and $\bar{p}$ operation,
- low beam intensity, three orders of magnitude lower than in the PS.

In these conditions using our standard oxide-coated Al alloy high voltage electrode is not possible. On the other hand screening the HV electrode against beam-produced ions is not necessary.

The SE1 is presented in Fig. 19 (cross-section) and Fig. 20 (longitudinal section). On the C shaped grounded electrode a 0.1 mm molybdenum foil is stretched which acts as the septum facing the titanium high voltage electrode. The latter can be connected by the HV feedthrough to a 300 kV generator, either positive or negative. Titanium potential deflectors are mounted on the feedthrough bushing and the stand-off insulators of the HV electrode. The positions and angles of both electrodes with respect to the axis can be remotedly adjusted, using computer-controlled motorized micrometric supports.

With the length of 860 mm available for the SE1 the equivalent length of the electric field is about 700 mm. The field strength in operation will be at least 8 MV/m across 1 cm and 6 MV/m across 2 cm for both polarities. In Table 4.6-1 (p. 29) the mechanical parameters of the SE1 are given.

The polarity of the SE1 cannot be changed instantaneously. The HV cable must be moved from one generator to the other and then the SE1 must be reconditioned in the other polarity. According to the performance which is expected in this new polarity, the total time requested may vary from half an hour to several hours.

TABLE 4.6-1 MECHANICAL PARAMETERS OF SE1

1. The tank

Total length between end flanges	860 mm
Material : 316 L+N stainless steel	
The SE1 will be designed for a 300°C bakeout under vacuum	

2. The septum electrode

The C shaped frame is made of 316 L+N stainless steel		
Inside dimensions	width	125 mm
	height	70 mm
The 70 mm high septum is made of a 0.1 mm molybdenum foil stretched on the C shaped frame		
Adjustment of the septum foil position, from axis at the upstream support		45 to 65 mm
Resolution		0.05 mm
Adjustment of the septum angle with respect to axis, by adjusting the downstream support		-8 to +2 mrad
Resolution		0.1 mrad

3. The high voltage electrode

Polished round-edged titanium bar, withstanding high voltages of both polarities	
Adjustment of the active face position, from axis at the upstream support	50 to 85 mm
Adjustment of the angle with respect to axis, by adjusting the downstream support	-8 to +2 mrad
The HV feedthrough is at an angle with the horizontal plane, so as to leave clearance for the injected beam.	

4.7 Injection/Ejection Septum

The principle adopted is to use a common thin magnetic septum SM 1 for both injection and ejection in SL1, and to add a second thicker septum (SM2) to give an additional deflection to the ejected beam.

SM1 is optimized in thickness, length, and position in SL1 from the following considerations :

- angles of injected and ejected beams given by width of the quadrupole and the kicker located in the same straight sector (Fig. 21)
- phase relation between electrostatic septum ES and EM1.
- thickness compatible with the shadow cast by the ES
- strength of the kicker.

The main parameters are indicated in Table 4.7-1. The septum magnets consist of C-shaped cores with watercooled coils and are located outside the vacuum. The coil must be dismountable to allow baking of the vacuum chamber; coil and core are therefore made of symmetrical halves which can be withdrawn in vertical direction. The magnetic screen is incorporated in the vacuum chamber.

TABLE 4.7-1 - TYPICAL SEPTUM PARAMETERS

		SM1	SM2
Kick at injection		175 mrad	
Kick at ejection		52 mrad	26 mrad
Max. amper turns	NI	∿22000 AT	∿ 30000 AT
Max. magnetic flux density	B	∿ 0,45 T	∿ 0,5 T
Apparent thickness		9 mm	30 mm
Cu thickness		5,3 mm	22 mm
Total length		0.9 m	0.4 m
Gap height		55 mm	75 mm
Magnet aperture		150 mm	180 mm
Center position (from middle SL1)		- 1,8 m	+ 0,7 m

4.8 INJECTION KICKER

The injection kicker is a two-module device mounted within the machine vacuum and which follows closely the principles already employed for the PS full aperture kicker and the AA injection kicker. Each module is a delay line magnet of 16 cells and characteristic impedance of 15.7 Ohms. The excitation pulse is derived from a pulse generator of standard PS design, employing gas pressurized coaxial cable and thyratron switching. Pulsed resonant charging is employed, the charging time being approximately 3 ms and the maximum charging voltage 80 - 85 kV. A current inversion switch is foreseen for each module, mounted directly on the atmospheric side of the injection kicker vacuum tank, which will permit kick polarity reversal by remote actuation.

The injection kicker is designed to withstand in situ backe-out, subject to the prior disconnection of its pulse cables, to a temperature of 300°C. Previous experience suggests that an injection kicker tank pressure of 10^{-11} Torr will be possible.

A kick strength of 10 mrad for a 0.6 GeV/c beam is guaranteed for each module with 5/95% rise/fall times of 100 ns. Absolute kick ripple, both on the flat top and after the pulse fall, will not exceed 2¼% of the nominal strength.

A summary of mechanical, electrical and magnetic properties of the injection kicker system is contained in Table 4.8-1 and Fig. 22 is a section through the magnet module.

TABLE 4.8-1 : LEAR INJECTION KICKER MAGNET PARAMETERS

Mechanical	Number of modules	2
	Horizontal aperture	150 ± 0.5 mm
	Vertical aperture	66 ± 0.5 mm
	Module overall length	468 mm
	width	565 mm
	height	850 mm
	Module weight (approximately)	450 kg
	Inter-module spacing	≥ 20 mm
	Max. bake-out temperature	300°C
Electrical and Magnetic	Number of cells per module	16
	Ferrite weight per module	43 kg
	Ferrite surface area per module	1.31 m^2
	Characteristic impedance	15.7 Ω
	Wave propagation delay	≃ 83 ns
	Module $\int Bd\ell$ for 80 kV PFN voltage (maximum value)	207 Gauss.m
	Corresponding kick strength for 0.6 GeV/c beam	10.3 mrad
	Kick rise time 5/95%	94 ns
	Kick fall time 95/5%	100 ns
	Flat-top kick ripple	2,2% absolute
	Kick ripple after pulse fall	2.0% absolute
	Gap flux density	480 Gauss
	Maximum ferrite flux density	2800 Gauss
	Remanent $\int Bd\ell$ per module	0.4 Gauss-m
	Kick pulse length	100-700 ns
	Kick polarity	± by motorized switch

4.9 STOCHASTIC COOLING

4.9.1 The need for cooling

As the cooled beam from the AA is used, the initial operation of LEAR does not have to rely on transverse cooling. It is, however, advantageous to install some momentum cooling from the beginning as this system can be used to assist the ultra-slow extraction (cf. section 3.3).

During deceleration, both the momentum spread and the transverse emittances increase. In fact, the bunched beam momentum spread may be written as

$$\frac{\Delta p}{p} = \pm \frac{A}{8 B_f \beta\gamma} \simeq \pm 1.8\ 10^{-3}/p \left[\mathrm{GeV/c}\right] \qquad (1)$$

where a bunch area of 12×10^{-3} rad was assumed and a bunching factor (defined here as bunch length/circumference), $B_f = 0.8$, was taken. In the stretcher mode, the momentum acceptance of LEAR is of the order of 1% but a large fraction (at least ½) of this has to be reserved for the extraction process.

Bearing this in mind one concludes from (1) that momentum cooling is necessary for stretcher operation below, say, 0.35 GeV/c.

In a similar way, both the horizontal and vertical emittances increase as 1/p during deceleration. Assuming $E_H = 30\ \pi\ 10^{-6}$ rad m $E_V = 15\ \pi\ 10^{-6}$ rad m at injection, the vertical emittance will meet the bare acceptance limit at about 0.2 GeV/c and the horizontal one grows to the aperture limitation at about 0.1 GeV/c . For clean deceleration, it is important to stay sufficiently far from these limits.

We may thus conclude that the first system needed is a momentum cooling system and that vertical and later horizontal cooling are essential for clean deceleration below, say, 0.3 GeV/c.

In addition, stochastic cooling will be useful in the options (jet target and collider), or if a very sharply collimated beam is to be extracted for special experiments. Anyway, cooling in all three planes can compensate beam degradation due to insufficient vacuum, high order resonances and beam mishandling

4.9.2 A simple system

The implementation of a simple stochastic cooling system is given in Fig. 23. The critical elements are the pick-up stations which have to be long (1 to 2 m) to obtain a good signal to noise ratio. Three pick-up stations (similar in conception to those used in ICE) are foreseen: one for Δp cooling (in SS41), one for vertical cooling (SS12 extending into the quadrupoles QF 12, QD 12), and the one for horizontal cooling (centre of magnet BH 4).

In a first stage, cooling will be limited to injection energy and short kickers (20 cm long) will be installed in SS21 and SS22 . At a later stage, when cooling at higher energies becomes desirable, auxiliary kickers would be installed in SS31 and SS32 to permit a diagonal signal path at particle velocities close to c where the correction needs an efficient short-cut to catch up with the particles. At lower energies, it is advantageous to have the shorter signal path in order to avoid particle mixing between pick-up and corrector. This is especially important for the two transverse systems because of the high frequency band adopted. For momentum cooling the diagonal path will probably be adequate at lower energies as well.

Note that the proposed implementation uses only the "cheap" space available in the magnets and in the short straight sections but that none of the long sections is touched. Also the correctors are made very compact at the expense of a somewhat higher power requirement for the final amplifiers and a high frequency band has been chosen for transverse cooling to keep the pick-ups ($\ell = \lambda/4$) short. All phase advances have been optimized for the stretcher mode. For some options (jet, $H^- - \bar{p}$) where a different horizontal tune is preferable, it may be advantageous to add a horizontal corrector and a pick-up.

Experiments in ICE have established the possibility of bunched beam cooling provided that the bunches are long [11]. It will thus be necessary to reduce the RF voltage as Δp cooling progresses, in order to keep the bunch long, but the more delicate operation of complete debunching and recapture after cooling can hopefully be avoided. As the off momentum function is large, mixing persists when Δp is effectively cooled and transverse and longitudinal cooling can work simultaneously One notes from Table 4.9-1 that, with the "ICE type system", times of, say, one to two minutes are needed to effectively precool the beam at injection.

TABLE 4.9-1

STOCHASTIC COOLING AT 0.6 GeV/c

1) Momentum cooling (filter system)

Number of pick-up gaps	16
Length of pick-up station	0.6 m
Number of correction gaps	2
Length of corrector	0.2 m
Pass-band*	20 - 220 MHz
Lower/upper revolution harmonic *	10 / 110
Electric length of filterline	72 m
Preamplifier noise figure	3 dB
Number of particles	10^9
Initial momentum spread assumed	$\pm 2.5 \times 10^{-3}$
Off momentum function $\eta = \frac{1}{\gamma_t^2} - \frac{1}{\gamma^2} = -\Delta f/f / \Delta p/p$	-0.72
Optimum electronic gain	10^6 (60 dB)
Initial cooling time constant	∿ 0.5 min
Increase of central density of Δp distribution after 1 min cooling	∿ 6.0
Corresponding decrease of momentum spread (at 10% height of distribution)	∿ 4.0

2) Vertical cooling system

Number of pick-up loop pairs	8
Length of pick-up	2.0 m
Number of kicker loop pairs	1
Length of corrector	0.1 m
Pass-band	250 - 750 MHz
Lower/upper revolution harmonic	125/375
Preamplifier noise figure	3 dB
Initial emittance assumed	$20\ \pi\ 10^{-6}$ rad.m
Emittance after cooling time of:	
- 1 min	$7\ \pi\ 10^{-6}$ rad.m
- 2 min	$4.2\ \pi\ 10^{-6}$ rad.m

A similar system is foreseen for horizontal cooling. Damping times are shorter since space is available for more pick-up loops.

---

* The alternative of a higher frequency band (∿ 150 - 400 MHz) is under study.

More details of the computed performances at 0.6 GeV/c are given in Fig. 24-26. Fig. 24 shows the evolution of the longitudinal density assuming an initially rectangular distribution of the number of particles vs. momentum. The initial width was taken to be $\Delta p/p = \pm 2.5 \times 10^{-3}$.

Fig. 25 and 26 refer to vertical cooling. For a detailed simulation of vertical and horizontal cooling simultaneously with momentum damping, the evolution of the longitudinal distribution (Fig. 24) has to be included into the calculation of the transverse heating by Schottky noise. As a simplified model we have inserted only a parabolic momentum distribution with a width of $\pm 1.25 \times 10^{-3}$, constant in time. It approximates circumstances after some momentum cooling but neglects the change in time of the beam energy spread. Fortunately this is not very critical in the present case as the Schottky noise is dominated by the amplifier noise.

In transverse phase space, an initial emittance of $20\,\pi \times 10^{-6}$ rad.m was assumed for all momentum bins of the beam, emittance being defined here in terms of the rms oscillation amplitude σ_V by $E_V = \pi(2\sigma_V)^2/\beta_V$. The evolution of the emittance is given in Fig. 25 . Note that the gain of the cooling system is reoptimized every 40 s. More details of the vertical cooling process are given in Fig. 26 . It shows the computed signals which would be observed at a Schottky band near $(n \pm Q_V)f_{rev}$ i.e., the evolution in time is given of the rms amplitude of particles in the momentum bin at $p \pm dp$ as a function of p. The beam emittance of Fig. 25 was obtained as $4\pi/\beta_V$ times the mean square oscillation amplitudes averaged over the momentum distribution.

All figures refer to the case of an unbunched beam but similar results are expected for long bunches.

4.9.3 Future possibilities

More advanced systems using for instance "travelling wave pick-ups" at lower energy and/or techniques permitting cooling during deceleration (continuously or in steps) can be developed and installed at a later stage. The coexistence of electron and stochastic cooling, which are to a large extent complementary, will open interesting possibilities.

For the collider mode, where very strong cooling is needed near the top LEAR energies, an extended stochastic system needing more space than the "poor man's version" described above will be desirable, together with an electron cooling device working at momenta up to 2 GeV/c.

4.10 Beam transfer lines PS - LEAR and LINAC - LEAR

The general layout is shown on Figs 1 and 2. The main functions of the transfer lines are :

- the transfer of fast-ejected $\bar{p}$ from the PS, at a fixed momentum of 600 MeV/c ;
- the transfer of 50 MeV particles (protons or H^- ions) produced by the old linac ;
- the injection of these particles into LEAR straight section SL1 and, at a later stage, the injection of protons into straight section SL4.

The transfer lines are designed to convey transverse emittances of 40π and 20π mm.mrad respectively in horizontal and vertical planes with a momentum bite of ±0.5 %. The use of the old linac as an injector for the PS (protons and ions) remains possible.

Existing equipment (beam transfer elements, power supplies) will be used as far as possible.

4.10.1 The PS ring area

Antiprotons will be fast-ejected from SS26 by a new septum magnet, designed also to inject into the PS ring 50 MeV particles produced by the Linacs. The new $\bar{p}$ transfer line will be parallel to the old Linac in its first part, before entering the tunnel (see 4.9.2).

A special 180° loop [12)] is designed to inject 50 MeV p^+ or H^- from the old linac. The loop consists of four bending magnets (2x107° and 2x17°) and five quadrupoles arranged in such a way that the system is symmetric, achromatic and maintains the transverse phase planes unchanged. The design of the C-shaped bending magnets is under study. Four new quadrupoles are also required ; these will be of the Linac Q7 type with pulsed power supplies.

Some modifications in the PS ring area will be necessary in order to accomodate the new transfer lines (turning MU 24, pumping station in SD23 to be moved, IB21 magnet and vacuum chamber to be modified, a few changes in the Linac beam lines, etc.).

4.10.2 The tunnel

A new 50 m long tunnel will be excavated between the PS ring and the South Hall. A 19^{o} bend in the downstream part of the Linac no. 1 area leads the transfer line to the beginning of the tunnel whence it follows a straight line to the South Hall. The rectangular cross-section of the tunnel (2.60×2.40 m^2) has been defined in order to accommodate PS standard quadrupoles with the passage of other beam transport elements just possible.

The LEAR ring in the South area being 1.66 m above ground level (0.40 m more than usual), the tunnel will have a slight slope of 10 mrad. The tunnel construction should be carried out during the next long PS shutdown (August - October 1980).

4.10.3 The injection part

The final position of LEAR has been determined together with the users of the machine in order to provide appropriate flexibility for experiments and further developments. Large bends ($\sim 45^{o}$) close to the machine are necessary to inject particles into LEAR straight sections 1 and 4; they make matching between the optical parameters of the transfer line and of LEAR difficult (mainly αp).

The beam is injected into LEAR with a large aperture septum magnet (deflection 155 mrad), followed by a full aperture kicker magnet (deflection $\simeq$ 20 mrad) placed in straight section SL1.

Injection of protons from LINAC 1 in SL4 is planned, but not in the first stage of the project. (It will be used for p-$\bar{p}$ collisions.)

4.10.4 Beam observation

The instrumentation required for setting-up and control of the transfer lines must be studied. The intensities concerned being of the order of 10^7 - 10^9 particles per pulse, one can envisage the use of transformers, TV screens with image intensifiers, and/or secondary emission monitors for the higher intensities. The interactive monitors will be required to work in a very good vacuum and will be retractable.

4.11 Experimental area layout

Fig. 2 shows a very preliminary layout, possible as far as the optics are concerned, but which will be subject to further discussions and studies together with the users.

The area can potentially, budgets permitting, accommodate several experiments. This model layout (Fig. 2) provides four locations for large-size experiments of which two can receive beam simultaneously ; it will be difficult to accommodate more such experiments within the given dimensions of the South Hall and also the use of more than one splitter magnet does not appear possible.

Another way to increase the yearly throughput of experiments would be to provide for the exchange en bloc of one experiment having taken a set of data, against another one, while data treatment is underway. These experiments would have to be assembled on a platform on rails or rollers so that they can be moved fairly easily. ("Storage" locations would however have to be found.)

A neutral beam from SS1 for the $(p\bar{p})$ experiment and experiments from internal targets could be accommodated along the lines indicated in Fig. 2.

The $\bar{p}$ ejected from LEAR at 78 mrad may be directed to a dump or a measurement line, or switched to the external beam line where they are divided into two branches by a simple splitter magnet giving a deflection of at least 120 mrad. Two vertical steering magnets placed in front of the splitter magnet allow the intensity in each branch to be adjusted between 0 and 100 % with low losses. Each branch may feed two experiments alternatively.

Special instrumentation (i.e., retractable proportional multi-wire chambers) will have to be provided for beam observation.

The vacuum system (no window between LEAR and the ejected beams) will be made of pipes (stainless steel close to LEAR, aluminum downstream) with metallic seals, pumped by turbo-molecular and ionic pumps and a few sublimation pumps are planned in the ultra-high vacuum part close to the machine.

4.12 SHIELDING

4.12.1 Shielding layout

The layout (Fig. 1) shows the LEAR shielding for the first stage of operation. The shielding enclosure consists of concrete walls (1.60 m thick) joining on the North side the shielding of the PS machine. The shielding wall will reach a height of 5.60 m (East and South) and 4 m (West). This avoids a "direct view" of the LEAR machine from the upper floors of the South Hall, but allows use of one of the cranes for construction work and modifications. Access to the gangway outside the South Hall between MCR and Booster will not be possible.

No roof concrete shielding is envisaged for the first stage but the machine is positioned so as to allow for additional shielding blocks to support a roof which may be required for future options.

Concrete blocks for the shielding walls will be made available by dismantling the ICE shielding.

4.12.2 Basic assumptions

The LEAR shielding is based on the estimations in Ref. 13 and on recent experience with the ICE machine. The following assumptions are made for LEAR operating during the first stage of exploitation:

- LEAR can be tuned for momenta up to 2 GeV/c,
- the $\bar{p}$ intensity in LEAR will be $\leq 10^9$ particles per 500 s.
- protons (used for setting-up) or H^- (used for tests) are injected with intensities $\leq 10^{11}$ particles/s for short periods only .

With these assumptions, beam losses during p or H^- operations determine the radiation situation. Adequate lateral shielding* can be provided. Therefore, the most stringent limitations are given by sky-shine due to the absence of roof shielding. The shortest distance from LEAR to the CERN boundary is about 100 m. A total dose of 100 mrem/year at the fence should not be exceeded. Monitors will be provided to survey the top of the chimney-like shielding.

4.12.3 Beam dump

The dump line (see Fig. 2) of the beam is inside the LEAR enclosure and directed towards the PS wall. It is shielded by 80 cm iron and 160 cm concrete before the end-stop (iron).

---

* It is assumed that in LEAR section 1 (injection and ejection section) larger losses may occur than in other LEAR sections. However, the C-shaped yoke of the magnet provides shielding for higher energy particles, and in addition the boundary along section 1 is the PS machine shielding. In other sections of LEAR the situation is less favourable, since the C-shaped magnet is open to the outside. However, the shielding may be reinforced by iron at beam level.

5. BUDGET, STAFFING AND PLANNING

5.1 Budget

Every effort has been made to reduce the material budget for LEAR to the strict minimum. The estimate given in Table 5.1 is based on the availability of the infrastructure of the PS South Hall and the use of existing beam transport magnets and power supplies. Particular items concerned are beam transport equipment of the external proton beam leading to ICE and the (ex-Gargamelle) power supply now used for the ICE magnet. In this spirit, it has also been decided to link LEAR to the Linac control system, which leads to a substantial saving in hardware and software.

The budget is expected to suffice for the construction of a first version of LEAR, with the capability of an accelerator/decelerator and beam stretcher, and including the beam transfer lines into LEAR and the external beam line up to the beam dump, though certain refinements (e.g. more refined instrumentation) are not included in the project budget. Owing to the strained manpower situation in the division, a sizeable fraction of the budget must be reserved for temporary and contract labour. No money is included for the experimental areas nor the preparation of any of the options.

Table 5.1-1 : LEAR BUDGET

Dipoles and quadrupoles	2'100 KFS
Power supplies for above (including installation)	700 KFS
Correction magnets (including power supplies)	500 KFS
Fast kicker	250 KFS
Electrostatic septum	300 KFS
Magnetic septa	600 KFS
RF system	550 KFS
Data acquisition system	550 KFS
Beam diagnostics + stochastic cooling	500 KFS
Injection line (PS + Linac to LEAR)	300 KFS
Injection line tunnel	500 KFS
Vacuum system (including pick-up electrodes integrated into chamber)	1'700 KFS
General installations	700 KFS
Temporary and contract labour	1'400 KFS
	10'650 KFS

Aspects of the layout of the experimental area, including the number of simultaneous experiments, the possibility to use beam transport elements from closed-down low energy accelerators, and its cost, are still being investigated. A proposal will be submitted before the end of 1980.

5.2 Staffing

It is not intended to create a special group responsible for this project; rather there will be a very small nucleus of staff who will co-ordinate the contributions from the various teams of technical experts. The total effort required is estimated at 65 man-years of CERN staff for the construction period 1980-1982. Almost 30 man-years of contract labour will be financed from the material budget.

5.3 Planning

The construction planning showing the shortest technically possible construction time for LEAR is given in Fig. 27. Basic elements in the planning are the shut-downs of the PS (for the injection tunnel and beam installation) and the estimated delivery of the magnet, for which the tendering is already under way. The schedule is quite tight for some of the necessary subsystems and that is even more so as the teams involved have responsibilities towards the AA project which obviously has priority over LEAR.

Concerning the options, attention should be given to the substantial delays occurring between the approval of a major development and its implementation in the machine. It is obvious that no more than one of the options can be implemented before 1985.

6. OPTIONS

6.1 Electron cooling

An electron cooling system installed in LEAR can be useful in many ways.. Depending on the operating conditions of the machine (average pressure, etc.) it can be used to increase the beam lifetime and to decrease beam emittance and momentum spread for special experiments *). It is specially important for jet target operation when high luminosity is required, and for the $\bar{p}H^-$ and the $p\bar{p}$ collision options (see Chapters 6.3 and 6.4). Below, design parameters are given for a cooling system corresponding to the requirements of experiments with LEAR. The possibility to adapt the ICE system [14], as a first step, to LEAR is being studied at present.

General parameters [15]

The layout of the cooling arrangement will be similar to the one in ICE [16a]. The assumed interaction length would be preferred. The beam diameter will be 2.5 cm. Using spacecharge limited operation with a perveance of 10^{-7} $AV^{-1.5}$, the electron gun would work as shown in the table (transverse cooling time scaled from ICE [16b]).

(anti-)proton momentum (MeV/c)	kinetic energy (MeV)	e-gun voltage (kV)	current (mA)	transverse cooling time (s)
100	5.3	2.9	15.5	35
310	50	27.2	450	2.8
600	175	95	2950	1.5

These values permit operation at all energies below injection energy (for target thicknesses between 2.10^{-11}g/cm^{-2} at 175 MeV). We keep the option of changing the perveance of the gun remotely by modifying the potentials of the gun electrodes.

Cooled beam characteristics

The equilibrium beam radii (rms) at an average pressure of 10^{-11} mbar are smaller than 1 mm, and with the H_2 jet target in operation they will be 2 to 5 mm with target densities as quoted above. The corresponding $\Delta p/p$ could be smaller than 10^{-4}.

Construction

The gun will use the classical pierce geometry with a flat cathode immersed in the solenoidal field. Space-charge limited operation is preferred as this should give a better electron beam quality even if the emissivity of the cathode is not constant over its surface. The ICE gun can serve as a model but attention must be paid to degassing and better cooling of the electrodes in order to achieve higher voltage holding.

Solenoid

For the solenoid and the toroides a construction similar to ICE can be used, with an increase in the toroid angle up to 45 degrees in order to keep the length of the overall assembly down. The field level at full gun voltage will be around 1 kG. The effect of the toroidal fields on the circulating beam has to be corrected for by auxiliary dipoles.

Collector

If the present tests on the ICE gun and collector to achieve higher voltages are successful this design could be used. Otherwise, deceleration inside the solenoidal field could be envisaged with a small reacceleration afterwards to stop backstreaming secondary electrons. Special precautions are needed on the collector surfaces to minimize the quantity of backscattered electrons which might outgas the anode structure and upset the high voltage.

Instrumentation

In view of the complexity of the system proper diagnostics are vital. We need to know exactly the characteristics of the electron beam, because final adjustments of different parameters will be essential to achieve the desired beam quality. In addition, the cooling performance of the e-beam on the $\bar{p}$ (or p, H^-) beam must be measured accurately.

e-beam diagnostics

Some measurements will be made with conventional means like screens, crossed wires or miniature Faraday cups. For these measurements the beam may be limited in pulse length or energy. Some measurements will be performed using a small e-gun, mainly to establish beam trajectories.

In addition, the transverse and longitudinal temperatures and the sensity distribution of the e-beam must be monitored. For the transverse temperature the best choice seems to be to measure the synchrotron radiation emitted by the spiralling electrons with a system similar to that used in ICE [17]. The longitudinal temperature and the density distribution of the e-beam can be obtained from measurements on the backscattered light of an infrared laser beam [16].

It must be stressed that both methods are important especially as for normal $\bar{p}$ operation there will be no neutral beam available for checking the cooling efficiency.

Circulating beam diagnostics

The cooling process of the circulating beam in the radial dimensions should be measured with a profile monitor and in the longitudinal dimension it should be observed by Schottky pick-ups in conjunction with a spectrum analyser.

In addition, protons must be available for test purposes (this requires inverting the LEAR fields). Provision has to be made for observation of the atomic hydrogen beam that comes then out along the straight section. It has also been pointed out that cooling of H^- would be feasible (at least for $\Delta p/p < 10^{-3}$). Naturally this does not directly produce a neutral beam, but a neutral beam for diagnostic purposes could be obtained by stepping the e-gun voltage within a short time up or down in order to strip the second electron of the H-ion .

6.2 Gas jet targets

Internal gas jet targets are required for several experiments [18) proposed for LEAR. While giving a very good definition of the interaction energy they permit at the same time a very efficient use [19) of the available $\bar{p}$ Particularly when used in conjunction with phase-space cooling which compensates the beam blow-up due to multiple Coulomb scattering, internal targets will yield the maximum luminosity for a given beam.

It is proposed to use a gas jet (polarized or unpolarized) as interaction target of experiments installed in a straight section (SL2) where the beam size is depressed by a set of additional quadrupoles (Fig. 3). As a source of antineutron beams a jet can be installed in the center of a magnet sector (Fig. 3) in order to improve the useful solid angle at the $\bar{n}$ experiment.

6.2.1 Unpolarized targets

The required target densities [18), 19) between 10^{-11} and $5 \cdot 10^{-9}$ g/cm^2 can be produced by a condensed molecular beam as developed by the group at the Kernforschungszentrum Karlsruhe (Ref. 20)). A target of this type is being built at CERN in view of a possible use as an internal target for the SPS [21). The principle of the condensed molecular beam is shown in Fig. 28 (from Ref. 20)). The gas enters with an input pressure p_o (a few atmospheres) and temperature T_o (about 20 to 30^{o}K). After the throat of the nozzle (diameter $\sim$ 0.1 mm) the gas expands adiabatically, decreasing in pressure and temperature, until saturation condition is reached. Small clusters are formed soon after, and grow as long as they are in the diverging part of the nozzle. After leaving the nozzle, the clusters form a beam with a divergence of about half the solid angle of the nozzle, and consisting of about 2 to 10% of the total gas input.

By a system of skimmers and diaphragms, acting as separations between differential pumping stages, a beam is extracted from this central cone, which has the required shape at the crossing with the LEAR beam. Due to their great mass the clusters are practically not scattered by background gas, and the beam keeps a very well-defined boundary.

A schematic view of a target system is shown in Fig. 29. The basic parameters for such a target would be:

target thickness: $5 \cdot 10^{-9}$ g/cm^2 $\hat{=}$ $1.5 \cdot 10^{15}$ molecules/cm^3;
target dimensions at crossing: diameter $\sim$ 30 mm;
target density: $\sim 10^{15}$ molecules/cm ;
distance, nozzle to crossing: $\sim$ 45 cm;
cluster dimension: $\sim 10^5$ to 10^7 molecules/cluster;
cluster speed: $\sim$ 500 m/s;
total gas input: $\sim 10^{22}$ molecules/s = 400 mbar ℓ/s;
useful gas flow in the target beam: $\sim 3.5 \cdot 10^{20}$ molecules/s - 14 mbar ℓ/s.

Due to the operation of the target, the ring vacuum will be locally perturbed by gas diffusing out of the last differential pumping stage or back from the cluster beam dump. The estimated pressure bump produced in the LEAR vacuum chamber, see Fig. 29 , varies linearly with the target thickness. In the presence of a cooling system its only effect will be to cause a loss of $\bar{p}$ in addition to the beam decay due to the interactions in the target volume. An estimate 22) shows that for the anticipated pressures and an extension of the pressure bump of a few meters, the additional $\bar{p}$ loss can be less than 10% of the loss caused by the target alone.

Up to now only hydrogen targets have been considered. Deuterium clusters can be produced without any modifications since the thermodynamic properties are almost identical. Because of the large gas input, a recuperation of the deuterium will be required. Cluster beams of heavier gases can be produced after modification of the nozzle cooling system.

6.2.2 Polarized target

The vacuum system of the straight section target will be designed such as to allow as well the installation of a polarized atomic hydrogen beam target. A target of this type being built at CERN has the following planned performance (Ref. 23)):

target thickness: $\sim 10^{12}$ atoms/cm^2 $\sim 2 \cdot 10^{-12}$ g/cm^2;
target diameter at crossing: $\sim$ 1 cm;
polarization: $\sim$ 90%.

The polarization axis can be oriented in any direction by a field of $\sim$ 10 Gauss (static or changing in direction, say, every few milliseconds). Due to the very small density of jet an experiment using it could run parasitically while the external beam is the main user.

6.3 CO-ROTATING BEAMS OF ANTIPROTONS AND H^-

Antiproton - proton atoms (Protonium) can be formed in highly excited states by having an "H^- target" moving together with antiprotons at the same velocity[24]. This can be realized in principle by storing H^- ions together with antiprotons in LEAR. Beams of neutral states formed in flight would come out of the straight sections and merge into the neutral beam lines foreseen (Fig.3).

Due to the mass difference between $\bar{p}$ and H^- the two co-rotating beams will in general be slightly displaced with respect to each other. If the two particle species are kept by the same RF system or by a stochastic cooling system imposing the same revolution frequency, the difference in mean radial position (Δr) and in mean longitudinal velocity $\Delta\beta_{//}$ at the interaction point will be given by

$$\Delta r = \alpha_p \gamma_t^2 \left(\frac{1}{\gamma_t^2 - \gamma^2}\right) \frac{\Delta m_o}{m_o}$$

$$\frac{\Delta\beta_{//}}{\beta_{//}} = \left(\frac{1}{\gamma_t^2 - \gamma^2}\right) \frac{\Delta m_o}{m_o}$$

With $\Delta m_o/m_o = 10^{-3}$, $\alpha_p = 2.7$ m (long straight section), $\gamma_t^2 = -6.3$, $\gamma \approx 1$ one obtains a very small longitudinal velocity difference

$$\frac{\Delta\beta_{//}}{\beta_{//}} = 1.4 \times 10^{-5}$$

and a radial separation of the two beam centres by

$$\Delta r = 2.4 \text{ mm}$$

If alternatively the average velocity of the two species is equalized (as may be the case with electron cooling if the electron velocity is very little dependent on radial position) than

$$\Delta r = \alpha_p \frac{\Delta m_o}{m_o}$$

giving a radial separation of 2.7 mm.

As particles perform betatron oscillation, the beam will have a transverse velocity spread

$$\frac{\Delta\beta_{\perp}}{\beta} = \sqrt{\frac{E}{\pi\beta_c}}$$

which assuming $E = 10\ \pi\ 10^{-6}$ rad m, $\beta_c = 5$m, will be of the order of $\frac{\Delta\beta}{\beta} = 1.4 \times 10^{-3}$ ($\Delta\beta \simeq 5 \times 10^{-4}$ at $p = 0.3$ GeV/c). The concurrent beam size $\sqrt{\frac{E}{\pi}\beta}$ is about 7 mm.

Estimations [25] indicate that the cross-section for protonium formation increases dramatically when the total velocity difference ($\Delta\beta$) between the two species is of the order of $2 \cdot 10^{-4}$ or less. Only a small fraction of the beam particles will be in these conditions until very strong cooling of both H^- and antiprotons can be used to reduce the beam sizes to about 2 mm and $\Delta p/p$ to a few 10^{-4}. Under these conditions, the two beams will no longer overlap in most of the machine, with the exception of the achromatic points where the orbit dispersion (α_p) passes through zero. With the working point proposed for $H^- - \bar{p}$ operation (Table 3.1-2), these points are in the short straight sections (Fig. 8), giving thus well defined interaction points for protonium formation

A problem is the stripping of H^- ions by other H^- ("intra-beam-stripping") or by antiprotons. In fact, model calculations [26] indicate that the cross-sections (σ) for both these processes may be as high as $3 \times 10^{-14}\ cm^2$ unless both beams are cool and very well synchronised ($\Delta\beta \lesssim 10^{-4}$). With an average luminosity (L) of, say, $1.5 \times 10^{21}\ cm^{-2}\ sec^{-1}$, a figure typical for the 7 mm radius beams with 10^9 particles, the loss rate is

$$\frac{dN}{dt} = 2\ L\ \sigma \approx 10^8 \quad H^-/sec \tag{6.3.1}$$

and the corresponding beam lifetime

$$\tau = N/d\ /dt \simeq 10\ s \tag{6.3.2}$$

(The factor 2 in (6.3.1) assumes equal cross-section for $\bar{p} - H^-$ and $H^- - H^-$ stripping and a similar intensity for both beams).

Again when the velocity difference $\Delta\beta$ is reduced below about 1.5×10^{-4}, the stripping cross-section is expected [26] to drop very sharply, thus improving the lifetime of the highly cooled and synchronized beam. However, present day Linac beams have a velocity spread of almost an order of magnitude larger (compare e.g. the longitudinal spread $\Delta\beta_{/\!/} = \beta\gamma^2 \frac{\Delta p}{p} = \pm 5 \times 10^{-4}$ resulting from the "typical" $\Delta p/p = \pm 1.5 \times 10^{-3}$).

We may thus conclude that frequent re-injection of H^- (say 10^9 every 5 to 10 s) and if possible strong cooling have to be devised. The time scales and the desired beam temperatures will probably exclude stochastic cooling of H^- for this purpose. On the other hand, electron cooling presents the danger of stripping the H^- by the electron beam. No detailed calculations of this mechanism exist to our knowledge. As a rough but apparently realistic [27] estimate, one can assume that the cross-section becomes very small when the velocity difference is $\Delta\beta \lesssim 1.7 \times 10^{-3}$ such that the electron energy in the H^- rest system does not exceed the binding energy (0.75 eV) of the outer shell.

Clearly, the whole complex of H^- cooling and synchronisation needs further study. In a first stage, one can envisage working with uncooled H^- ($\Delta\beta \approx 10^{-3}$) in which case only a fraction of the beam participates in protonium formation and stripping is so fast that frequent refilling is essential. Fortunately, the protonium formation cross-sections are high so that even under these more difficult conditions useful experiments can be done and the apparatus can be made selective enough to discriminate protonium from the large background of H^0 created by stripping of H^- [28].

The H^- ions of 50 MeV energy can be obtained from the old PS Linac and injected into LEAR through the 180° loop (Fig. 1) also used (with reversed polarity) for the injection of "cheap" protons for machine tests. For H^- operation, the proton duoplasmatron has to be replaced by an H^- source. Such devices [29] giving Linac currents of the order of 10 to 40 mA have in fact been developed in other laboratories and are operational, e.g., at FNAL and LAMPF.

To reinject H^- into LEAR, the antiprotons will be bunched into, say, half of the LEAR circumference. The free part (about 400 ns at

50 MeV energy) can be used to inject a 200 ns pulse of H^- leaving about 100 ns for rise of the kicker field and 100 ns for its fall. Prior to injection the RF would be jumped to the second harmonic, keeping the $\bar{p}$ in one bucket and leaving the second for H^- capture. Assuming 50% capture efficiency and 10 mA Linac current, the number of H^-

$$N = \eta_c \, I \, \Delta t/e \approx 6 \times 10^9$$

is in excess of the 10^9 assumed above. This permits us to select to some extent the small emittance, small Δp core of the beam, thus alleviating the stripping problems discussed above. After injection, the RF would be turned down adiabatically and $\bar{p}$ and H^- merge due to the frequency spreads. Continuous (stochastic) cooling of the $\bar{p}$ or short periods of electron cooling of the antiprotons would be essential to avoid degradation of the antiproton beam as 10^9 fresh $\bar{p}$ can be added only every, say, 10 min i.e. after some hundred H^- injection cycles.

Most considerations made above apply equally well to schemes which need extracted beams of H^- as e.g., the proposal to measure proton-antiproton mass difference by comparing H^- and antiprotons, in a mass spectrometer [30].

However, intra beam stripping is of less concern as these schemes need probably less particles and beam is required for shorter times in LEAR. In fact, various beam density limitations like intra beam scattering and the danger of destructive beam self-bunching will anyway put limits on the number of particles which can be cooled to the momentum spread of 10^{-5} as contemplated for the mass difference experiment.

If appropriate for the experiment, H^- and $\bar{p}$ can be decelerated simultaneously in LEAR.

6.4 Colliding beams of $\bar{p}$ and p

To work out an upper limit on the luminosity for this option [31], we assume head-on collisions of a proton and an antiproton bunch of 6×10^{11} particles each. This is the design intensity of the AA beam for 24 hours of stacking.

Following the procedure used to determine performance limits of electron storage rings [32], we start from the general luminosity formula

$$L = \frac{N_{\bar{p}} N_p f_{rev}}{4 A_{int}} \tag{6.4.1}$$

where the interaction area is given by the effective width (a_H) and height (a_V) (twice the rms width) of the larger of the two beams

$$A_{int} = \frac{\pi}{4} a_H \cdot a_V \tag{6.4.2}$$

Next we introduce the tune shift characterizing the beam-beam effect. The antiproton tune shift is determined by the intensity and the size of the proton beam

$$\Delta\nu_{\bar{p}} \simeq r_p \frac{N_p \beta_v^*}{A_{int,p}} \left(\frac{1 + \beta^{-2}}{\gamma} \right)$$

Here we have assumed that the vertical tune shift dominates and that the beam is flat (w >> h).

The proton tune shift is given by the corresponding expression inserting antiproton intensity and area on the r.h.s. Since both tune shifts have to be limited, it follows from (6.4.1) and (6.4.2) that optimum luminosity is reached if both beams are designed to the tune shift limit ($\hat{\Delta\nu}$) and if both have similar size ($A_{int,\bar{p}} = A_{int,p}$) and similar intensity ($N_{\bar{p}} = N_p$). The optimum luminosity is

$$L = \frac{N f_{rev} \hat{\Delta\nu} \gamma}{(1 + \beta^{-2}) r_p \beta_v^*} \tag{6.4.3}$$

The only "free" parameters in (6.4.3) are $\hat{\Delta\nu}$ and β_v^*, the value of the focusing function in the interaction region.

As to $\hat{\Delta\nu}$, it is usually assumed that in proton (and antiproton) beams the tune shift should be

$$\hat{\Delta\nu} \lesssim 0.005$$

in order to avoid rapid beam decay. More recent studies insist on a smaller permissible value for machines working with short bunches, especially for multibunch machines. We shall however take the canonical 0.005 for LEAR with only one bunch of each species.

The value of the focusing function in the straight section is $\beta_v^* \simeq 5$ for the usual working point of LEAR. Betas of 2 m could be reached by going to higher vertical tune and probably smaller values with a special low β insertion. However, in all cases, the focusing function increases parabolically with the distance (s) from the low β point ($\beta = \beta_o + s^2/\beta_o$) reaching twice the central value at $s = \beta_o$. To avoid beam interaction outside this region of low β values, it is of no use to have β^* smaller than the bunch length. In fact, this is a potential drawback of the head-on collision scheme where the length of the interaction region is given by the bunch length.

Bearing this in mind, we may rewrite (6.4.3), replacing β_v^* by ℓ_b. It seems difficult to obtain bunches shorter than 5 m in LEAR as will be discussed below. With this restriction, one obtains a luminosity at 2 GeV/c in LEAR of

$$L \lesssim 1.4 \times 10^{34} \frac{\Delta\nu}{\ell_b(\mathrm{cm})} \simeq 1.4 \times 10^{29}\ \mathrm{cm}^{-2}\ \mathrm{s}^{-1} \qquad (6.4.3')$$

Clearly this is an upper limit given by beam-beam effect and bunch length limitations only. We can work out the required beam area (and assuming $a_h = 3a_v$) the corresponding beam size and emittances from (6.4.1) and (6.4.2). Results are compiled in Table 6.4-1.

The RF voltage needed to contain a bunch of length ℓ_b and a given $\Delta p/p$ may be written as

$$U = \frac{\pi}{2} |\eta|\ \beta^2\ \gamma \left(\frac{\Delta p}{p}\right)^2 h_{RF} \left(\frac{1}{y(\ell_b)}\right)^2 \times 938\ \mathrm{MV} \qquad (6.4.4)$$

where the "bunch height function" y (approximated by $y \approx 1.6\ \ell_b/2\pi R$ for $y \lesssim 0.5$) is about 0.1 for a 5 m long bunch in LEAR ($h_{RF} = 1$).
For the usual working point $|\eta| = 0.18$ at 2 GeV/c. Taking $\Delta p/p = 10^{-3}$ for the bunched beam momentum spread and assuming a first harmonic RF system ($h_{RF} = 1$) one needs

$$U = 54 \text{ kV}$$

It will take very powerful cooling to get to the assumed $\Delta p/p = 10^{-3}$ (corresponding to $\Delta p/p = 6 \times 10^{-5}$ for a debunched beam). In fact, the bunch area of the circulating beam

$$A = \pi \frac{\ell_b}{2\ R} \beta\gamma \frac{\Delta p}{p} \simeq 1.3 \times 10^{-3}$$

is at least 10 times smaller than the value expected for the injected bunches.

A possibility to reduce the voltage requirement (6.4.4) is to reduce $\eta = 1/\gamma_t^2 - 1/\gamma^2$ by tuning transition energy closer to the working range. This can be done in principle by tuning LEAR to a different working point. However, this method is limited as the longitudinal beam stability becomes very critical.

In fact, the impedance of the beam environment has to be

$$\left|\frac{Z_n}{n}\right| \leq \frac{B_f |\eta|\ \beta^2 \gamma}{\hat{I}} \left(\frac{\Delta p}{p}\right)^2$$

to avoid beam destructive selfbunching. At 2 GeV/c and with $|\eta| = 0.18$ this gives a permissible $|Z_n/n| \lesssim 60\ \Omega$ which is about twice the impedance value reached in PS and ISR after work to "clean up" the beam environment. Although 60 Ω thus seem acceptable, there is little margin left to work at decreased $\Delta p/p$ (and extended bunch length) as it will be desirable during beam preparation (cooling). It is for this reason that we exclude η reduction for the time beeing. Another possibility for further bunch compression is the use of a higher harmonic RF system as proposed by M. Conte[33]. This may be feasible if the extra space can be found in one of the straight sections and if the strong intra beam scattering can be compensated.

The alternative possibility has briefly been studied using a "Doris type" scheme where the two beams are separated by electrostatic fields over most of the circumference and cross under an angle in the interaction point. Then, the interaction length is given by the crossing angle rather than by the bunch length. The difficulty is that the incorporation of the separating fields needs a major change of the machine.

In addition, very small transverse beam size is now required to obtain luminosities comparable to the head-on collision case thus needing strong transverse cooling until again one can work with short bunches. More work is needed to finalize the design. In all cases, the luminosity obtainable depends very critically on strong phase-space cooling, on the assumed tight bunching and/or very small transverse emittances. We estimate that a luminosity of an order of magnitude lower than the limiting value (6.4.3) could be expected after a considerable number of changes of the machine.

The protons needed for the collider option would be injected directly from the old linac. Prior to this the antiprotons would be filled in at 0.6 GeV/c using a transverse 10 turn injection procedure together with cooling if necessary. After deceleration to 0.3 GeV/c the p bunch would be added onto the free part of the circumference using another 3 to 5 turn injection into the proton bucket. Although these multiturn procedures are rather delicate, they are somewhat facilitated by the fact that the horizontal acceptance of the machine is about 20 times larger than the emittance of the incoming beams. Injection procedures could be simplified if a direct proton injection path from the PS was built.

In any case, the collider option will need a major shut-down and modifications of LEAR and delicate techniques of filling and running of the machine in order to reach respectable luminosities. Very strong cooling is needed to compress the beam to the required small momentum spread and to compensate intra beam scattering. Stochastic cooling may be used to precondition the large beam after injection, whereas electron cooling will be essential to compete with the blow-up mechanisms in the final beam. It will therefore be important to device some sort of electron cooling working in the momentum range foreseen for the collider mode.

TABLE 6.4-1

COLLIDING BEAM PROPERTIES

1. Lattice parameters ($Q_H \simeq 2.3$, $Q_V \simeq 2.7$)	
Lattice functions (average) in interaction region $\beta_H \simeq \beta_V$ (m)	5
Momentum compaction α_p (m)	3.9
Transition energy γ_t^2	$-(14)^2$
2. Beam parameters and luminosity	
Momentum (GeV/c)	2
Number of particles ($N_{\bar{p}} = N_p$)	6×10^{11}
Beam size (2 rms) horizontal x vertical (mm^2)	29 x 10
Corresponding emittances $E_H \times E_V$ (mm.mrad)^2	170 π x 20 π
Bunched beam momentum spread $\pm \Delta p/p$	1×10^{-3}
Bunch length, total (m)	5
Luminosity limit (cm^{-2} s^{-1})	1.4×10^{29}
3. Auxiliary quantities	
RF voltage/turn (kV)	55
Frequency, h = 1 (MHz)	3.45
Off energy function $1/\gamma_t^2 - 1/\gamma^2$	-0.18
Beam-beam tune shift $\Delta\nu$	5×10^{-3}
Laslett space-charge tune shift ΔQ at 2 GeV/c	0.01
Tolerable impedance at n^{th} revolution harmonic $\lvert Z_n/n \rvert$ (Ω)	60
Growth time of Δp and bunch length due to intra beam scattering (hours) (without cooling)	$\approx$ 0.6

REFERENCES

1) U. Gastaldi, K. Kilian and D. Möhl
Deceleration of antiprotons for physics experiments at low energy (a low-energy antiproton factory)
in Proc. 10th Int. Conf. on High-Energy Accelerators, Protvino, 1977 (Institute for High-Energy Physics, Serpukhov, 1977).

P. Dalpiaz
Electromagnetic Annihilation in Low Energy $p\bar{p}$ Colliding Beams
CERN-$p\bar{p}$ Note 06 (May 1, 1977)

2a) P. Dalpiaz, U. Gastaldi, K. Kilian and M.A. Schneegans,
Low Energy Antiproton Experiment with Antiproton Factory,
Memorandum to the Workshop of Medium Energy Physics
CERN - September 1977.

2b) R. Klapisch
CERN Workshop on Intermediate Energy Physics :
Chairman's report, CERN-PS-CDI-77-50 (1977)

B. Povh
Unconventional tools for physics, beams of antiprotons and relativistic heavy ions,
CERN-PS-CDI-77-49 (1977),

2c) A. Astbury, P. Dalpiaz, U. Gastaldi, K. Kilian, E. Lohrmann, B. Povh and M.A. Schneegans,
Possible Experiments with Antiprotons at low and intermediate Energies,
Memo to PS and SC Committees dated 6th February 1978.

3a) Proc. Joint CERN-KfK Workshop on Physics with Cooled Low-Energetic Antiprotons,
Karlsruhe, 1979, KfK Report 2836 (ed. H. Poth).

3b) U. Gastaldi, K. Kilian and G. Plass,
A low-energy antiproton facility at CERN : physics possibilities and technical aspects,
CERN/PSCC/79-17 (1979).

4) CERN/PS/AA 78-3,
Design study of a proton-antiproton colliding beam facility (1978)

5) W. Hardt, L. Hoffmann, P. Lefèvre, D. Möhl, G. Plass and D. Simon
Conceptual study of a facility for low-energy antiproton experiments,
CERN/PS/DL/Note 79-1 (1979).

6) H. Koziol,
Private communication.

7) S. van der Meer
Stochastic Extraction, a Low-Ripple Version of Resonant Extraction,
CERN/PS/AA 78-6,March 1, 1978.

8) R. Cappi, W.E.K. Hardt,
Ultra Slow Extraction with Good Duty Factor,
Paper submitted to the XIth Intern. Conf. on High Energy Accel., Geneva, July 7-11, 1980.

Stochastic Extraction at 10 GeV/c
Machine Development Report PS/OP/MD 80-5 (27.3.80).

8a) D. Blechschmidt, E. Jones, H. Schuhback
Private communication and
Memo ISR-VA/DB/gm du 16.8.79

9) A. Susini
CERN/PS/LR Note in preparation.

10) A. Cheretakis, J. Knott, P. Mead, A. van der Schueren and U. Tallgren,
The Control System of the CERN New Linac,
Ibid., p. 49,

P. Mead
The System Software of the New Linac Control System,
Proc. of the Digital Equipment Users Society, p.93, Vol. 4, No. 1 (1977).

11) G. Carron, H. Herr, G. Lebée, H. Koziol, F. Krienen, D. Möhl, G. Petrucci, C. Rubbia, F. Sacherer, G. Sadoulet, G. Stefanini, L. Thorndahl, S. van der Meer and T. Wikberg,
Experiments on stochastic cooling in ICE,
CERN EP/79-16 (1979), presented at the Particle Accelerator Conference, San Francisco, 1979.

H. Herr, D. Möhl,
Bunched Beam Stochastic Cooling,
CERN-PS-DL Note 79-3

12) D.J. Simon
A possible scheme to transfer 50 MeV H^- ions (and protons) from the old PS Linac to LEAR,
CERN $\bar{p}$ LEAR-Note 37 and CERN/PS/MU/BL/Note 79-10

13) M Höfert,
HS-RP/TM 79-28 and HS-RP/IR 77-19

14) M. Bell, J. Chaney, S. Citolin, H. Herr, H. Koziol, F. Krienen, G. Lebée, P. Møller-Petersen, G. Petrucci, H. Poth, T. Sherwood, G. Stefanini, C. Taylor, L. Tecchio, C. Rubbia, S. van der Meer and T. Wikberg
Phys. Lett. 87B, 275 (1979).

15) H. Haseroth, C. Hill, P. Møller-Petersen, H. Poth
Electron Cooling for LEAR
To be published.

16a) M. Bell, J.E. Chaney, F. Krienen and P. Møller Petersen
Report on the CERN Electron Cooler
Proc. Joint CERN-KfK Workshop on Physics of Low-Energetic Antiprotons (Karlsruhe 1979 Kfk Report 2836)
CERN $\bar{p}$ LEAR-Note 29

16b) P. Møller-Petersen
Ph.D Thesis University of Aarhus (unpublished)

17) C.S. Taylor
Private communication

18) P. Dalpiaz, P.F. Dalpiaz, B. Dickinson, J. Duclos, L. Faure,
F. Gasparini, M. Ibbotson, S. Limentani, A. Magnon, A. Meneguzzo,
M. Nigro, C. Peroni, L. Pescara, M. Posocco, P. Sartori,
M.A. Schneegans, L. Tecchio, C. Voci,
CERN/PSCC/79-56.

A.S. Clough, N.M. Stewart, D.V. Bugg, J. Chaney, J.A. Edgington,
CERN/PSCC/79-66

J.C. Kluyver
CERN/PSCC/80-10

19) K. Kilian
Comment concerning internal gas targets in LEAR
CERN/PSCC/80-8

20) E.W. Becker and W. Henkes,
Z. Phys. 146, 320 (1956)

E.. W. Becker, K. Bier and W. Henkes,
Z. Phys. 146, 333 (1956)

E.W. Becker, R. Klingelhöfer and P. Lohse,
Z. Naturforschung 17A, 432 (1962)

R. Klingelhöfer, H. Röhl,
Z. Naturf. 25a (1970) 402

O.F. Hagena, W. Obert, J. Chem,
Phys. 56 (1972) 1793.

W. Obert
6th ICEC, Grenoble, (May 1976)

W. Obert,
Progress in Astronautics and Aeronautics 51, 2 (1977) 1153.

W. Ensslen,
Diplomarbeit Univ. Karlsruhe, (1977)

W. Obert,
11th Rarefied Gas Dynamics Symposium, Cannes (1978)

21) CERN-Lausanne-Lund-Michigan-Rockefeller Collaboration
CERN/SPS/78-23, SPSC/M 106, (14th Feb. 1978)
and CERN/SPSC/79-72, (21st June 1979).

22) K. Kilian, D. Möhl
LEAR-note 82 (in preparation).

23) CERN-Lund-Rockefeller Collaboration
CERN/SPSC/77-71 (26 August 1977)

24) U. Gastaldi,
Protonium spectroscopy in flight
CERN/PSCC 79-67 and references given therein.

U. Gastaldi,
$\bar{p}p$ experiments at very low energy using cooled antiprotons
In Proc. 4th European Antiproton Conf., Barr-Strasbourg, 1978
(Editions du CNRS, Paris, Ed. A. Friedman)

25) L. Bracci, G. Fiorentini, D. Pitzurra,
Protonium formation in flight
Instituto di Fisica, Pisa, Report IFUP 79

26) G. Fiorentini,
Private communication

27) A.N. Skrinski,
Private communication

28) U. Gastaldi
Private communication

29) C. Hill,
H^- sources - a summary,
CERN $\bar{p}$ LEAR-Note 37 and CERN/PS-LR/Note 79-6

30) C. Thibault, R. Klapisch, G. Audi, M. Epherre, M. De Saint Simon,
F. F. Touchard,
A high precision measurement of the proton antiproton mass difference ...
CERN/PSCC/80-7

31) P. Dalpiaz, P.F. Dalpiaz, F. Gasparini, V. Graccnoh, M. Macri,
M.H. Schneegans, L. Tecchio, C. Voci,
Charmonium Fine Spectroscopy with LEAR operating as a Minicollider
CERN/PSCC/79-57

32) M. Sands,
The Physics of Electron Storage Rings
SLAC Report 121 (1970).

33) M. Conte,
Head-on collisions in LEAR
CERN $\bar{p}$-LEAR Note 46 (1979).

APPENDIX

GLOSSARY OF SYMBOLS

A	Bunch area in units of $\Delta(\beta\gamma).\phi_{RF}$
A_{int}	Effective collidiňg beam interaction area $A_{int} = \frac{\pi}{4} a_V a_H$ (one bunch per beam)
$a_{H\beta}$, a_{Hp}, a_V	Peak amplitudes (2σ) for horizontal betatron motion, horizontal motion due to momentum spread and vertical betatron motion respectively
$a_H = (a_{H\beta}^2 + a_{Hp}^2)^{\frac{1}{2}}$	Horizontal beam half-width (2σ)
B	Magnetic flux density
B_f	Bunching factor = average current over peak current
D	Diffusion constant, $D = \frac{1}{2\Delta f}\left(\frac{U_n}{2\pi R\ B\rho}\right)^2$ with U_n : rms noise voltage Δf : noise bandwidth
E_H, E_V	Horizontal, vertical emittances, respectively. $E_H = \pi a_{H\beta}^2 / \beta_H$; $E_V = \pi a_V^2 / \beta_V$
$f_{rev} = \frac{\beta c}{2\pi R}$	Revolution frequency
g	Quadrupole gradient, $g = \frac{\partial B}{\partial x}$
h, h_{RF}	RF harmonic number
$\hat{I}$	Peak current, $\hat{I} = N e f_{rev} / B_f$ for circulating beam
k	Normalized quadrupole gradient, $k = (-\partial B/\partial x) / (B\rho)$
k'	Normalized sextupole moment , $k' = \partial k/\partial x$
L	Luminosity
ℓ_b	Total bunch length
N, $(N_p , N_{\bar{p}})$	Number of particles (protons, antiprotons) per beam
Q_H, Q_V	Number of horizontal or vertical betatron oscillations per turn
ΔQ	Laslett tune shift (single beam)

$2\pi R$	Circumference of machine
r_p	Classical proton radius ($1.53\ 10^{-18}$ m)
Δr	Horizontal (radial) deviation from equilibrium orbit
U	RF voltage (amplitude)
$y(\ell_b)$	Bunch height / bucket height
$\|Z_n\|$	Modulus of beam equipment coupling impedance at frequency $n \cdot f_{rev}$
α_p	Momentum compaction function $\alpha_p = \Delta r/(\Delta p/p)$
β_H, β_V, β_c	Betatron functions (reduced instantaneous wavelength) for horizontal, vertical or either plane respectively
β_H^*, β_V^*, β_c^*	Beta values in the interaction region
β,γ	Relativistic factors : $\beta = v/c$; $\gamma = (1 - \beta^2)^{-\frac{1}{2}}$
γ_t	γ at transition energy for machines with $\gamma_t^2 > 1$, in general : $\gamma_t^{-2} = <\frac{\alpha p}{\rho}>$
η	Off-momentum function, $\eta = (-\Delta f/f) / (\Delta p/p) = \frac{1}{\gamma_t^2} - \frac{1}{\gamma^2}$
$\Delta\nu$	Beam-beam tuneshift (vertical)
ρ	Magnetic bending radius
ξ_H, ξ_V	Chromaticity (horizontal, vertical), $\xi = (\partial Q/Q) / (\partial p/p)$
σ_H, σ_V	rms beam size, horizontal and vertical ($\sigma_H = a_H/2$; $\sigma_V = a_V/2$)

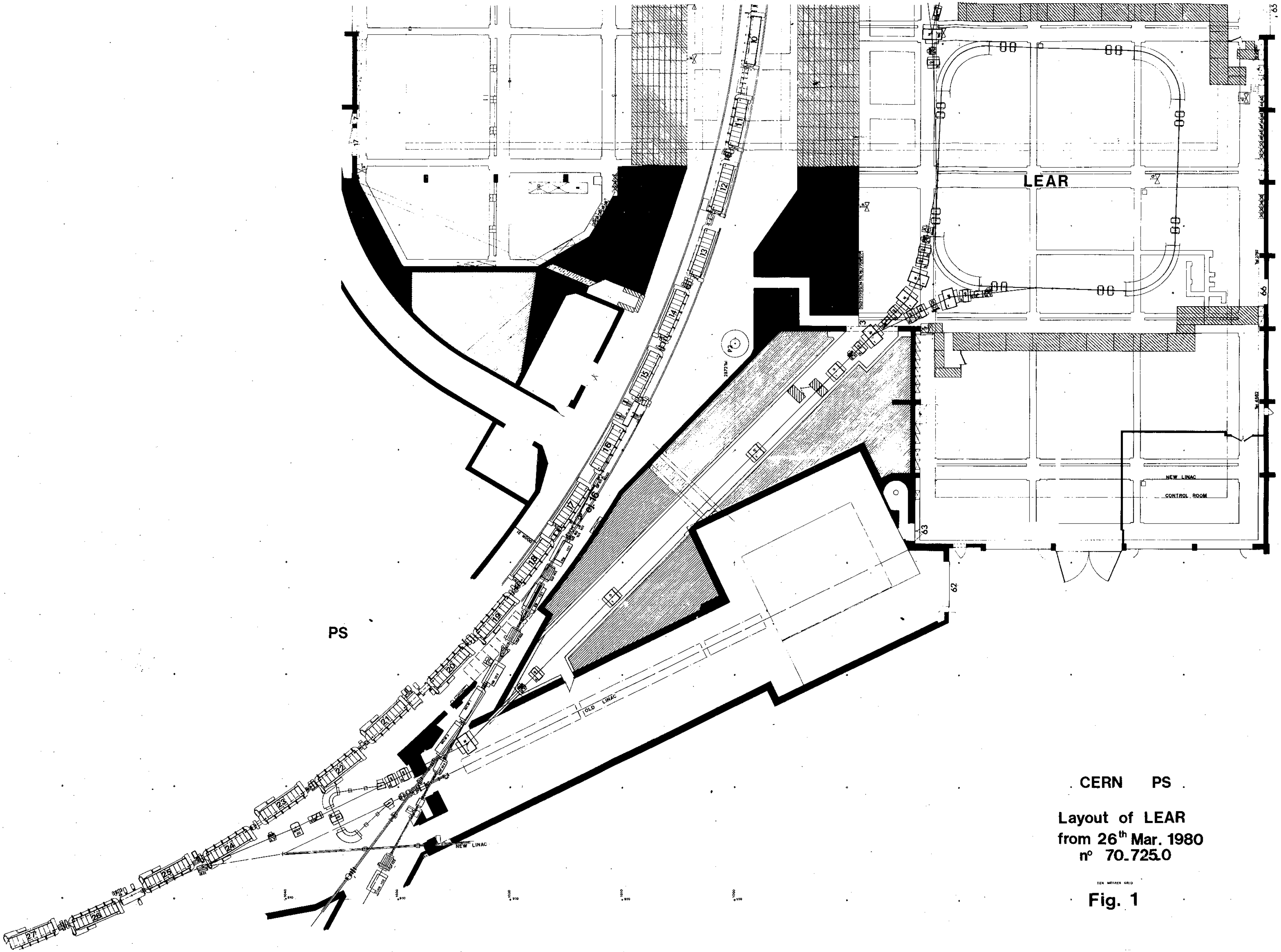

CERN PS

Layout of LEAR
from 26th Mar. 1980
n° 70.725.0

Fig. 1

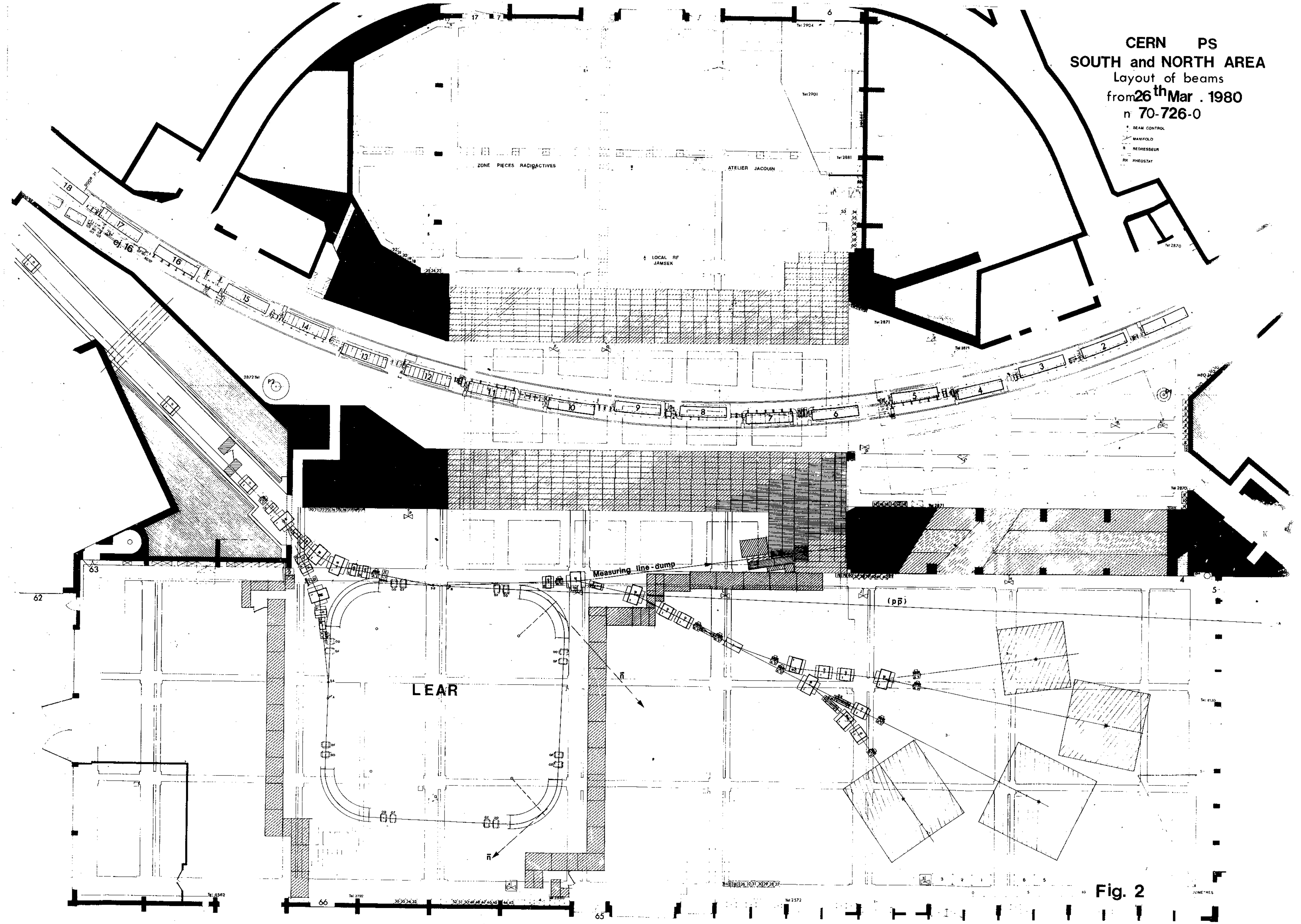
CERN PS
SOUTH and NORTH AREA
Layout of beams
from 26th Mar. 1980
n 70-726-0
ZONE PIECES RADIOACTIVES
ATELIER JACQUIN
LOCAL RF JAMSEK
Measuring line-dump
(pp̄)
LEAR
ej.16

Fig. 2

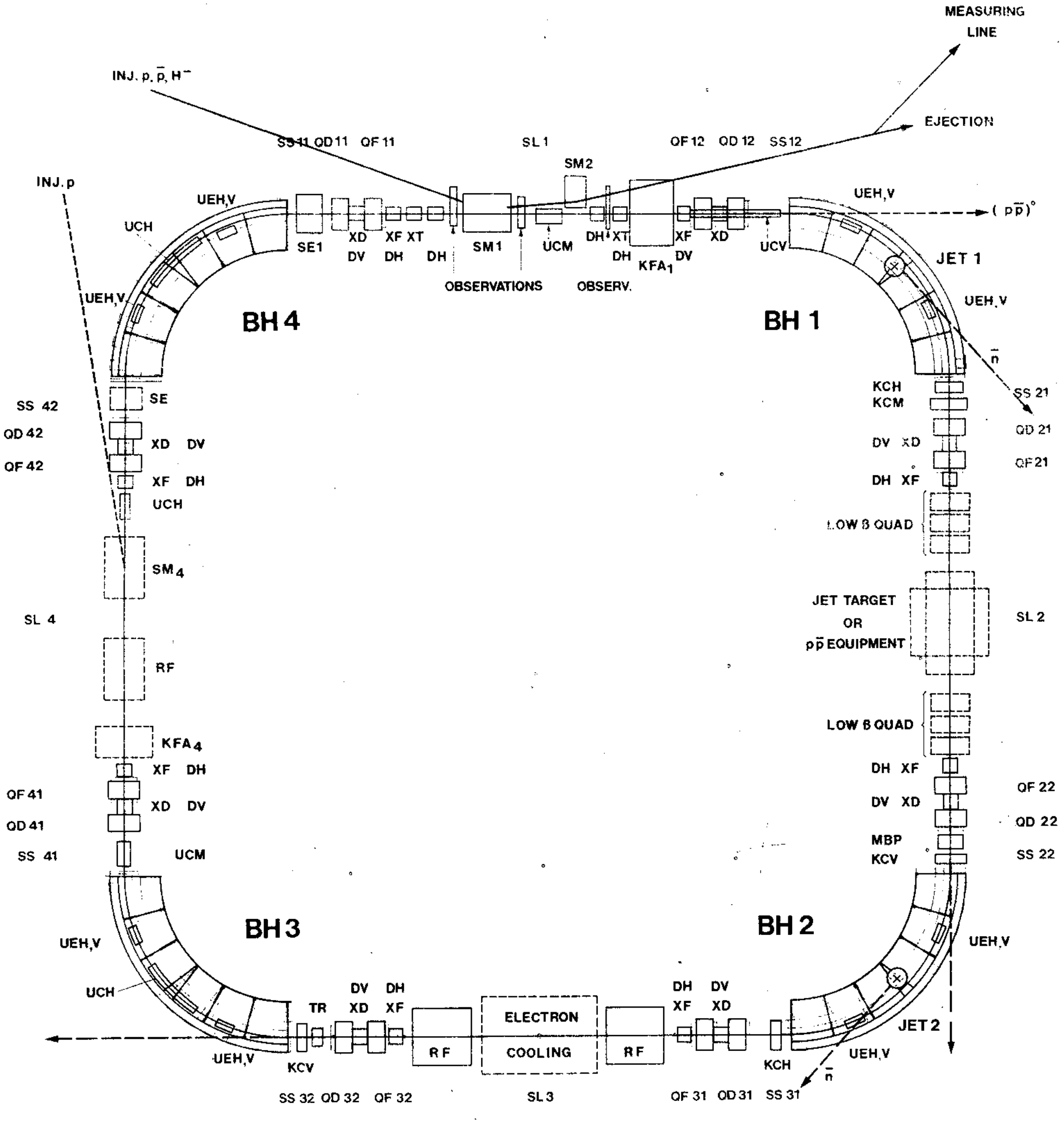

Fig. 3

LEAR General Lay out

(TENTATIVE, ELEMENTS OUT OF SCALE)

SCALE 1:50

0 5M.

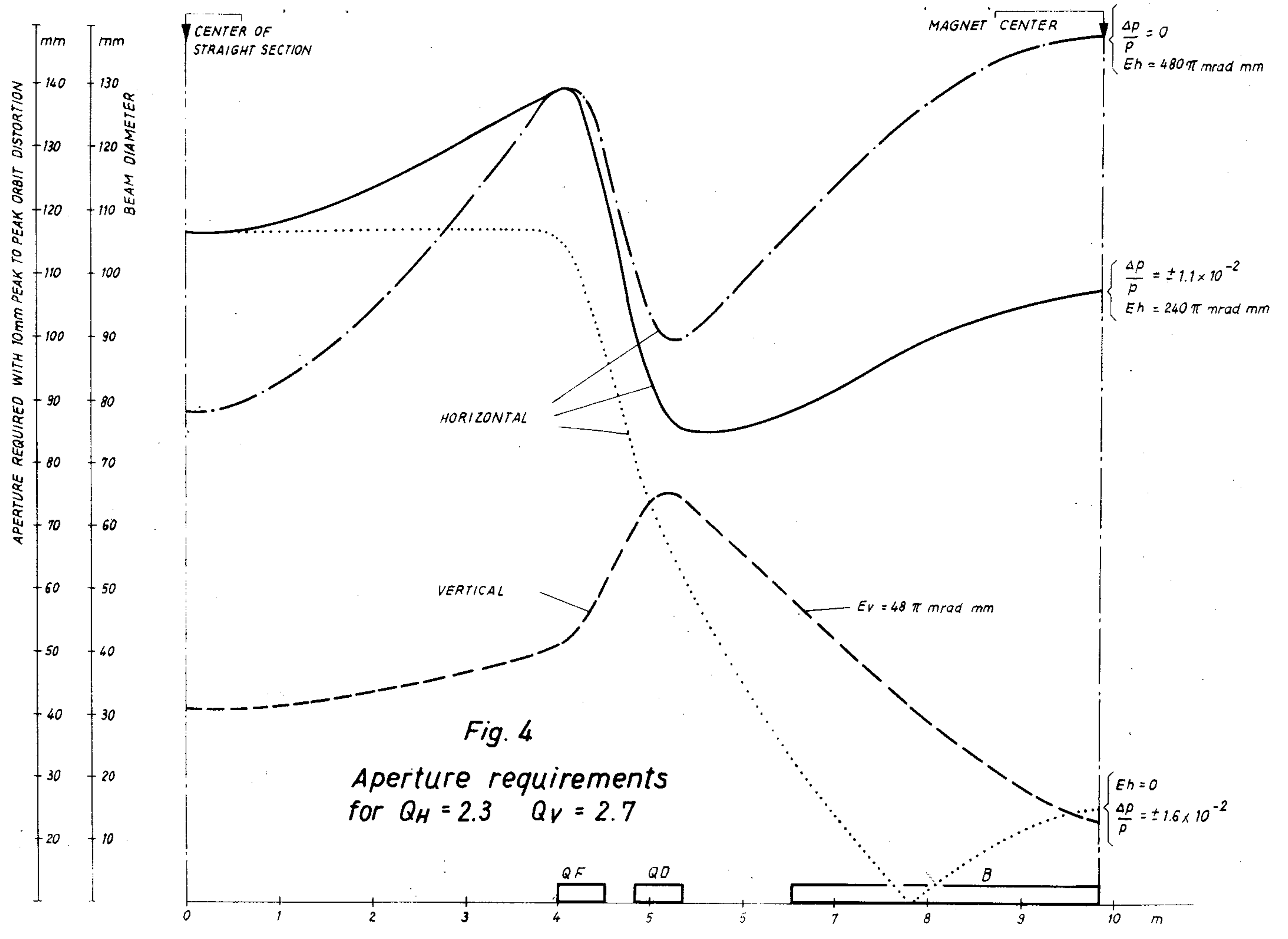

Fig. 4

Aperture requirements for $Q_H = 2.3 \quad Q_V = 2.7$

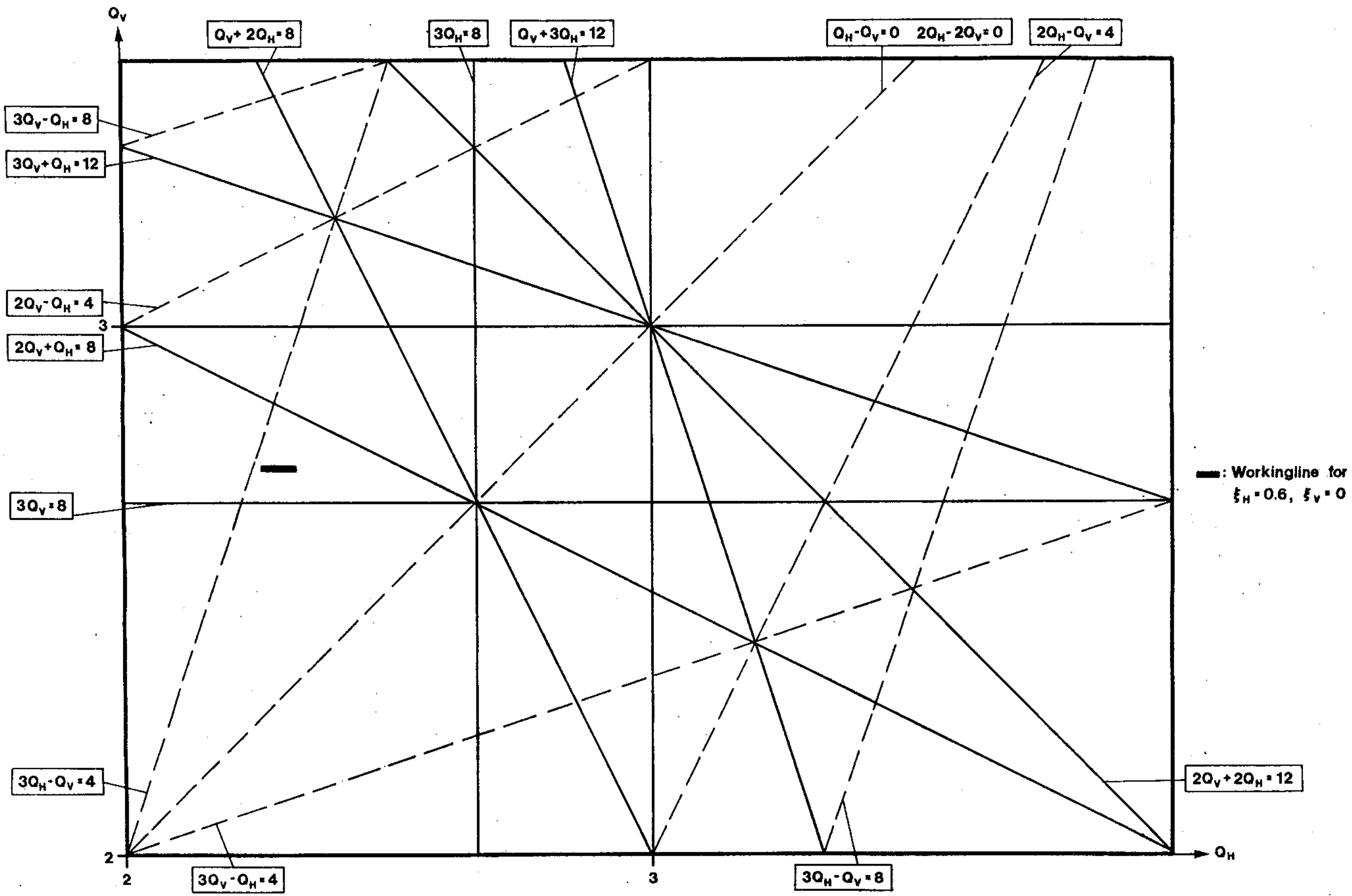

Fig. 5: Systematic resonances of order 1 to 4 for lattice with four superperiods

1). 2.4.80

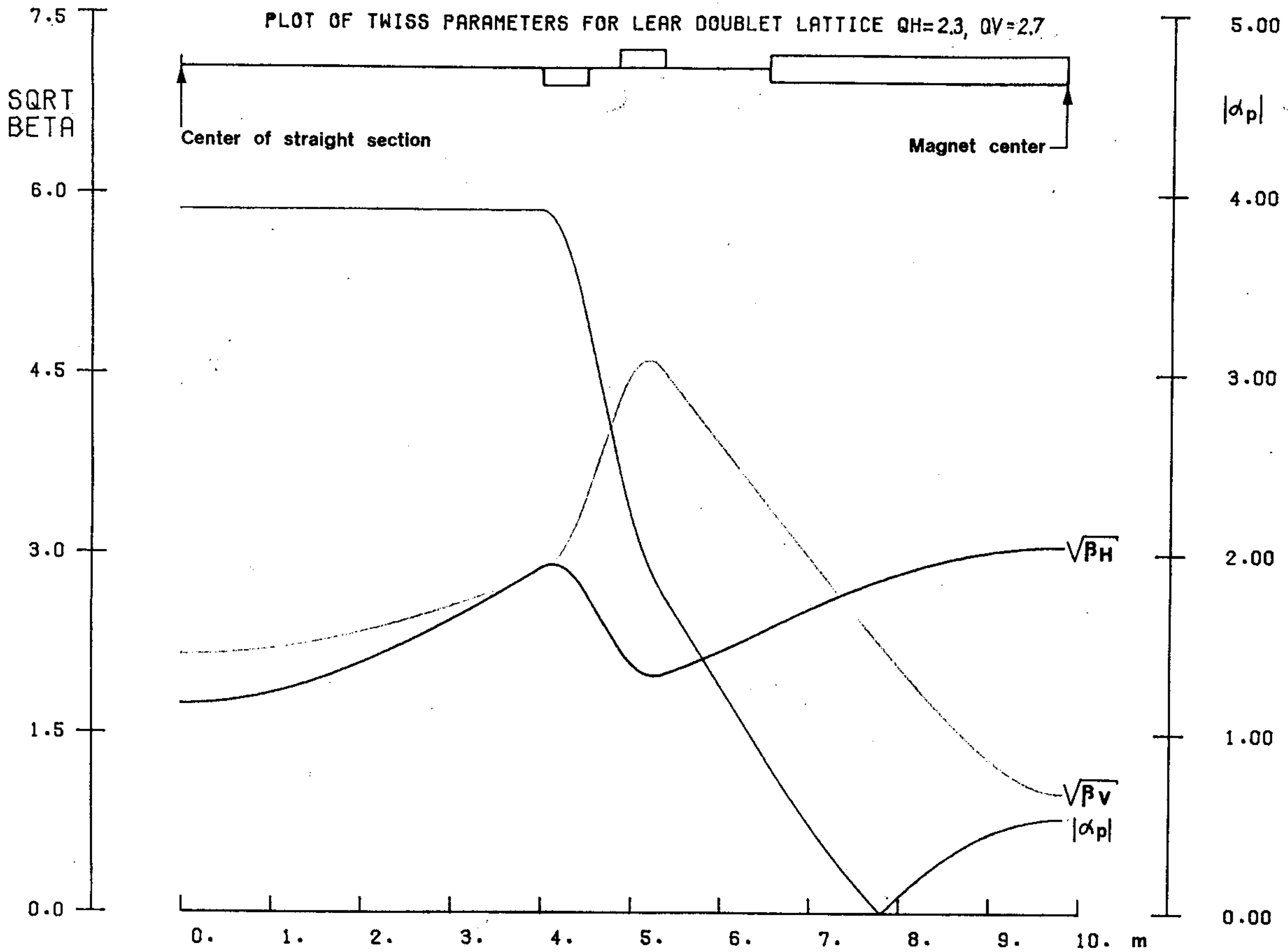
PLOT OF TWISS PARAMETERS FOR LEAR DOUBLET LATTICE QH=2.3, QV=2.7
SQRT BETA
Center of straight section
Magnet center
|αp|
√βH
√βV
|αp|
7.5
6.0
4.5
3.0
1.5
0.0
5.00
4.00
3.00
2.00
1.00
0.00
0. 1. 2. 3. 4. 5. 6. 7. 8. 9. 10. m

FIG. 6

Fig. 7

AGS OUTPUT FOR LEAR WITH $Q_H = 2.33$, $Q_V = 2.75$

LEAR AT WORKINGPOINT FOR STRETCHER OPERATION AGS VERSION 75.03 19/03/80 09.43.40

CIRCUMFERENCE = 78.54000 4 HALF SUPERPERIODS WEDGE MAGNETS ALL VALUES AT EXIT OF ELEMENTS

XXXXXXXXXXXXXXXXXXXXXXXXXXXXXXXXXXXXXXXXXXXXXXXXXXXXXXXXXXXXXXXXXXXXXXXXXXXXXXXXXXXXXXXXXXXXXXXXXXXXXXXXXXXX

NO	ELEM	L(M)	DIST(M)	ANG(MR)	K(1/M2)	BETAV(M)	BETAH(M)	ALPHAV	ALPHAH	MUV/2PI	MUH/2PI	ALPHAP(M)	ALPHAP'
INITIAL			0.0000			4.64731	3.04018	0.00000	0.00000	0.00000	0.00000	3.90864	-.000000
1	SS	.5000	.5000	0.00000	0.0000000	4.70110	3.12241	-.10759	-.16446	.01706	.02594	3.90864	-.000000
2	SS	.5000	1.0000	0.00000	0.0000000	4.86248	3.36911	-.21518	-.32893	.03373	.05058	3.90864	-.000000
3	SS	.5000	1.5000	0.00000	0.0000000	5.13146	3.78027	-.32277	-.49339	.04969	.07295	3.90864	-.000000
4	SS	.5000	2.0000	0.00000	0.0000000	5.50802	4.35589	-.43036	-.65786	.06468	.09261	3.90864	-.000000
5	SS	.5000	2.5000	0.00000	0.0000000	5.99217	5.09593	-.53795	-.82232	.07855	.10953	3.90864	-.000000
6	SS	.5000	3.0000	0.00000	0.0000000	6.58391	6.00053	-.64554	-.98678	.09123	.12394	3.90864	-.000000
7	SS	.5000	3.5000	0.00000	0.0000000	7.28324	7.06955	-.75312	-1.15125	.10273	.13617	3.90864	-.000000
8	SS	.1750	3.6750	0.00000	0.0000000	7.55342	7.48256	-.79078	-1.20881	.10649	.14000	3.90864	-.000000
9	CORRE	.1500	3.8250	0.00000	0.0000000	7.79550	7.85260	-.82306	-1.25815	.10960	.14312	3.90864	-.000000
10	CORRE	.1500	3.9750	0.00000	0.0000000	8.04726	8.23745	-.85533	-1.30749	.11262	.14608	3.90864	-.000000
11	GAP	.0250	4.0000	0.00000	0.0000000	8.09016	8.30303	-.86071	-1.31571	.11311	.14657	3.90864	-.000000
12	QF	.2500	4.2500	0.00000	-1.2237075	9.19128	8.32888	-3.65548	1.21493	.11778	.15129	3.76012	-1.180575
13	QF	.2500	4.5000	0.00000	-1.2237075	11.93490	7.14910	-7.59736	3.38328	.12163	.15638	3.32885	-2.271432
14	GAP	.0250	4.5250	0.00000	0.0000000	12.31784	6.98102	-7.72036	3.33975	.12196	.15694	3.26907	-2.271432
15	CORRE	.1500	4.6750	0.00000	0.0000000	14.71465	6.01827	-8.45836	3.07860	.12373	.16063	2.92835	-2.271432
16	CORRE	.1500	4.8250	0.00000	0.0000000	17.39285	5.13386	-9.19636	2.81745	.12522	.16492	2.58764	-2.271432
17	GAP	.0250	4.8500	0.00000	0.0000000	17.85575	4.99408	-9.31936	2.77393	.12545	.16571	2.53085	-2.271432
18	QD	.2500	5.1000	0.00000	1.4068296	21.02112	4.08855	-2.96885	.95374	.12747	.17465	2.06672	-1.468605
19	QD	.2500	5.3500	0.00000	1.4068296	20.65360	3.98344	4.39558	-.52105	.12935	.18466	1.78564	-.796274
20	GAP	.5837	5.9337	0.00000	0.0000000	15.85712	4.70052	3.82123	-.70738	.13449	.20620	1.32082	-.796274
21	GAP	.5837	6.5175	0.00000	0.0000000	11.73117	5.63514	3.24689	-.89371	.14130	.22429	.85600	-.796274
22	BMAG	.0249	6.5424	3.95000	0.0000000	11.56996	5.67968	3.22237	-.89359	.14164	.22499	.83622	-.791526
23	BMAG	.5459	7.0882	129.91000	0.0000000	8.34525	6.64278	2.68531	-.86087	.15049	.23911	.43374	-.681093
24	BMAG	.5459	7.6341	129.91000	0.0000000	5.70685	7.53824	2.14825	-.77037	.16309	.25136	.09476	-.559182
25	BMAG	.5459	8.1799	129.91000	0.0000000	3.65476	8.30594	1.61119	-.62815	.18216	.26232	-.17500	-.427847
26	BMAG	.5459	8.7258	129.91000	0.0000000	2.18898	8.89436	1.07412	-.44376	.21306	.27241	-.37101	-.289301
27	BMAG	.5459	9.2716	129.91000	0.0000000	1.30952	9.26399	.53706	-.22959	.26531	.28196	-.48995	-.145880
28	BMAG	.5459	9.8175	129.91000	0.0000000	1.01636	9.39002	-.00000	-.00000	.34375	.29125	-.52982	.000000

DP/P	COSMU(H)	Q(H)	QPRIME(H)	BETAMAX(H)	COSMU(V)	Q(V)	QPRIME(V)	BETAMAX(V)	XMAX(P)	GAMMA TR.
0.0000	-.86363	2.3300	-2.2303	9.3900	-.38268	2.7500	-5.4609	21.0211	3.9086	-14.6626

XXXXXXXXXXXXXXXXXXXXXXXXXXXXXXXXXXXXXXXXXXXXXXXXXXXXXXXXXXXXXXXXXXXXXXXXXXXXXXXXXXXXXXXXXXXXXXXXXXXXXXXXXXXX

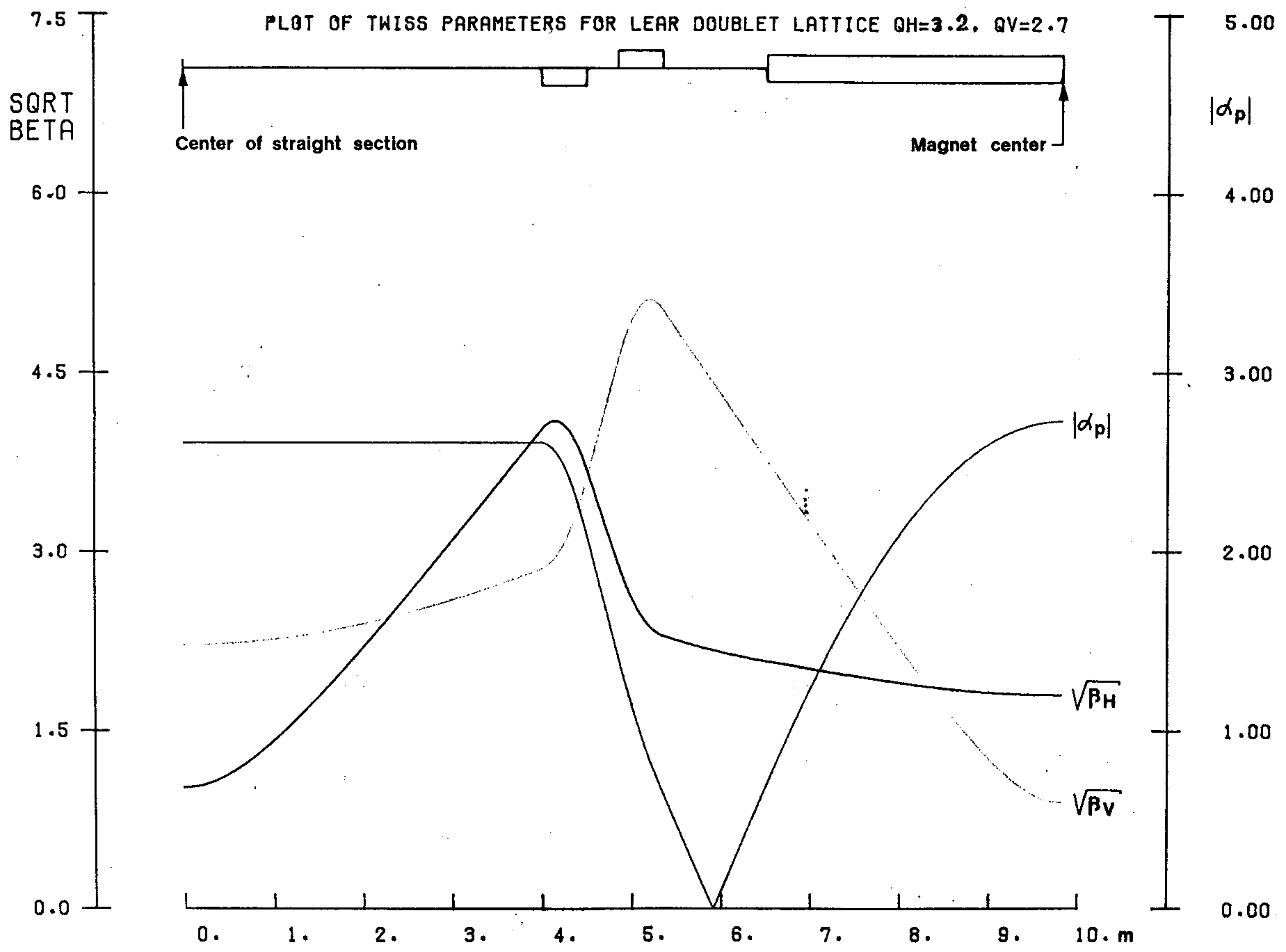
PLOT OF TWISS PARAMETERS FOR LEAR DOUBLET LATTICE QH=3.2, QV=2.7
Center of straight section
Magnet center
SQRT BETA
7.5
6.0
4.5
3.0
1.5
0.0
$|\alpha_p|$
5.00
4.00
3.00
2.00
1.00
0.00
$\sqrt{\beta_H}$
$\sqrt{\beta_V}$
0.
1.
2.
3.
4.
5.
6.
7.
8.
9.
10. m

FIG. 8

Fig. 9

AGS OUTPUT FOR LEAR WITH $Q_H = 3.2$, $Q_V = 2.75$

LEAR WITH HIGHER HORIZONTAL TUNE   AGS VERSION 75.03   02/04/80   23.39.42

CIRCUMFERENCE = 78.54000   4 HALF SUPERPERIODS   WEDGE MAGNETS   ALL VALUES AT EXIT OF ELEMENTS

XXXXXXXXXXXXXXXXXXXXXXXXXXXXXXXXXXXXXXXXXXXXXXXXXXXXXXXXXXXXXXXXXXXXXXXXXXXXXXXXXXXXXXXXXXXXXXXXXXXXXXXXXXXXXXXXXXXXXXXXXX

NO	ELEM	L(M)	DIST(M)	ANG(MR)	K(1/M2)	BETAV(M)	BETAH(M)	ALPHAV	ALPHAH	MUV/2PI	MUH/2PI	ALPHAP(M)	ALPHAP'
	INITIAL		0.0000			4.96399	1.27273	0.00000	0.00000	0.00000	0.00000	2.69162	-.000000
1	SS	.5000	.5000	0.00000	0.0000000	5.01435	1.46916	-.10073	-.39286	.01598	.05958	2.69162	-.000000
2	SS	.5000	1.0000	0.00000	0.0000000	5.16544	2.05844	-.20145	-.78571	.03164	.10599	2.69162	-.000000
3	SS	.5000	1.5000	0.00000	0.0000000	5.41725	3.04058	-.30218	-1.17857	.04670	.13802	2.69162	-.000000
4	SS	.5000	2.0000	0.00000	0.0000000	5.76979	4.41558	-.40290	-1.57143	.06096	.15980	2.69162	-.000000
5	SS	.5000	2.5000	0.00000	0.0000000	6.22306	6.18343	-.50363	-1.96428	.07425	.17505	2.69162	-.000000
6	SS	.5000	3.0000	0.00000	0.0000000	6.77705	8.34414	-.60435	-2.35714	.08652	.18614	2.69162	-.000000
7	SS	.5000	3.5000	0.00000	0.0000000	7.43176	10.89771	-.70508	-2.74999	.09774	.19449	2.69162	-.000000
8	SS	.1750	3.6750	0.00000	0.0000000	7.68471	11.88427	-.74033	-2.88749	.10143	.19694	2.69162	-.000000
9	CORRE	.1500	3.8250	0.00000	0.0000000	7.91134	12.76820	-.77055	-3.00535	.10449	.19888	2.69162	-.000000
10	CORRE	.1500	3.9750	0.00000	0.0000000	8.14704	13.68748	-.80077	-3.12321	.10746	.20068	2.69162	-.000000
11	GAP	.0250	4.0000	0.00000	0.0000000	8.18720	13.84413	-.80580	-3.14285	.10795	.20097	2.69162	-.000000
12	QF	.2500	4.2500	0.00000	-1.5724152	9.46135	14.04557	-4.45664	2.36367	.11255	.20378	2.56044	-1.040842
13	QF	.2500	4.5000	0.00000	-1.5724152	12.94162	11.63231	-9.91754	6.97106	.11620	.20684	2.17969	-1.980229
14	GAP	.0250	4.5250	0.00000	0.0000000	13.44230	11.28642	-10.10947	6.86447	.11650	.20719	2.13018	-1.980229
15	CORRE	.1500	4.6750	0.00000	0.0000000	16.64788	9.32301	-11.26108	6.22493	.11810	.20952	1.83315	-1.980229
16	CORRE	.1500	4.8250	0.00000	0.0000000	20.19894	7.55147	-12.41268	5.58539	.11940	.21236	1.53611	-1.980229
17	GAP	.0250	4.8500	0.00000	0.0000000	20.82438	7.27486	-12.60462	5.47880	.11959	.21290	1.48661	-1.980229
18	QD	.2500	5.1000	0.00000	1.5573258	25.22811	5.36081	-4.43507	2.42423	.12130	.21937	1.05641	-1.489167
19	QD	.2500	5.3500	0.00000	1.5573258	24.97721	4.69024	5.40589	.34451	.12286	.22744	.72988	-1.144229
20	GAP	.5837	5.9337	0.00000	0.0000000	19.07827	4.36930	4.69953	.20528	.12712	.24802	.06195	-1.144229
21	GAP	.5837	6.5175	0.00000	0.0000000	14.00399	4.21092	3.99318	.06605	.13280	.26975	-.60598	-1.144229
22	BMAG	.0249	6.5424	5.95000	0.0000000	13.80572	4.20762	3.95303	.06608	.13309	.27069	-.63441	-1.137398
23	BMAG	.5459	7.0882	129.91000	0.0000000	9.83982	4.13640	3.30252	.06366	.14055	.29152	-1.21276	-.978709
24	BMAG	.5459	7.6341	129.91000	0.0000000	6.59499	4.07018	2.64202	.05697	.15134	.31269	-1.69986	-.803526
25	BMAG	.5459	8.1799	129.91000	0.0000000	4.07124	4.01340	1.98151	.04645	.16813	.33419	-2.08751	-.614802
26	BMAG	.5459	8.7258	129.91000	0.0000000	2.26856	3.96989	1.32101	.03282	.19688	.35596	-2.36916	-.415716
27	BMAG	.5459	9.2716	129.91000	0.0000000	1.18695	3.94255	.66050	.01698	.25085	.37793	-2.54007	-.209624
28	BMAG	.5459	9.8175	129.91000	0.0000000	.82641	3.93323	.00000	-.00000	.34375	.40000	-2.59736	.000000

DP/P	COSMU(H)	Q(H)	QPRIME(H)	BETAMAX(H)	COSMU(V)	Q(V)	QPRIME(V)	BETAMAX(V)	XMAX(H)	GAMMA TR.
0.0000	.30902	3.2000	-4.5302	14.0456	-.38268	2.7500	-7.1991	25.2281	2.6916	-2.5518

XXXXXXXXXXXXXXXXXXXXXXXXXXXXXXXXXXXXXXXXXXXXXXXXXXXXXXXXXXXXXXXXXXXXXXXXXXXXXXXXXXXXXXXXXXXXXXXXXXXXXXXXXXXXXXXXXXXXXXXXXX

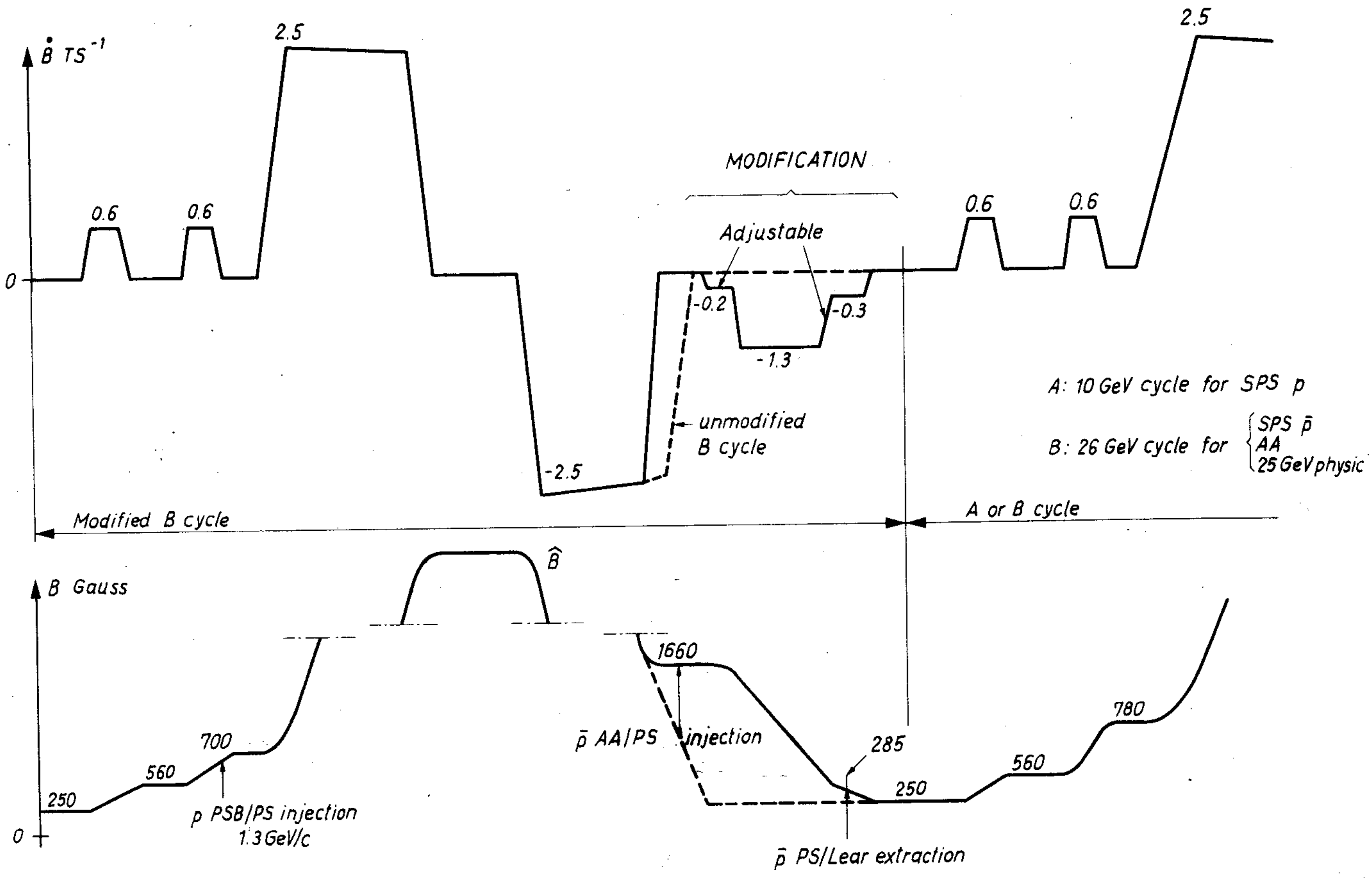

Fig. 10 TYPICAL DECELERATION PS CYCLE

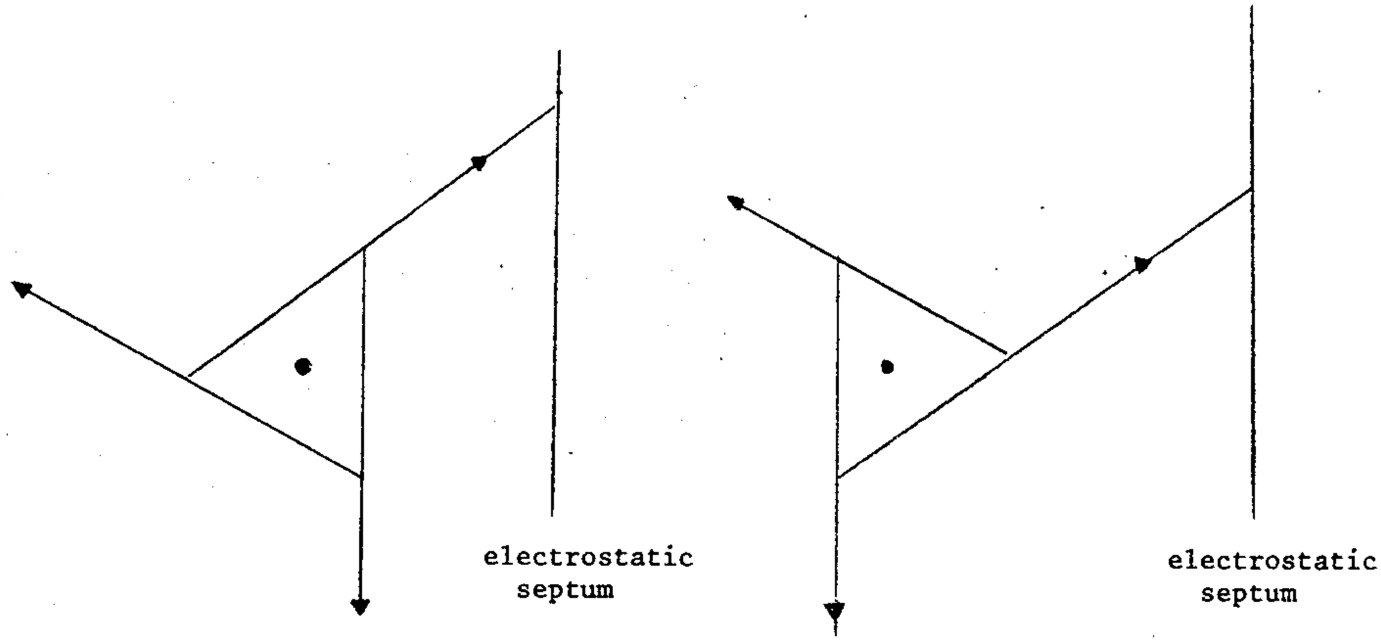

Fig. 11: a) $\Delta Q < 0$, $\xi > 0$ b) $\Delta Q > 0$, $\xi < 0$

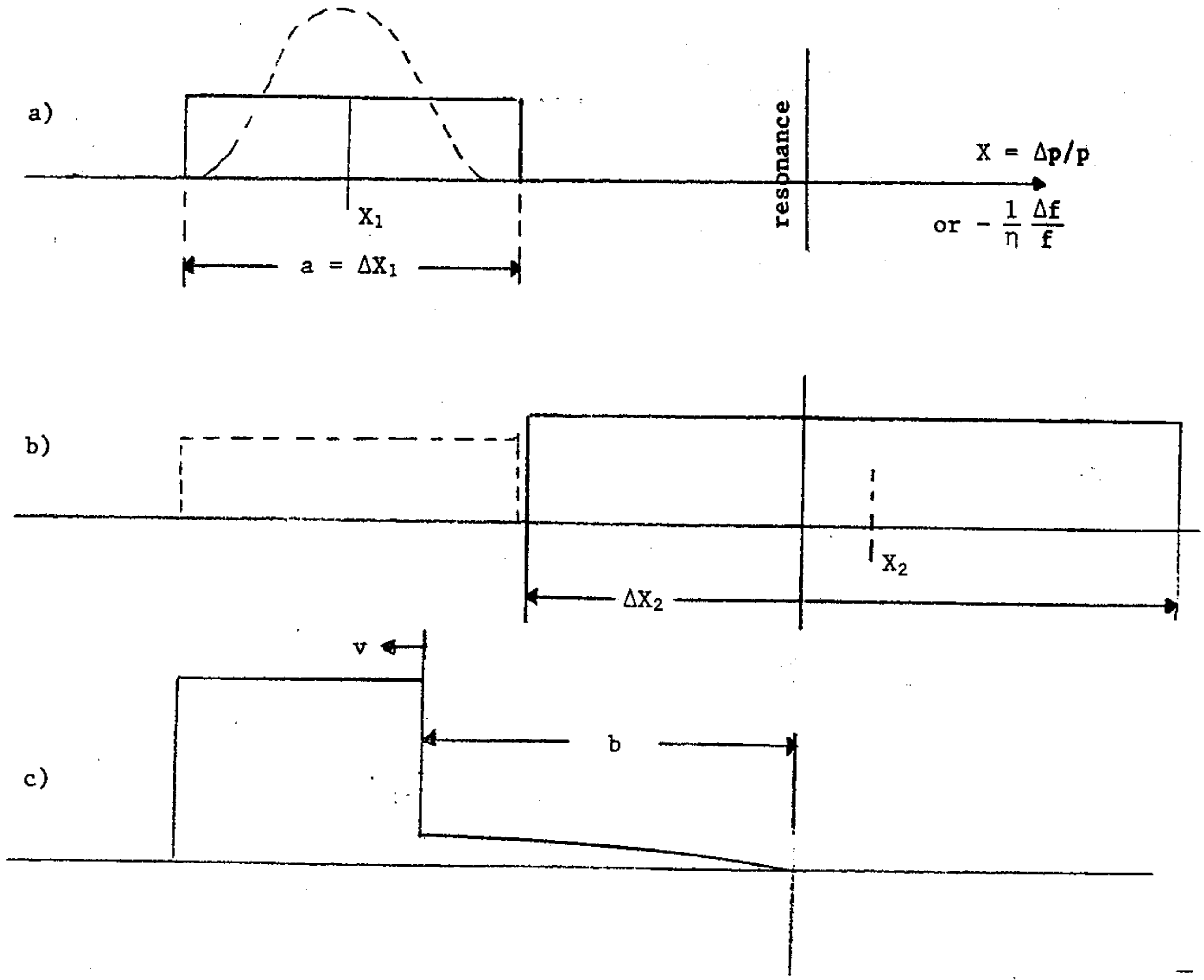

Fig. 12

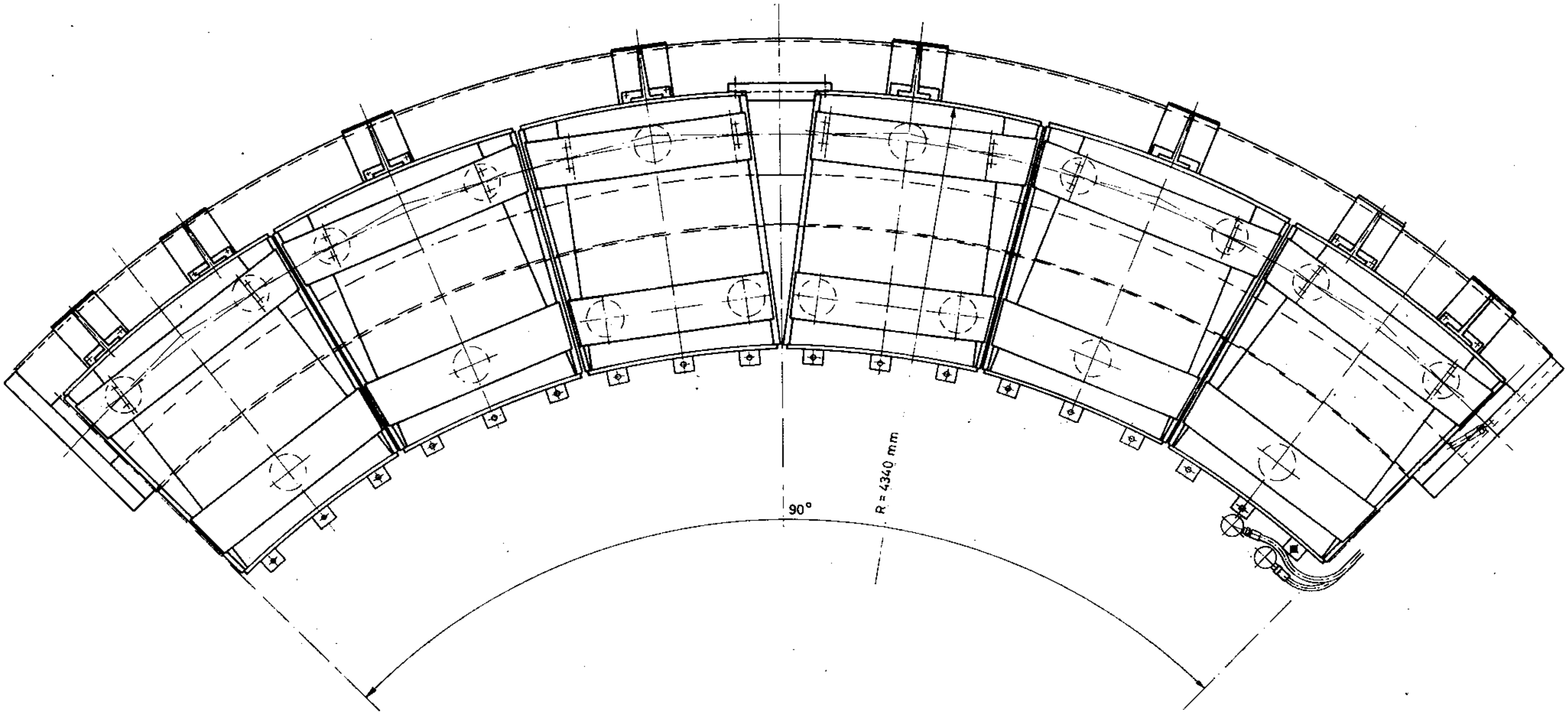

Fig. 13 : LEAR bending magnet

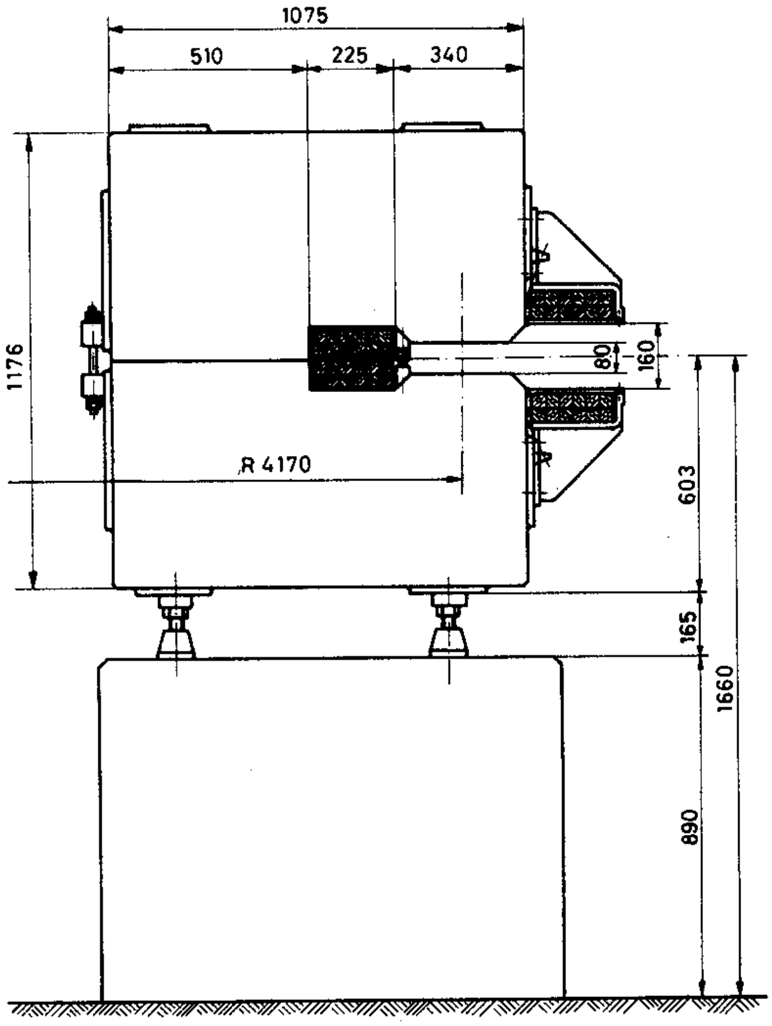

Fig. 14 : LEAR bending magnet

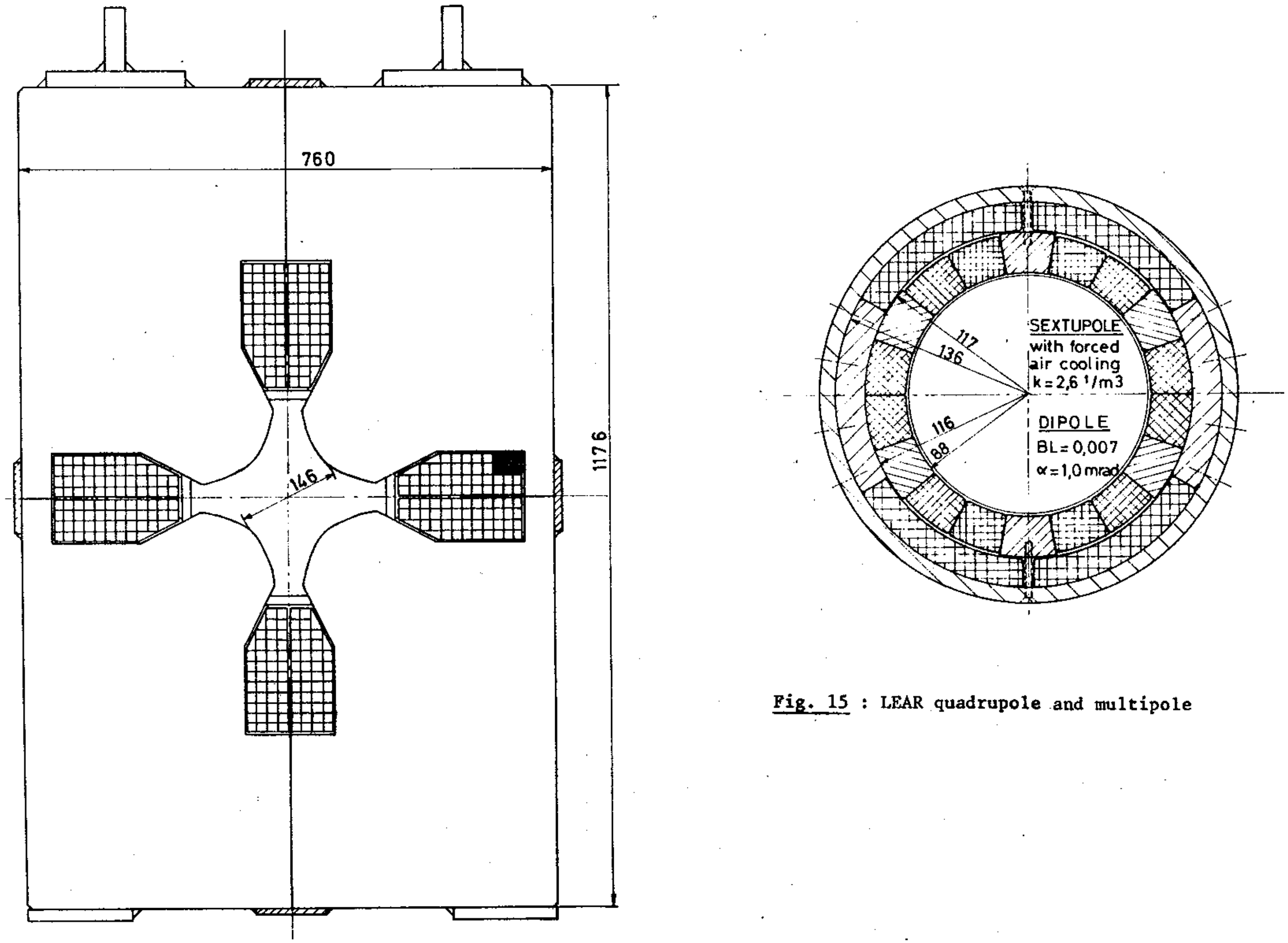

Fig. 15 : LEAR quadrupole and multipole

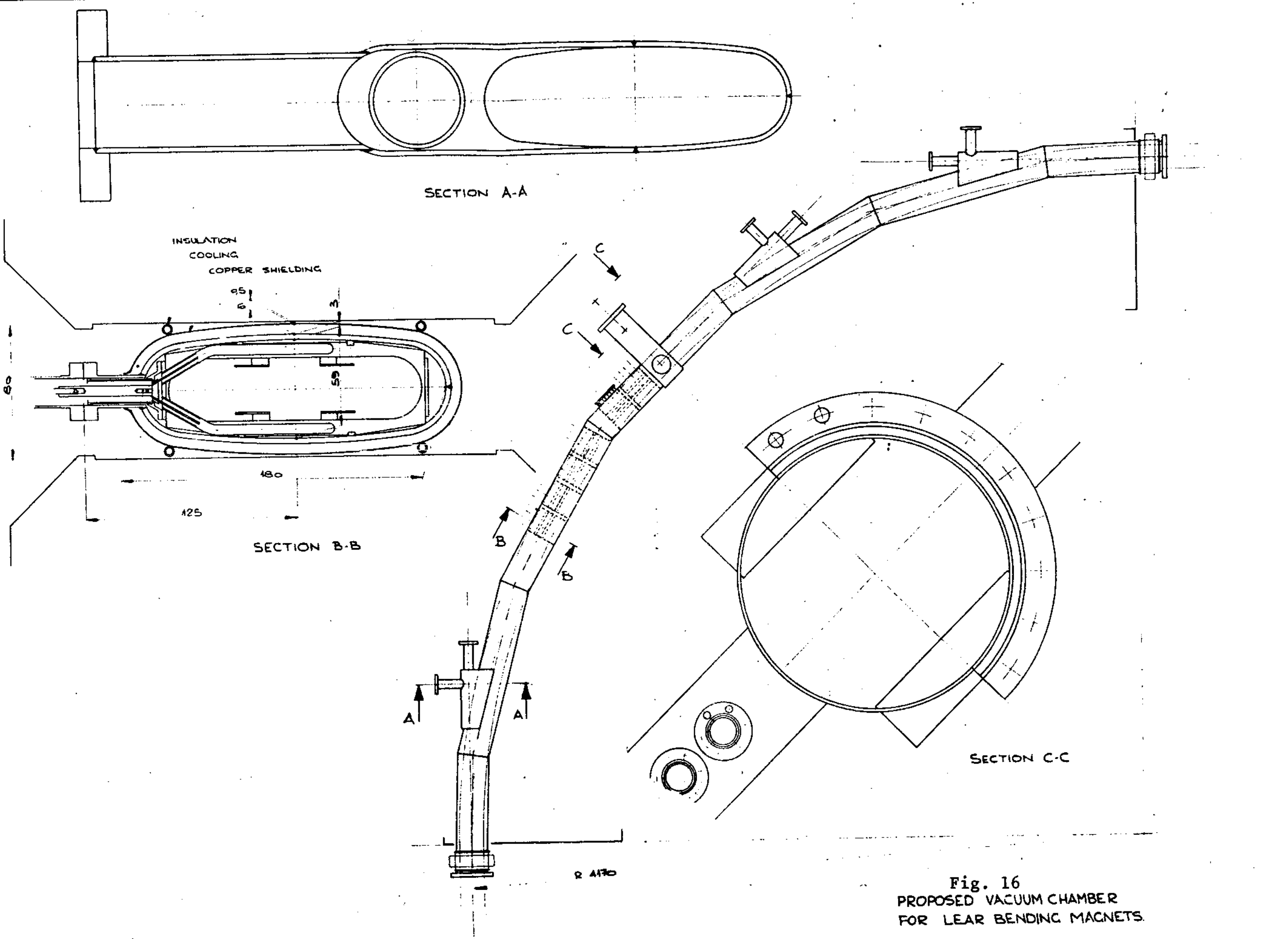

Fig. 16
PROPOSED VACUUM CHAMBER
FOR LEAR BENDING MAGNETS.

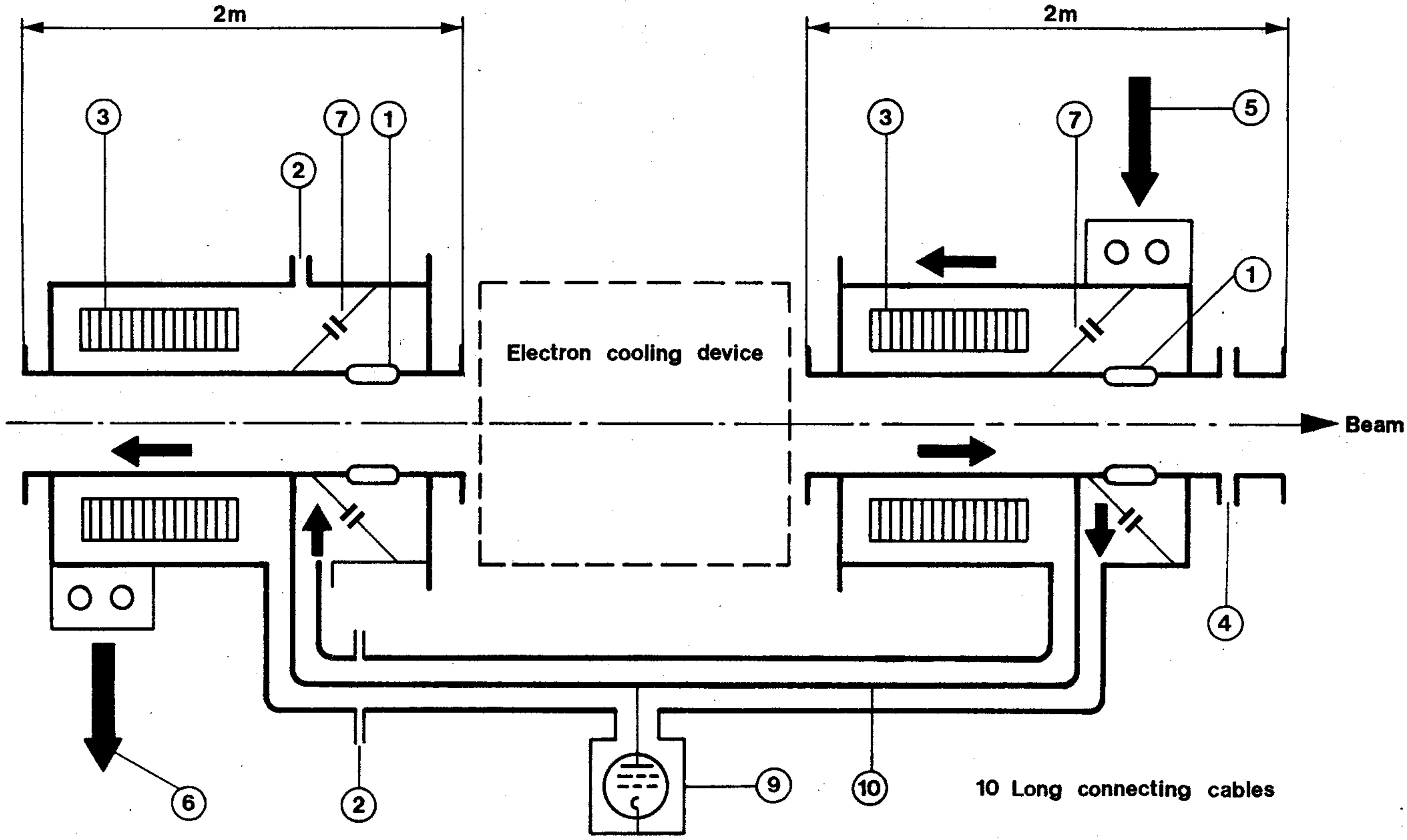

PROPOSED LEAR RF CAVITY

Fig. 17

21.3.80

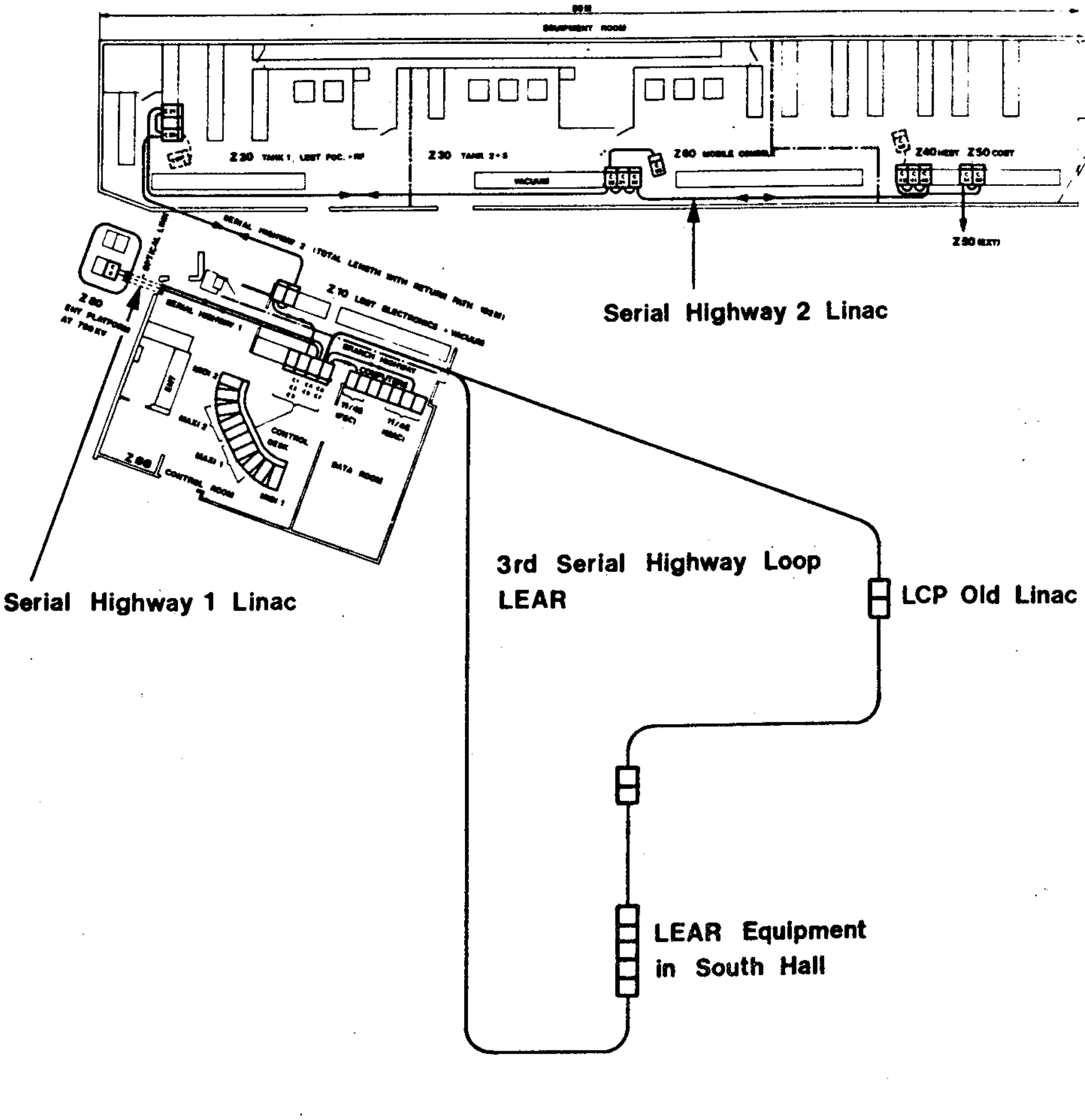

Fig. 18: Proposed addition of a third Serial Highway for LEAR and the Old Linac

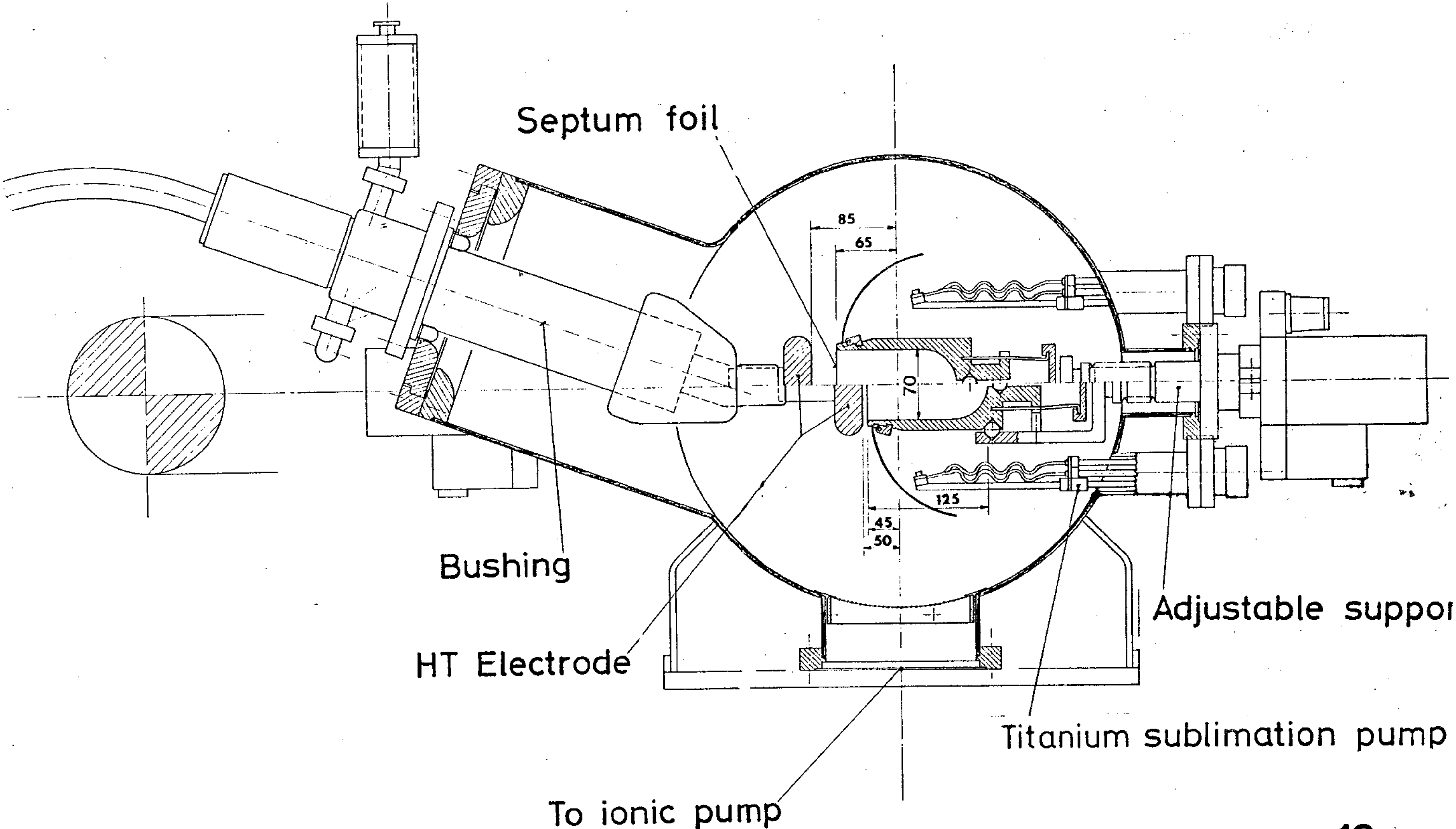

Fig. 19

ELECTROSTATIC SEPTUM Cross section

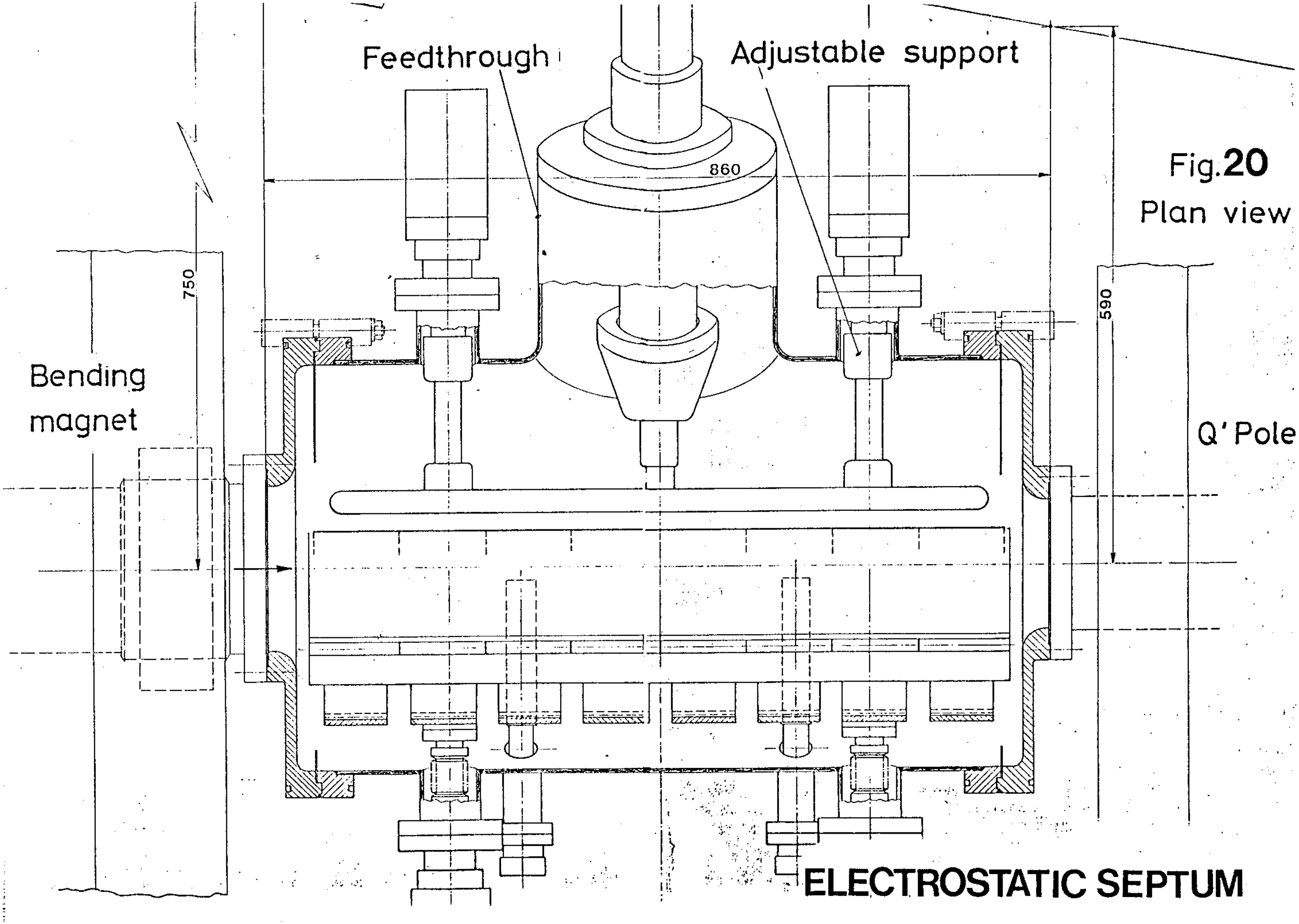

Fig. 20
Plan view

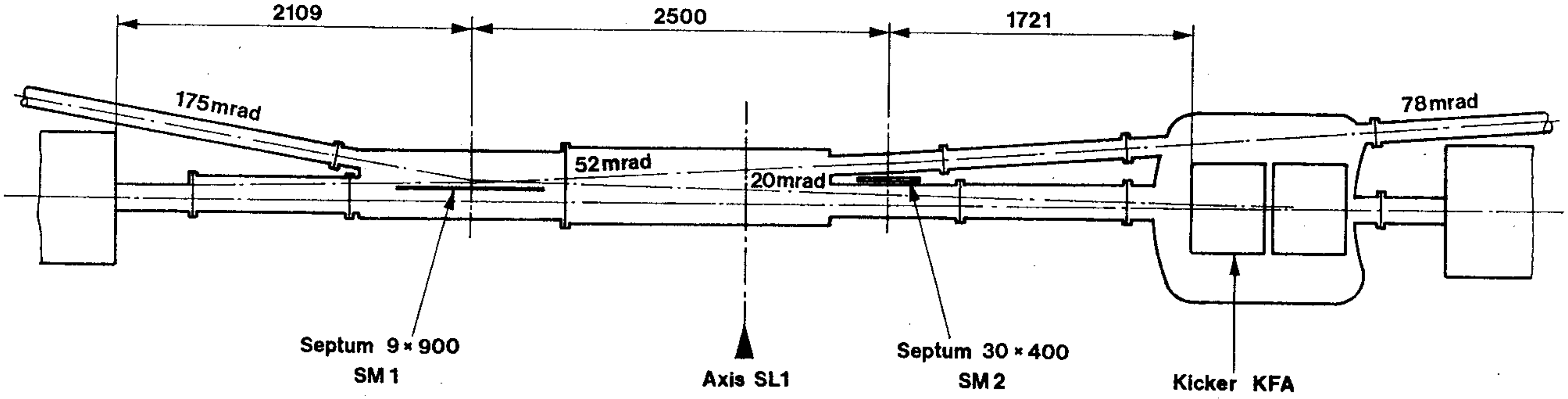

Fig. 21: General lay-out of SL 1 (Injection / ejection elements)

18.4.80 [signature]

Fig. 22 _ Injection kicker _ LEAR _

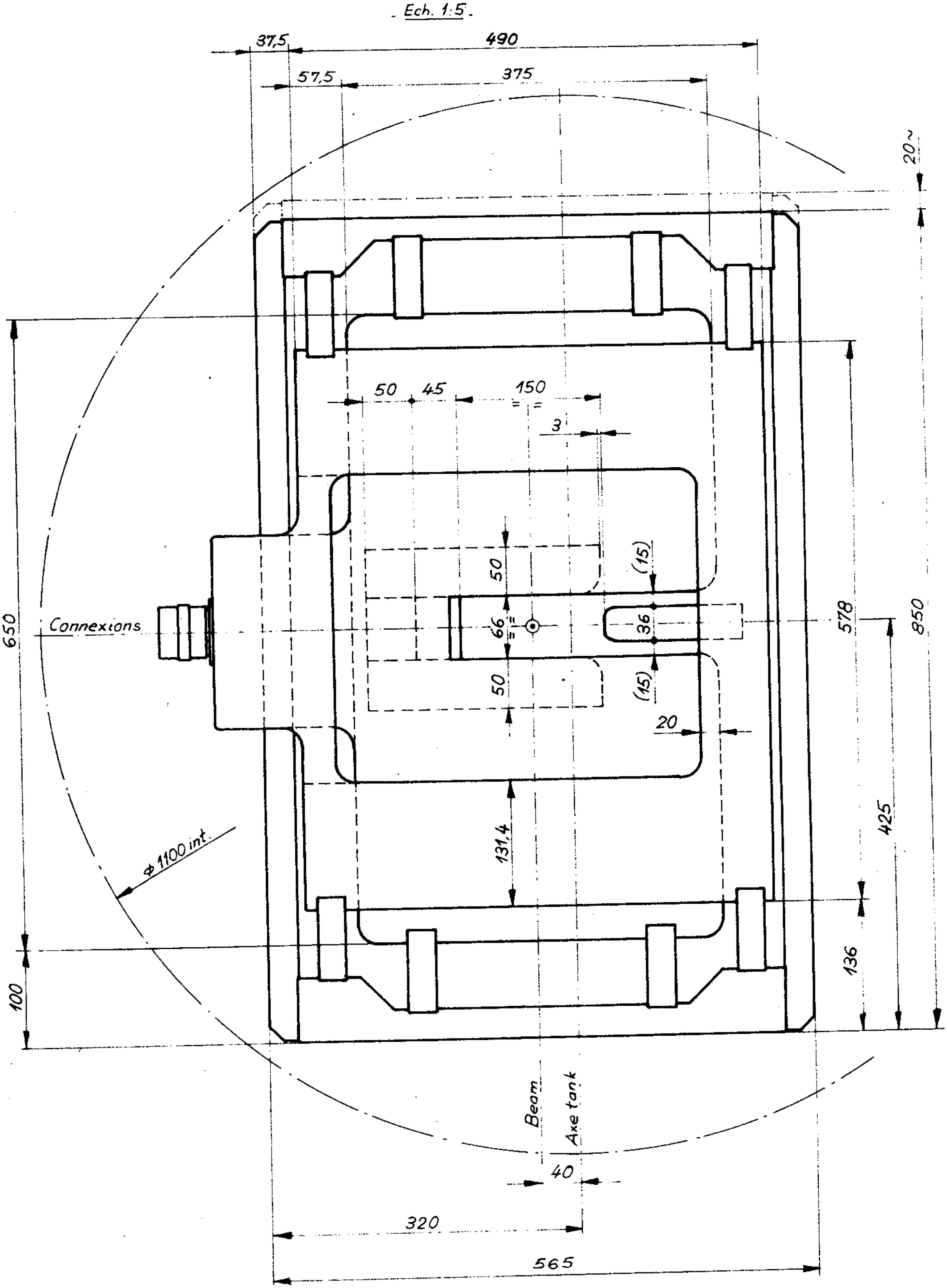

Fig. 23 -IMPLEMENTATION OF STOCHASTIC COOLING SYSTEM -(schematic)

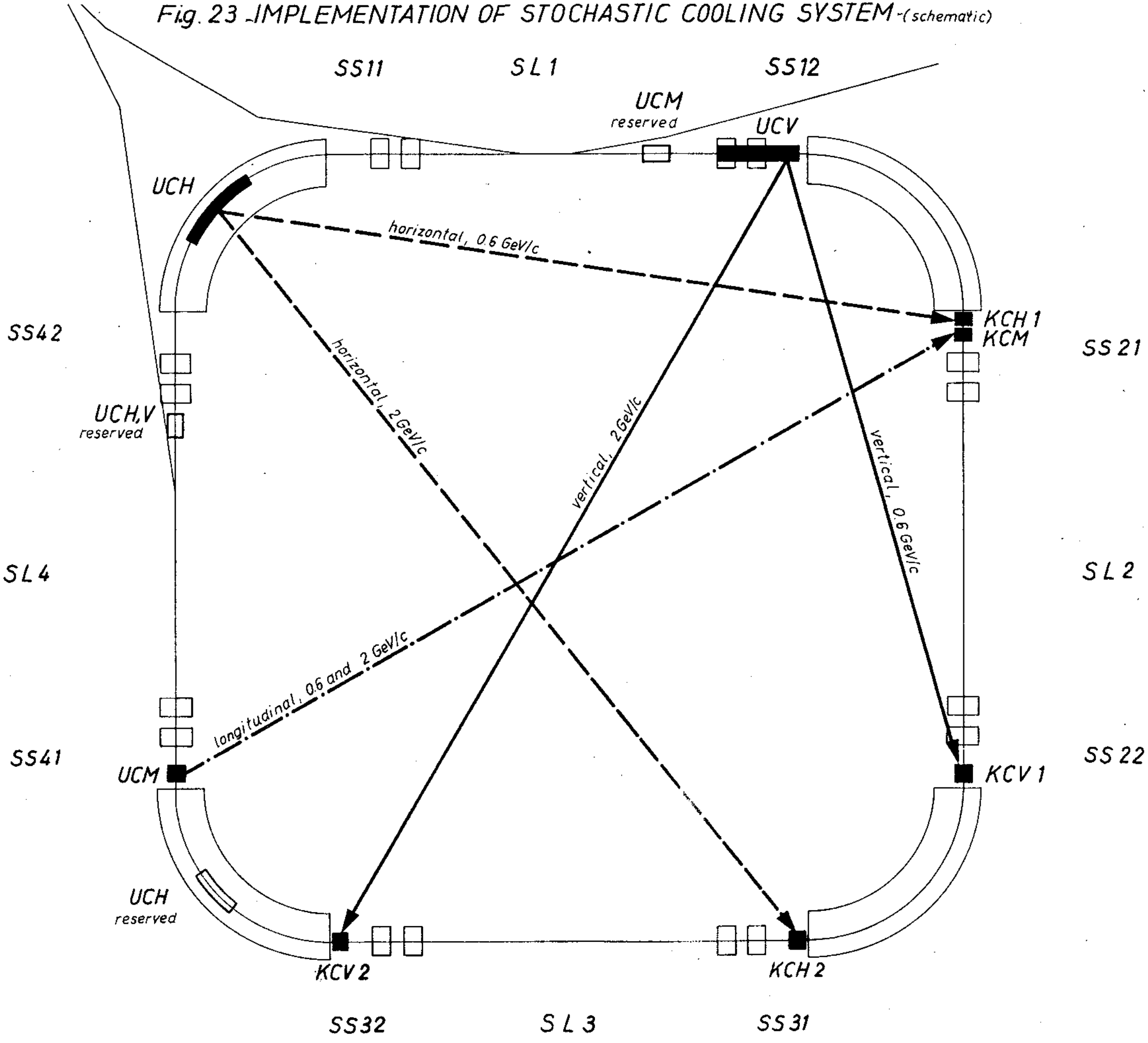

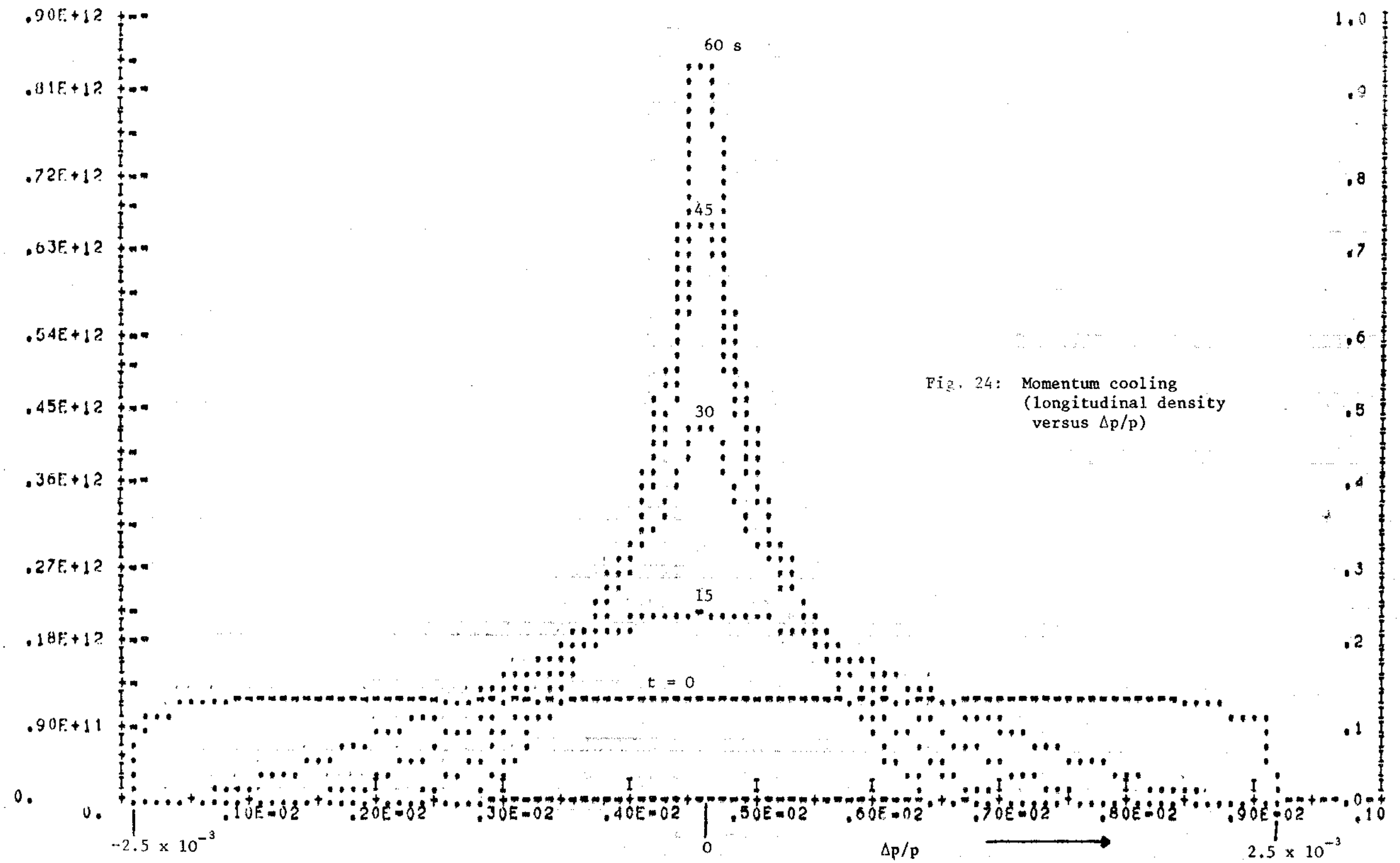

Fig. 24: Momentum cooling (longitudinal density versus $\Delta p/p$)

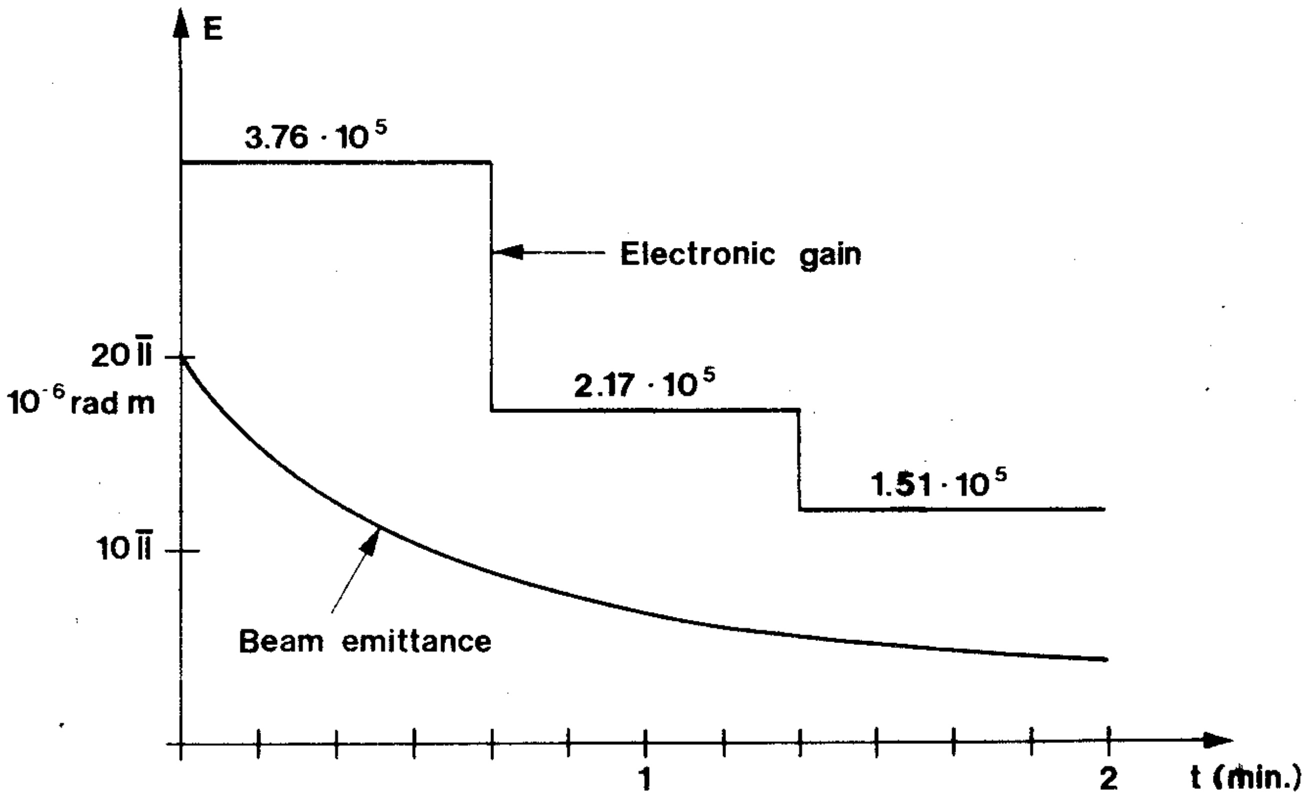

Fig. 25: Cooling of vertical emittance at 0.6 GeV/c

8.4.80

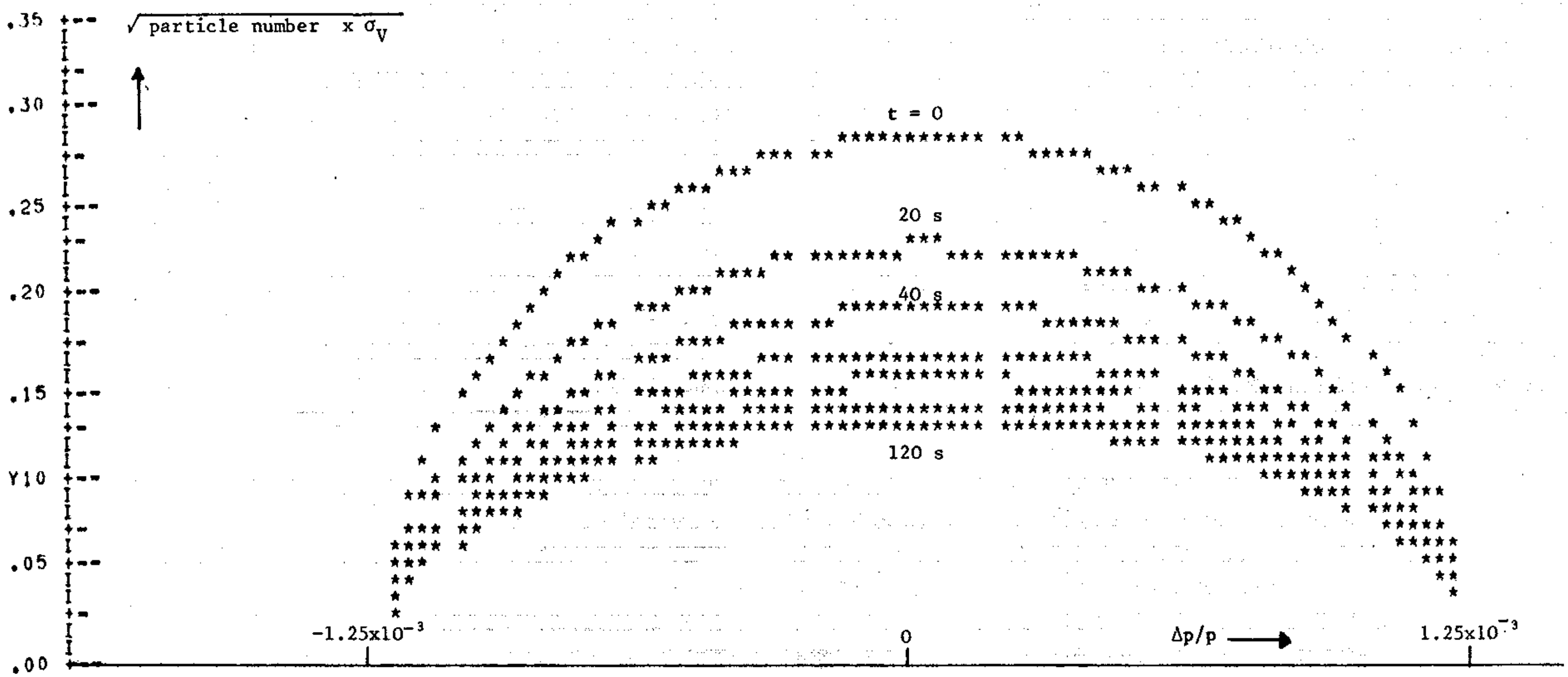

Fig. 26: Schottky signals during vertical cooling

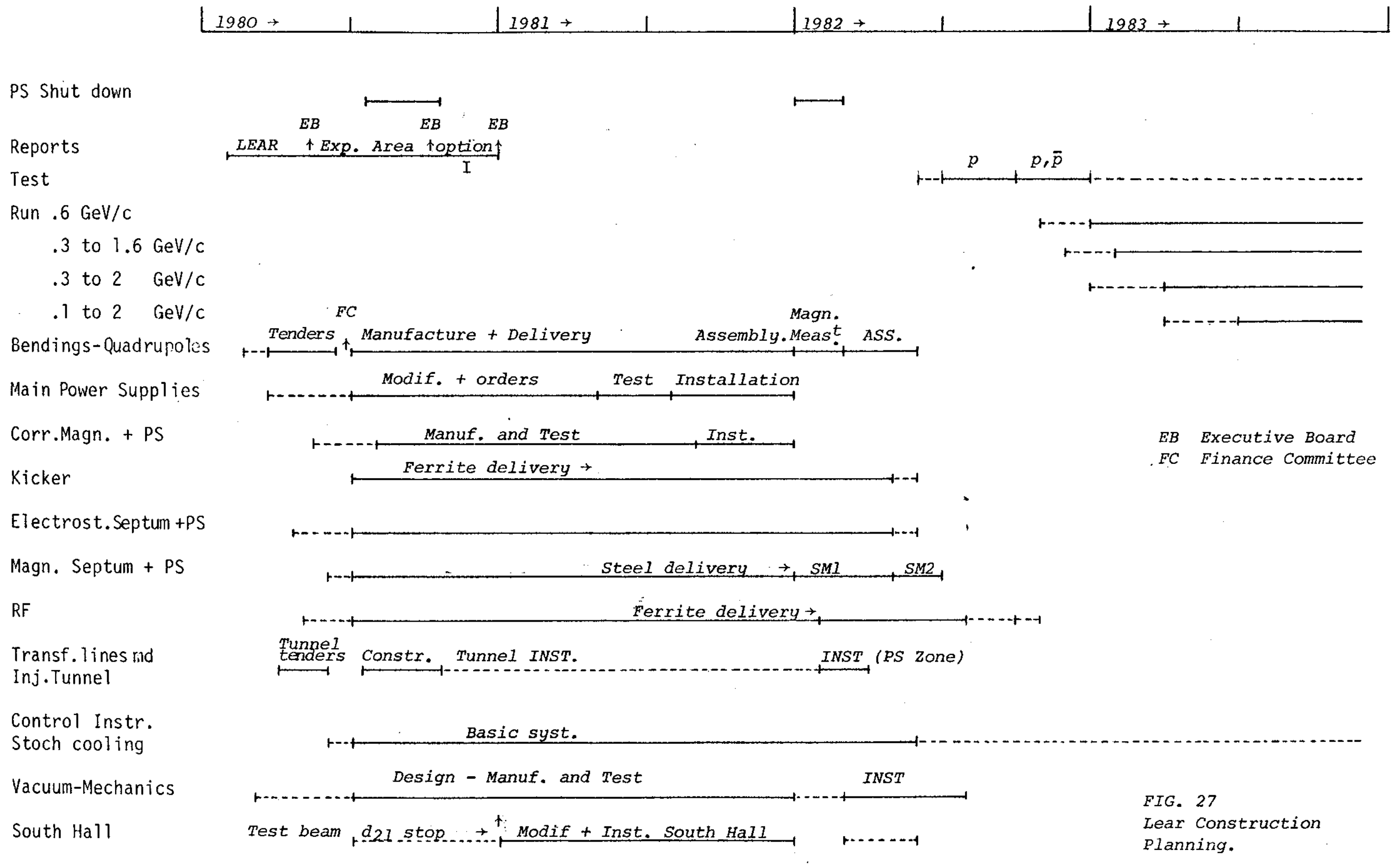

FIG. 27
Lear Construction
Planning.

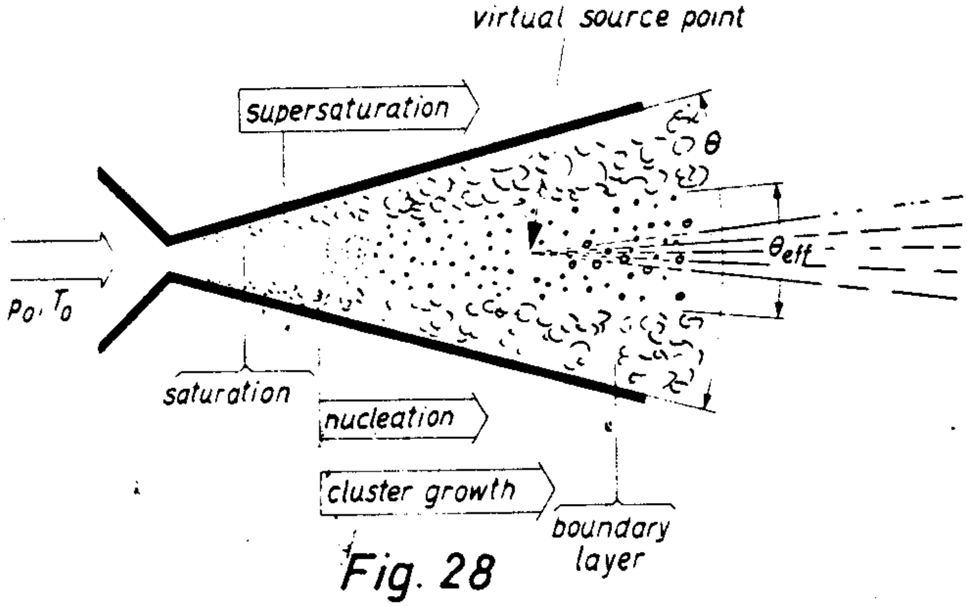

Fig. 28

PRODUCTION OF CLUSTER BEAMS

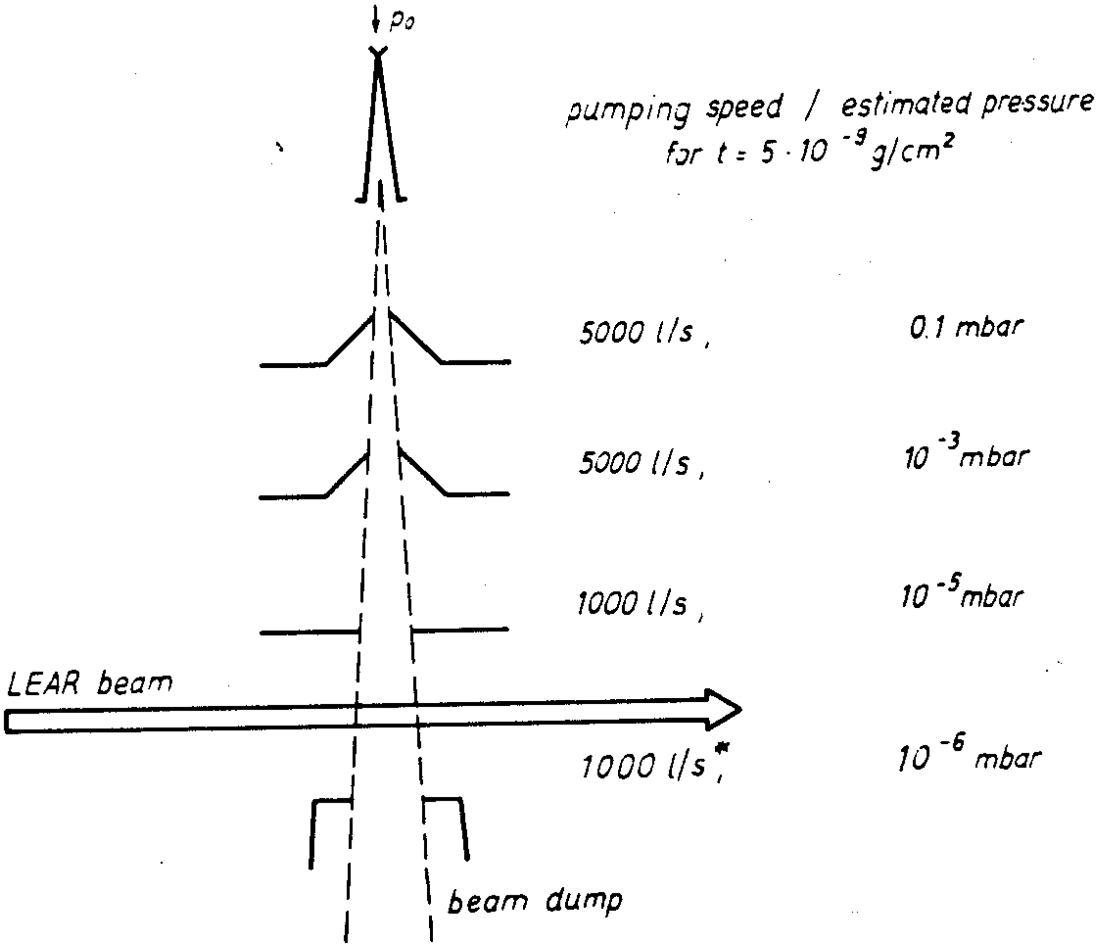

* Depending on the geometry of the experiment, the pumping speed in the crossing region may be up to an order of magnitude higher, resulting in a lower pressure

Fig. 29

SCHEMATIC LAYOUT OF A CLUSTER BEAM TARGET. PRESSURES FOR A TARGET DENSITY OF $2.5 \cdot 10^{-11}$ g/cm², THE MAXIMUM FOR 100 MeV OPERATION WILL BE A FACTOR OF 100 LOWER.